

**CHARACTERISATION OF THE GENETICALLY MODIFIED
CYTOCHROME SYSTEMS AND THEIR APPLICATION TO
BIOHYDROGEN PRODUCTION IN *RHODOBACTER CAPSULATUS***

YAVUZ ÖZTÜRK

DECEMBER 2005

CHARACTERISATION OF THE GENETICALLY MODIFIED
CYTOCHROME SYSTEMS AND THEIR APPLICATION TO
BIOHYDROGEN PRODUCTION IN *RHODOBACTER CAPSULATUS*

A THESIS SUBMITTED TO
THE GRADUATE SCHOOL OF NATURAL AND APPLIED SCIENCES
OF
MIDDLE EAST TECHNICAL UNIVERSITY

BY

YAVUZ ÖZTÜRK

IN PARTIAL FULFILLMENT OF THE REQUIREMENTS
FOR
THE DEGREE OF DOCTOR OF PHILOSOPHY
IN
BIOTECHNOLOGY

DECEMBER 2005

Approval of the Graduate School of Natural and Applied Science

Prof. Dr. Canan ÖZGEN
Director

I certify that this thesis satisfies all the requirements as a thesis for the degree of Doctor of Philosophy.

Assoc. Prof. Dr. Candan GÜRAKAN
Head of the Department

This is to certify that we have read this thesis and that in our opinion it is fully adequate, in scope and quality, as a thesis for the degree of Doctor of Philosophy.

Assoc. Prof. Dr. Sevnur MANDACI
Co-Supervisor

Prof. Dr. Meral Yücel
Supervisor

Examining Committee Members

Prof. Dr. İnci EROĞLU (METU, CHE) _____

Prof. Dr. Meral YÜCEL (METU, BIOL) _____

Prof. Dr. Hüseyin Avni ÖKTEM (METU, BIOL) _____

Assoc. Prof. Dr. Candan GÜRAKAN (METU, FDE) _____

Assist. Prof. Dr. Füsün EYİDOĞAN (Başkent Univ.,) _____

I hereby declare that all information in this document has been obtained and presented in accordance with academic rules and ethical conduct. I also declare that, as required by these rules and conduct, I have fully cited and referenced all material and results that are not original to this work.

Name, Last name: Yavuz Öztürk

Signature :

ABSTRACT

CHARACTERISATION OF GENETICALLY MODIFIED CYTOCHROME SYSTEMS AND THEIR APPLICATION TO BIOHYDROGEN PRODUCTION IN *RHODOBACTER CAPSULATUS*

Öztürk, Yavuz

Ph.D., Department of Biotechnology

Supervisor: Prof. Dr. Meral YÜCEL

Co-Supervisor: Assoc. Prof. Dr. Sevnur MANDACI

December 2005, 164 pages

Facultative phototrophic bacterium *Rhodobacter capsulatus* has two *c*-type electron carrier cytochromes (cyt); the soluble cyt *c*₂ and the membrane-attached cyt *c*_y, that act as electron carriers during respiratory and photosynthetic growth of this species. Previously, a soluble form of cyt *c*_y was constructed by fusing genetically the signal sequence of cyt *c*₂ to the cyt *c* domain of cyt *c*_y. The obtained novel soluble cyt *c*_y (cyt S-*c*_y) was unable to support photosynthetic growth of *R. capsulatus* but yielded photosynthetically functional (Ps⁺) revertants frequently. In the first part of this study, photosynthetic electron transfer properties of some of Ps⁺ revertants of cyt S-*c*_y were analyzed by biochemical and biophysical methods and compared with the cyt *c*_y and cyt *c*₂. Reduction-oxidation titration of membrane supernatants showed that the redox midpoint potential of cyt S-*c*_y was +338 mV which is similar to midpoint potentials of cyt *c*_y or the cyt *c*₂. However,

light-activated, time resolved spectroscopy revealed that reaction center mediated oxidation kinetics of cyt S-*c_y* exhibited only a slow phase, unlike cyt *c₂* which has both fast and slow phases. It therefore appeared that during electron transfer cyt S-*c_y* does not interact with the reaction centre as tightly as cyt *c₂*. These findings imply that attaching electron carrier cyts to the membrane allowed them to weaken their interactions with their partners, while restricting their spatial diffusion, so that they accomplish rapid multiple turnovers.

In the second part of this study, hydrogen production of various *R. capsulatus* strains harboring the genetically modified electron carrier cytochromes, cyt *cbb₃* deleted and Qox deleted strains were compared with the wild type. Under photoheterotrophic growth conditions with limiting nitrogen source, the excess reducing equivalents generated by organic acid oxidation are consumed to reduce protons into hydrogen by the activity of nitrogenase in *R. capsulatus*. The results indicated that the hydrogen production of mutant strains with modified electron carrier cytochromes decreased 3-5 folds, and the hydrogen production rate of the cyt *cbb₃*⁻ mutant increased significantly. Moreover in this study, the hydrogen production efficiency of different *R. capsulatus* strains was increased by the chromosomal inactivation of uptake hydrogenase genes and enzymatic activity of uptake hydrogenase of *R. capsulatus* strains were determined.

Keywords: *Rhodobacter capsulatus*, Photosynthesis, Cytochrome, Hydrogen production.

ÖZ

RHODOBACTER CAPSULATUS BAKTERİSİNDE GENETİK OLARAK DEĞİŞTİRİLMİŞ SİTOKROM SİSTEMLERİNİN KARAKTERİZE EDİLMESİ VE BU SUŞLARİN HİDROJEN GAZI ÜRETİMİNDE KULLANILMASI

Öztürk, Yavuz

Doktora, Biyoteknoloji Programı

Tez Yöneticisi: Prof. Dr. Meral YÜCEL

Yardımcı Tez Yöneticisi: Doç. Dr. Sevnur MANDACI

Aralık 2005, 164 sayfa

Fakültatif fotosentetik *Rhodobacter capsulatus* bakterisi çözünür formdaki sitokrom c_2 (sit c_2) ve hücre zarına bağlı sitokrom c_y (sit c_y) olmak üzere iki farklı c -tipi elektron taşıyıcı sitokrom proteinine sahiptir. Bu sitokromlar fotosentezde elektronları sit bc_1 kompleksinden reaksiyon merkezine; solunumda ise, elektronları sit bc_1 kompleksinden sit cbb_3 oksidaz enzime aktarırlar. Rapor edilen önceki çalışmada sit c_y 'nin yeni çözünür formu ($S-c_y$) sit c_2 'nin işaret dizisi ile sit c_y 'nin sit c bölgesinin genetik yöntemler kullanılarak birleştirilmesi ile oluşturuldu. Elde edilen yeni çözünür sit $S-c_y$ 'nin fotosentetik büyümeye fonksiyonel olmadığı görüldü fakat çok sık olarak geri mutasyonla fotosentezde aktif (Ps^+) özelliği kazanan geri mutantlar verdiği görüldü. Bu çalışmanın ilk

kısmında elde edilen bazı Ps^+ özelliği kazanan revertantların elektron taşıma özellikleri biyokimyasal ve biyofiziksel metodlarla incelendi ve sit c_2 ve sit c_y ile karşılaştırıldı. Çözünür sit $S-c_y$ nin indirgenme-yükseltgenme titrasyonu bu sitokromun orta nokta potansiyelinin + 338 mV olduğunu ve bu değerin sit c_2 ve sit c_y ye ait değerler ile benzer olduğunu gösterdi. Ayrıca, ışık-aktiflenmiş zamanbağımlı spektroskopik ölçümleri bu sitokromun reaksiyon merkezi odaklı yükseltgenme kinetiğinin sit c_2 ' den farklı olarak sadece yavaş fazdan oluştuğunu gösterdi. Bu da sit $S-c_y$ nin elektron taşıma sırasında reaksiyon merkezi ile c_2 kadar kuvvetli etkileşime giremediğini göstermektedir. Tüm bu bulgular, sit c_y nin hücre zarına bağlı olmasının sadece difizyon etkisini ortadan kaldırmakla kalmayıp elektron taşıma zincirindeki kompleksler ile zayıf elektrostatik etkileşmeye girmesi sonucu daha etkili ve hızlı bir şekilde çoklu döngüsel elektron transferi yaptığı göstermektedir.

Çalışmanın ikinci kısmında, sitokrom sistemleri genetik olarak değiştirilmiş soylar ile künol oksidaz ve cbb_3 oksidaz enzimleri inaktif edilmiş soyların hidrojen üretim profilleri yaban soyu ile karşılaştırıldı. *R. capsulatus* bakterisinde, nitrojen kaynağının kısıtlı olduğu fotoheterotrofik büyümeye koşullarında, organik asitlerin oksitlenmesi sonucunda ortaya çıkan aşırı indirgen elektronlar nitrojenaz enziminin hidrojen üretme kapasitesi sayesinde protonların indirgenmesi ile hidrojene dönüştürülmektedir. Sonuçlar, elektron taşıyıcı sitokromları genetik olarak değiştirilmiş soylarda hidrojen üretiminin 3-5 kat düşüğünü ve cbb_3 oksidaz enzimi inaktif edilmiş soyda hidrojen üretim hızının kaydadeğer bir şekilde arttığını göstermiştir. Bunlara ek olarak, farklı *R. capsulatus* soylarına ait gerikullanım hidrojenaz enzimi genlerinin delesyonu gerçekleştirilerek hidrojen üretimi daha verimli hale getirilmiş ve *R. capsulatus* soylarının enzim aktivite ölçümleri yapılmıştır.

Anahtar kelimeler: *Rhodobacter capsulatus*, Fotosentez, Sitokrom, Hidrojen üretimi.

To my family for all their support and understanding

ACKNOWLEDGMENTS

I would like to express my deepest gratitude to my supervisor Prof. Dr. Meral Yücel for her invaluable guidance, advice and supervision throughout the study. She supported me and this study with her continued advice and close interest. She always has been model for me.

I would like to express my sincere gratitude to Prof. Dr. Fevzi Daldal for *Rhodobacter* strains, plasmids, and his great guidance, advice and supports throughout the research. Without his help and support, this work could not be completed. The most part of the soluble cyt S-*c_y* work was completed at his laboratory at University of Pennsylvania.

I would like to thank to Assoc. Prof. Dr. Sevnur Mandacı for her help and for permitting some *Rhodobacter* strains for biohydrogen experiments during this study.

I would like to thank to Prof. Dr. İnci Eroğlu, Prof. Dr. Ufuk Gündüz and Prof. Dr. Lemi Türker for their critical suggestions, comments and guidance throughout the biohydrogen study.

I would like to thank to Drs. Artur Osyczka and Roger C. Prince for their valuable help for chemical oxidation-reduction midpoint potential titration and light-activated, millisecond time scale kinetic spectroscopy experiments.

I wish to extend my thanks to institute acting director Assoc. Prof. Dr. Kemal Baysal, deputy director Prof. Dr. Altan Erarslan, deputy director Assoc. Prof. Dr. Aynur Başalp and all of TÜBİTAK-GMBAE members for their help and supports during this study.

I appreciate the cooperation of my colleagues Semra Aygün, Özlem Akkaya and Mehmet Öztürk for their help and friendship.

I am deeply grateful to METU Biohydrogen group members; Başar Uyar, Ela Eroğlu, Gökhan Kars and Süleyman Sarı for their friendship, collaboration and help when I needed.

I would like to thank all members of Plant biotechnology lab in Biology Department in METU for their friendship and help.

I am indebted to my family for their support during my education

Finally, I would like to thank TÜBİTAK- GMBAE and METU for research facilities where the work was supported by ICGEB Project No. CRP/TUR99-01 (Trieste-Italy) and METU Project No: BAP. 2004-07-02-00-10 respectively. The experiments carried out in Prof. Dr. Fevzi Daldal laboratory (University of Pennsylvania, USA) was supported by grants from NIH GM38237 and DOE 91ER20052.

ABBREVIATIONS

- ATP: Adenosine triphosphate
Bp: Base pair
Cyt: Cytochrome
Cyt S-*c*: Soluble cyt *c*
Cyt MA-*c*₂: Membrane-attached cyt *c*₂
Cyt *bc*₁ complex: Ubihydroquinone cyt *c* oxidoreductase
Cyt *cbb*₃ oxidase: *cbb*₃-type cytochrome *c* oxidase
*E*_{m7}: Oxidation-reduction midpoint potential at pH 7.0
ETC: Electron Transfer Chain
Gen^R: Gentamycin resistance
Hup: Uptake Hydrogenase
ICM: Intracytoplasmic membranes
Kan^R: Kanamycin resistance
Kb: Kilobase
KDa: Kilo Dalton
LHI and LHII: Light harvesting I and II complexes, respectively
Nif: Nitrogen fixation
ORF: Open reading frame
P: Primary donor
PC: Plastocyanin
PQ: Plastoquinone
Ps: Photosynthetic
PSI and PSII: Photosystem I and II, respectively
Q: Quinone pool
Q_A and Q_B: Primary and secondary quinone acceptors of the RC, respectively

Q_o : Ubihydroquinone oxidizing site of the cyt bc_1 complex

Q_{OX} : Quinol oxidase

RC: Photochemical reaction center

Rc and Rs: *Rhodobacter capsulatus* and *Rhodobacter sphaeroides*, respectively

Res: Respiratory

RT: Room temperature

Spe^R: Spectinomycin resistance

UQ: Ubiquinone

UQH₂: ubihydroquinone

Tet^R: Tetracycline resistance

TM: Trans membrane

TABLE OF CONTENTS

PLAGIARISM.....	iii
ABSTRACT.....	iv
ÖZ.....	vi
DEDICATION.....	viii
ACKNOWLEDGMENTS.....	ix
ABBREVIATIONS.....	xi
TABLE OF CONTENTS.....	xiii
LIST OF TABLES	xviii
LIST OF FIGURES	xix
CHAPTER	
 1. INTRODUCTION.....	1
1.1. General properties of energy metabolism	1
1.1.1. Electron transfer chains in energy metabolism.....	2
1.2. Energy metabolism of <i>Rhodobacter capsulatus</i>	3
1.2.1. <i>R. capsulatus</i> as a model for energy transduction.....	3
1.2.2. Metabolic diversity of <i>R. capsulatus</i> and RegB/RegA global regulatory system.....	5
1.2.3. Respiratory and photosynthetic growth of <i>R. capsulatus</i>	9
1.2.4. Inter-protein electron transfer during the photosynthetic growth.....	12
1.3. Cytochromes as electron carriers.....	16
1.3.1. Electron carrier cytochromes of <i>R. capsulatus</i>	17
1.3.1.1 Cyt <i>c</i> ₂ of <i>R. capsulatus</i>	17
1.3.1.2 Cyt <i>c</i> _y of <i>R. capsulatus</i>	19
1.3.2. Hybrid versions of cyt <i>c</i> ₂ and cyt <i>c</i> _y	21

1.3.2.1. Membrane- attached form of cyt <i>c</i> ₂ (cyt MA- <i>c</i> ₂).....	21
1.3.2.2. Soluble version of cyt <i>c</i> _y (cyt S- <i>c</i> _y).....	23
1.4. Biological hydrogen production	25
1.4.1. Photoheterotrophic hydrogen production by <i>R. capsulatus</i>	26
1.4.2. Electron transfer chain and hydrogen production in <i>R. capsulatus</i>	27
1.4.3. Enzyme systems for hydrogen metabolism in <i>R. capsulatus</i>	29
1.4.3.1. Nitrogenase	29
1.4.3.1.1. Genetics, structure and activity of nitrogenase.....	29
1.4.3.1.2. Regulation of nitrogenase.....	32
1.4.3.2. Uptake hydrogenase.....	34
1.4.3.2.1. Genetics, structure and activity of uptake hydrogenase.....	34
1.4.3.2.2. Regulation of uptake hydrogenase.....	35
1.4.4. Genetic studies for hydrogen production in <i>R. capsulatus</i>	37
1.5. Scope of the work.....	38
2. MATERIALS AND METHODS.....	39
2.1. Materials.....	39
2.1.1. Bacterial strains and plasmids.....	39
2.1.2. Bacterial growth mediums and culture conditions	40
2.1.3. Growth mediums and culture conditions for hydrogen production.....	40
2.1.4. Chemicals, restriction endonucleases and DNA modifying enzymes	44
2.2. Methods.....	44
2.2.1. Molecular genetic techniques.....	44
2.2.1.1. Plasmid DNA isolation.....	44
2.2.1.2. Chromosomal DNA isolation	45
2.2.1.3. Enzyme digestion.....	46
2.2.1.4. Purification and concentration of digested DNA samples.....	47

2.2.1.5. Isolation of DNA fragments from agarose gel	47
2.2.1.6. Ligation reaction.....	48
2.2.1.7. DNA sequencing.....	49
2.2.1.8. PCR based site directed mutagenesis.....	49
2.2.2. Bacterial genetic techniques.....	51
2.2.2.1. Competent cell preparation and CaCl ₂	
transformation	51
2.2.2.2. Triparental mating (conjugation).....	52
2.2.2.3. Photosynthetic growth.....	53
2.2.2.4. Photosynthetic reversion	54
2.2.2.5. Chromosomal inactivation of uptake	
hydrogenase: Gene transfer agent (GTA) cross.....	54
2.2.3. Biochemical and biophysical techniques.....	56
2.2.3.1. Isolation of chromatophore vesicles and	
membrane sheets.....	56
2.2.3.2. Determination of amount of the protein by	
lowry assay.....	58
2.2.3.3. Tricine SDS-PAGE (16.5 % Schägger) gel.....	58
2.2.3.4. TMBZ staining of <i>c</i> -type cytochromes.....	59
2.2.3.5. Spectroscopic analysis.....	60
2.2.3.6. Light-activated absorption spectroscopy.....	60
2.2.4. Cloning strategies for cyt S- <i>c_y</i> R5 (cyt S- <i>c_y</i>).....	61
2.2.5. Cloning strategies for double mutant cyt S- <i>c_y</i> R35	
(cyt S- <i>c_y</i>).....	61
2.2.6. Cloning strategies for <i>hupSLC</i>	65
2.2.7. Construction of the $\Delta hupSL::\text{gen}$ insertion-deletion allele.....	65
2.2.8. Bioreactor setup for hydrogen production.....	68
2.2.8.1. Experimental setup for hydrogen production	68
2.2.8.2. Sampling and analyses.....	69
2.2.9. Dry weight analysis.....	69
2.2.10. Assay of hydrogenase activity.....	70

3. RESULTS AND DISCUSSION.....	71
3.1. Isolation of Ps ⁺ revertants of soluble cyt S- <i>c_y</i> : cyt S- <i>c_y</i> R5 and FJ2-R4 chromosomal reversion	71
3.2. Sequence analysis of the Ps ⁺ revertants	72
3.3. Cloning of the Ps ⁺ revertant cyt S- <i>c_y</i> R5.....	73
3.4. Construction of double mutant cyt S- <i>c_y</i> R35.....	73
3.4.1. Site directed mutagenesis for double mutation.....	73
3.4.2. Cloning of double mutant cyt S- <i>c_y</i> R35.....	77
3.5. Ps growth properties of Ps ⁺ revertants.....	78
3.6. Characterization of cyt S- <i>c_y</i> produced by various Ps ⁺ revertants.....	80
3.6.1. SDS-PAGE/ TMBZ heme staining of <i>c</i> type cytochromes.....	80
3.6.2. Difference spectra (Red _{Ascorbate} - Ox _{Ferricyanide}) of supernatant fraction of S- <i>c_y</i> and its Ps ⁺ revertants.....	80
3.7. Midpoint potential of soluble cyt S- <i>c_y</i> variants.....	83
3.8. Multiple turnover ET kinetics of cyt S- <i>c_y</i> variants.....	84
3.9. Comparison of single turnover ET kinetics mediated by different electron carrier cyst.....	85
3.10. Cloning of <i>hupSLC</i>	89
3.11. Construction of Δ <i>hupSL</i> ::gen deletion-insertion allele.....	91
3.12. Generation of the knock-out uptake hydrogenase mutant strains of <i>R. capsulatus</i>	95
3.13. Confirmation of the chromosomal mutation of uptake hydrogenase.....	99
3.13.1. PCR amplification of chromosomal Δ <i>hupSL</i> ::gen insertion-deletion allele.....	99
3.13.2. Hydrogenase activity of Hup ⁻ <i>R. capsulatus</i> strains.....	99
3.14. Hydrogen production of mutant <i>R. capsulatus</i> strains with modified electron carrier cytochromes.....	101
3.15. Hydrogen production of Quinol oxidase and cyt <i>cbb</i> ₃ oxidase deficient mutants of <i>R. capsulatus</i>	102

3.16. Hydrogen production of uptake hydrogenase deleted derivatives of <i>R. capsulatus</i> strains.....	105
3.17. Hydrogen production of <i>R. capsulatus</i> strains in glucose/ glutamate medium.....	108
4. CONCUSSION.....	112
REFERENCES.....	119
APPENDIX.....	137
A. BACTERIAL GROWTH MEDIUMS.....	137
B. SOLUTIONS AND ANTIBIOTICS.....	142
C. BUFFERS.....	145
D. CHEMICALS.....	148
E. RESTRICTION ENDONUCLEASES AND DNA MODIFYING ENZYMES.....	150
F. <i>hupSLC</i> OPERON AND PLASMID MAPS.....	151
G. OPTICAL DENSITY-DRY WEIGHT CALIBRATION CURVES.....	155
H. EQUIPMENTS USED IN THIS STUDY.....	158
I. CALCULATIONS FOR SUBSTRATE CONVERSION EFFICIENCY.....	160
VITA.....	161

LIST OF TABLES

TABLE

2.1. Bacterial strains, and plasmids.....	41
3.1. Photosynthetic growth properties of soluble S- <i>c_y</i> and its Ps ⁺ revertants in FJ2 and FJ2-R4 strains.	78
3.2. Difference spectra (Red _{Ascorbate-} Ox _{Ferricyanide}) of supernatant fraction of S- <i>c_y</i> and its Ps ⁺ revertants in FJ2 and FJ2-R4 strains	83
3.3. GTA cross table for Hup ⁻ strains.....	98
3.4. Hydrogen production of wild type and different mutants of <i>R. capsulatus</i> in malate/glutamate (15/ 2 mM) growth medium.....	107
3.5. Hydrogen production of wild type and different mutants of <i>R. capsulatus</i> in glucose/glutamate (10/2 mM) growth medium.....	109

LIST OF FIGURES

FIGURE

1.1. Electron transfer chains for diverse metabolic pathways of <i>R. capsulatus</i>	7
1.2. Diagram of the various RegB/RegA-controlled systems that have been identified in <i>R. capsulatus</i> and <i>R. sphaeroides</i>	8
1.3. Respiratory and photosynthetic electron transfer chain in a <i>Rhodobacter capsulatus</i>	11
1.4. Complex formation between the cyt <i>c</i> ₂ and RC (cyt <i>c</i> ₂ :RC) from <i>R. Sphaeroides</i>	13
1.5. Type of hemes and ligands of the Fe atom	18
1.6. The three dimensional structure of <i>R. capsulatus</i> cyt <i>c</i> ₂	19
1.7. Primary structure of cyt <i>c</i> _y	21
1.8. Construction of membrane attached cyt <i>c</i> ₂ (cyt MA- <i>c</i> ₂).....	22
1.9. Construction of soluble form of cyt <i>c</i> _y (cyt S- <i>c</i> _y).....	24
1.10. Electron follows in the <i>R. capsulatus</i> membrane during the hydrogen production.....	30
2.1. Cloning strategy for pYO26 and pYO105	63
2.2. Site directed mutagenesis of R3 (H53Y) and cloning of resulted mutant cyt S- <i>c</i> _y R35 to pRK415 plasmid.....	64
2.3. Amplification of the structural genes of uptake hydrogenase (<i>hupSLC</i>) and cloning strategy to pBSII and pRK415 plasmids.....	66
2.4. Construction of the Δ <i>hupSL</i> :: <i>gen</i> insertion deletion allele and cloning of it to pRK415 plasmid.....	67
2.5. Bioreactor setup for hydrogen production.....	68
3.1. DNA sequence of the R5 (AAG to AGG -Lys19Arg) mutation on cyt S- <i>c</i> _y	72

3.2. Agarose gel (1%) electrophoresis results for the cloning of cyt S- <i>c_y</i> R5 on pBSII and pRK415.....	74
3.3. Agarose gel electrophoresis result of PCR based site directed mutagenesis for double mutant cyt S- <i>c_y</i> R35.....	75
3.4. Sequencing analysis of pYO27 carrying the double mutant S- <i>c_y</i> R35.....	76
3.5. Agarose gel (1%) electrophoresis result for the cloning of double mutant cyt S- <i>c_y</i> R35.....	77
3.6. Photosynthetic phenotypes of strains carrying the soluble derivatives of cyt <i>c_y</i> in Fj2 and in FJ2-R4 under anaerobic condition with saturated light on MPYE medium.....	79
3.7. SDS-PAGE/ TMBZ heme staining of <i>c</i> type cytochromes from different <i>R. capsulatus</i> strains.	81
3.8. Difference spectra (Red _{Ascorbate} - Ox _{Ferricyanide}) of supernatant fraction of S- <i>c_y</i> and its Ps ⁺ revertants.....	82
3.9. Redox midpoint potentials of cyt S- <i>c_y</i> R35	84
3.10. Transient kinetics of the flash induced oxidation and reduction of the cyt <i>c</i> components were followed at 550-540 nm for cyt <i>c</i> (A.) and at 490-475 nm for carotenoid band shift (B). The traces obtained with no inhibitor and stigmatellin by train of eight flashes.	87
3.11. Flash-induced electron transfer kinetics of the pFJ631/FJ2 (cyt <i>c_y</i> ⁺), pHM14/ FJ2-R4 (cyt <i>c₂</i> ⁺), and pYO135/FJ2-R4 (cyt S- <i>c_y</i> R35) strains in the presence of stigmatellin.....	88
3.12. PCR amplification of 4.1 kb <i>hupSLC</i> operon by mutagenic primers.....	89
3.13. Control enzymatic digestion of pYO39 with different restriction enzymes.....	90
3.14. Cloning of 4.1 kb <i>KpnI</i> / <i>XbaI</i> fragment (<i>hupSLC</i> operon) of pYO39 to 10.6 kb pRK415 vector.....	91
3.15. Construction of Δ <i>hupSL</i> ::gen deletion-insertion allele.....	92
3.16. Sequencing analysis of pYO41carrying the Δ <i>hupSL</i> ::gen deletion-insertion cassette.....	93
3.17. Sequencing analysis of the 3' extension of the Δ <i>hupSL</i> ::gen cassette on pYO41 (reverse sequence of <i>hupC</i>).	94

3.18. Cloning of $\Delta hupSL::gen$ insertion-deletion allele located on 3 kb <i>KpnI/XbaI</i> fragment of pYO41 to 10.6 kb pRK415 vector.....	95
3.19. The plasmid pYO42 carrying $\Delta hupSL::gen$ insertion-deletion allele was transferred from <i>E. coli</i> HB101 strain to <i>R. capsulatus</i> Y ₂₆₂ strain (GTA over-producer strain) by three parental conjugation.....	96
3.20. The results of GTA cross for YO3 strain.....	97
3.21. The results of GTA cross for YO4 and YO4 strains.....	98
3.22. Chromosomal DNA's of related strains were isolated and used as a template for PCR amplification of <i>hupSLC</i> and $\Delta hupSL::gen$	100
3.23. Hydrogenase activity of the Hup ⁻ strains were assayed by the methylene blue reduction linked to H ₂ oxidation.....	101
3.24. Hydrogen production (A), phototrophic growth (B) and pH (C) of mutant <i>R. capsulatus</i> strains with different electron carrier cytochromes in malate/glutamate BP medium (15 mM / 2 mM)	103
3.25. Hydrogen production (A), phototrophic growth (B) and pH (C) of Qox ⁻ and cyt <i>cbb3</i> ⁻ mutants of <i>R. capsulatus</i> in malate/glutamate BP medium (15 mM / 2 mM).....	104
3.26. Hydrogen production (A), phototrophic growth (B) and pH (C) of Hup ⁻ mutants of wild type, Quinol oxidase and cyt <i>cbb3</i> oxidase deleted strains of <i>R. capsulatus</i> in malate/glutamate BP medium (15 mM / 2 mM).....	106
3.27. Hydrogen production (A), phototrophic growth (B and pH (C) of mutant <i>R. capsulatus</i> strains with different electron carrier cytochromes in glucose/glutamate medium BP medium (10 mM/ 2mM)	110
3.28. Hydrogen production (A), phototrophic growth (B) and pH (C) of Hup ⁻ mutants of wild type, Quinol oxidase and cyt <i>cbb3</i> oxidase deleted strains of <i>R. capsulatus</i> in 10 mM / 2 mM glucose/glutamate BP medium.....	111
4.1. Structural model for the cyt <i>c</i> domain of cyt <i>c_y</i> built by homology modeling using the cyt <i>c₅₅₂</i>	114
4.2. Respiratory and photosynthetic electron transport pathways in <i>R. sphaeroides</i> and model for redox sensing and signal transduction.....	117
F1. Restriction Map of <i>hupSLC</i> operon.....	152

F2. Map of the pRK415 Plasmid vector.....	153
F3. Map of the pBluescript Plasmid vector (Stratagene).....	154
G1. Calibration curve and the regression trend line for dry cell weight versus OD ₆₆₀ of MT1131.....	155
G2. Calibration curve and the regression trend line for dry cell weight versus OD ₆₆₀ of GK-32.....	155
G3. Calibration curve and the regression trend line for dry cell weight versus OD ₆₆₀ of KZ1.....	156
G4. Calibration curve and the regression trend line for dry cell weight versus OD ₆₆₀ of YO3.....	156
G5. Calibration curve and the regression trend line for dry cell weight versus OD ₆₆₀ of YO4.....	157
G6. Calibration curve and the regression trend line for dry cell weight versus OD ₆₆₀ of YO5.....	157

CHAPTER 1

INTRODUCTION

1.1. General properties of energy metabolisms

Living organisms depend on a steady supply of available energy for their life. The energy that is necessary for all living cells and organisms is harnessed from various sources extend from oxidizing reduced carbon sources during respiration (Res) to capturing light during photosynthesis (Ps) and channeled into biological work as a fundamental property of all living organisms. Organisms and living cells have membrane bound multi-enzyme systems to convert chemical and light energy to electrochemical gradients, motion, heat and chemical bound. Oxidative phosphorylation and photophosphorylation are the most important forms of energy transduction in the biosphere (Mitchell, 1961). In both processes, electrons flow through a chain of redox intermediates containing several membrane-associated, multisubunit pigment proteins linked to each other by lipid and water soluble electron carriers. In this Electron Transfer Chains (ETC) electrons flow spontaneously from serially ordered lower oxidation potential carrier complexes to higher oxidation potential carrier complexes and this downhill (exergonic) electron flow is coupled to the uphill (endergonic) transport of protons across a proton-impermeable membrane, yielding a transmembrane electrochemical potential. By flowing down their concentration gradient through specific protein channels such as the ATP synthase, protons provide the necessary free energy needed for ATP

synthesis from ADP and phosphate (Mitchell, 1961). The major physiological pathways of electron transport chains located in the mitochondria of eukaryotic cells, in the chloroplast of plants, and in cytoplasmic membrane of bacteria. In living cells, a large number of biological processes including macromolecular synthesis, nitrogen fixation, carbon fixation, cellular movement and solute transport use ATP as an energy source (Lehninger et al., 1998). In metabolically diverse organisms like photosynthetic bacterium *Rhodobacter* species, energy-generating and energy-utilizing biological processes are under the control of regulatory systems for adaptation to different environmental condition, and for conservation of energy (Elsen et al., 2004).

1.1.1. Electron transfer chains in energy metabolism

To survive in different environmental condition with different nutrient and energy source, living cells developed different electron transfer chain for energy conversion. The mitochondria of higher organisms and a variety of bacteria contain enzymes that catalyze respiration by using molecular oxygen as the terminal electron acceptor in respiratory growth. These respiratory oligomeric, cytochrome-containing multi-pigmented enzyme complexes are embedded into the bacterial plasma membrane or inner mitochondrial membrane. The energy from oxidation of hydrogen-containing substrates is converted into a transmembrane proton electrochemical gradient, and then used by these respiratory enzymes for a variety of energy requiring reactions such as ATP production, transport of molecules, and cell motility (chemiosmotic theory of Mitchell) (Mitchell, 1966). In mitochondria of most species, NADH-1 type dehydrogenases transfer electrons from NADH to lipid soluble quinone, yielding quinol (or hydroquinone). The reducing equivalents thus accumulated in the quinol pool are transferred to molecular oxygen by the sequential actions of two enzyme complexes, the cytochrome *bc*₁ complex and the cyt *c* oxidase complex. The cyt *bc*₁ complex oxidizes quinol and reduces a cyt *c*, and cyt *c* oxidase complex oxidizes a cyt *c* by reducing O₂ to water to complete the

electron transfer processes. In addition to the cyt *bc*₁-dependent respiratory pathway, most microorganisms including photosynthetic bacteria, possess alternative quinol oxidases, which transfer electrons directly from quinol to oxygen. On the other hand, some bacteria like *Escherichia coli* have a simpler arrangement of respiratory cyt complexes without a cyt *bc*₁ complex. These bacteria oxidize quinol directly using molecular oxygen by either one of two-quinol oxidases (Trumper and Gennis, 1994).

In anoxygenic phototropic bacteria such as *Rhodobacter capsulatus* and *Rhodobacter sphaeroides* the cyt *bc*₁ complex also participates in light-driven cyclic electron transfer during photosynthesis (Amesz and Knaff, 1990; Kiley and Kaplan, 1988). These bacteria require electron donors such as molecular hydrogen (H₂), small reduced organic molecules (lactate, acetate, and malate), sulfide or other reduced sulfur compounds, and perform photosynthesis in the absence of air and without producing oxygen. Cyanobacteria, Algae and Plants are oxygenic phototrophs and contain two photosystems: PSI, homologous to the RC of green bacteria, and PSII, homologous to that of purple bacteria. In noncyclic photophosphorylation (Z scheme photophosphorylation) formation of the electrochemical gradient is coupled to a one way electron flow from H₂O to NADP⁺. In this chain, electrons from the cyt *b*₆*f* complex, which is the cyanobacterial and chloroplast version of the cyt *bc*₁ complex, are transferred to light oxidized PSI complexes by cytochrome the *c*₆ (cyt *c*₆) or plastocyanin (PC) (Meyer and Donohue, 1995).

1.2. Energy metabolism of *Rhodobacter capsulatus*

1.2.1. *R. capsulatus* as a Model for Energy Transduction

Anoxygenic phototropic bacteria are generally divided into the purple sulfur, purple nonsulfur, green sulfur and green nonsulfur bacteria according to

phenotypes (Tindall and Grant, 1986). The purple bacteria fall into the group of proteobacteria on the basis of the 16S rRNA analyses. Proteobacteria have 4 major subdivisions; α , β , γ , and δ subdivision and only α , β , and γ subdivisions contain photosynthetic organisms (Stackebrandt, 1988). The species of genera *Rhodospirillum*, *Rhodopila*, *Rhodopseudomonas*, *Rhodomicrobium* and *Rhodobacter* are included in α division (Prince, 1990).

R. capsulatus is a gram-negative, purple nonsulfur and facultative phototroph bacterium, and is able to perform different growth modes such as, aerobic respiration, anaerobic respiration, and photosynthesis for its growth. It is a member of the *Rhodospirillaceae* family and it belongs to the *Rhodobacter* genera. It has a rod-like cell shape with a diameter of 0.5-1.2 μm and has a 65.5-66.8 % G+C content (Imhoff, 1995). *R. capsulatus*, like most of the anoxygenic photosynthetic purple bacteria, has intracytoplasmic membranes (ICM) which are also described as chromatophores. Several external factors like oxygen tension and light intensity affect the formation of ICM (Drews and Golecki, 1995). The membrane-bound energy transducing complexes including the photosynthetic apparatus are the major components of the ICM, and the interior of the ICM structure is equivalent to periplasmic or the extra-cytoplasmic space.

R. capsulatus possesses energy transducing complexes homologous to those found in mitochondria and chloroplast. Remarkable similarities between ETC complexes in these bacteria and in higher organism are revealed by structural studies and nucleotide sequence data (Youvan and Bylina, 1989). A wide variety of growth modes, for example alternate respiratory branches terminating with quinol oxidases (Q_{ox}), allow these bacteria to survive when a lethal mutation occurs in the independent Ps and Res complexes (Daldal, 1987). The well-developed genetics of *Rhodobacter* species provide excellent materials for experiments (Kaplan and Donohue, 1992). In addition, easy preparation of chromatophore membrane vesicles, containing all of the components of energy transduction pathways in large quantities, provide good experimental materials for biochemical and biophysical

analysis, including overproduction and facile purification of membrane protein complexes and their associated components (Tiede and Dutton, 1993). Furthermore complete sequence of *Rhodobacter* genome is helpful in identifying new components of energy transduction systems. Because of these advantages, *Rhodobacter* species are readily used for genetic and biochemical analyses, and provide a powerful system for detailed analyses of prokaryotic and eukaryotic energy transduction (Myllykallio et al., 1998).

In this work *R. capsulatus* was used to obtain and analyze a new hybrid form of a *c*-type electron carrier cytochrome i.e. soluble form of cyt *c_y* and to analyze the interaction between ETC and hydrogen production metabolism.

1.2.2. Metabolic Diversity of *R. capsulatus* and RegB/RegA global regulatory system

R. capsulatus has developed various growth modes of energy metabolism to respond to different environmental conditions, in particular the presence or absence of light, electron donors and acceptors, by branched respiratory electron transport pathways (Imhoff, 1995). *Rhodobacter* uses photoheterotrophy and photoautotrophy metabolic modes in the presence of solar energy and absence of oxygen. Bacteria obtain their energy from sunlight and their carbon atoms from reduced compounds in photoheterotrophy. In photoautotrophy, bacteria obtain their energy from sunlight and they use CO₂ as their sole source of carbon. There are two aerobic growth modes, chemoheterotrophy and chemoautotrophy. Organic compounds are oxidized for energy and metabolized for carbon assimilation in chemoheterotrophy. In chemoautotrophy, cellular carbon comes from CO₂ and energy obtained from molecular hydrogen. Fermentative pathway and anaerobic respiration during which compounds other than oxygen are used as terminal electron acceptors are included in anaerobic growth modes (Youvan and Bylina, 1989). In *R. capsulatus* there are three main chains; cyclic photosynthetic chain,

aerobic respiratory chain and anaerobic respiratory chains terminating with trimethyl-amine-*N*-oxide (TMAO) reductase, dimethyl sulfoxide (DMSO) reductase, nitrous oxide (N_2O), nitric oxide (NO) or nitrate oxide (NO_3^-) reductases. Besides, *R. capsulatus* use alternate aerobic respiratory ET pathway, which directly branches out at the membrane quinone (Q) pool, and uses a quinol oxidase (Qox) as a terminal electron acceptor complex (Baccarini et al., 1973) (**Figure 1.1**).

To accommodate the divergent growth modes, *R. capsulatus* has a number of inter-dependent regulatory mechanisms. RegB/RegA global regulatory system, which is composed of the RegB histidine kinase and the RegA response regulator, controls such fundamental and diverse processes affecting the oxidation-reduction state of the ubiquinone pool (photosynthesis, respiration and hydrogen utilization) and processes functioning as electron sinks (CO_2 fixation, N_2 assimilation and formaldehyde dehydration) (**Figure 1.2**). Sensor kinase RegB of *R. capsulatus* is a 460-amino-acid (50.1- kDa) protein that is composed of two domains; a N-terminal transmembrane domain and a C-terminal cytoplasmic “transmitter” domain that function as histidine protein kinases. The RegB system senses the oxidation/reduction state of the cell by monitoring a signal associated with electron transport (Elsen et al., 2004). One of the redox signals that have been shown to regulate RegB is the redox state of the aerobic respiratory chain. In aerobic respiratory chain, cytochrome cbb_3 oxidase generates an “inhibitory” signal that represses the RegB/RegA two-component system. This signal may either inhibit the kinase activity or stimulate the phosphatase activity of RegB, which, in turn controls the amount of phosphorylated RegA (Oh et al., 2004). Response regulator RegA of *R. capsulatus* is a 184-amino-acid 20.4-kDa protein containing several highly conserved residues that are typically found in two-component response regulators. Conserved residues include a phosphate-accepting aspartate and an “acid pocket” containing two highly conserved aspartate residues in the N-terminal receiver domain. The N-terminal receiver domain is linked by a four-proline hinge to a 50 amino acid C-terminal output domain that contains a three-helix bundle

HTH (helix-turn-helix) DNA binding motif (Laguri et al., 2003). The response regulator RegA activates or represses gene expression through direct interaction with target gene promoters, where it often works in concert with other regulators that can be either global or specific (Elsen et al., 2004).

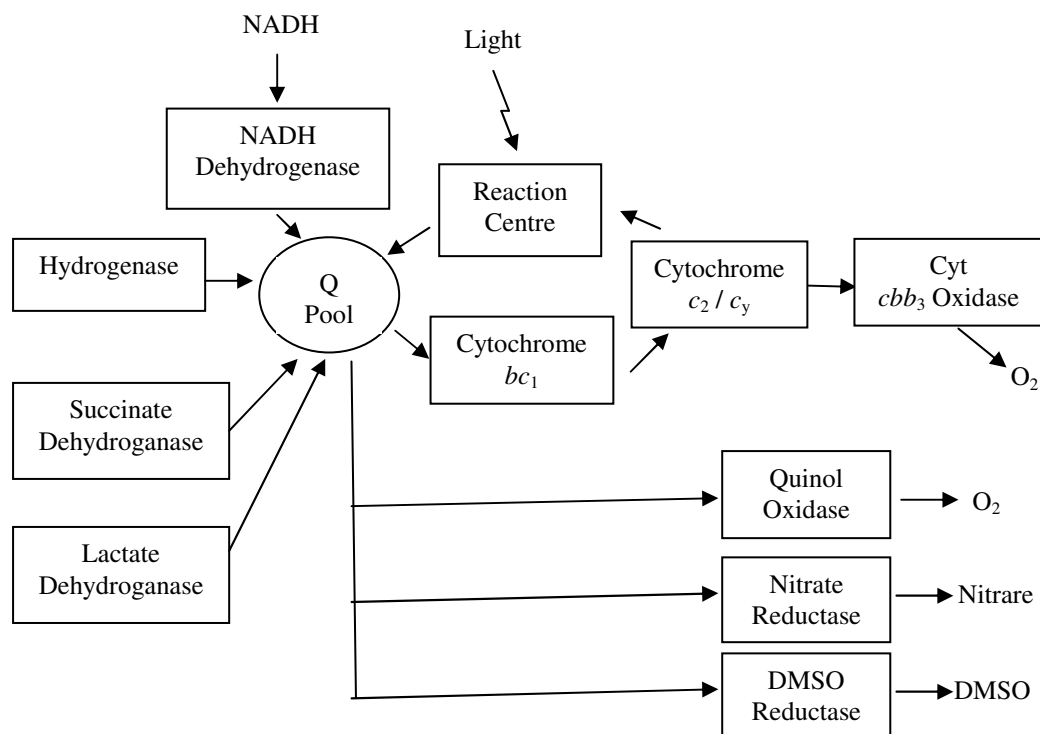


Figure 1.1. Electron transfer chains for diverse metabolic pathways of *R. capsulatus*. Alternative pathways branch from the ubiquinone pool and are independent of both photosynthesis and cyt *cbb*₃ dependent aerobic respiration. Arrows indicate the direction of linear electron flow.

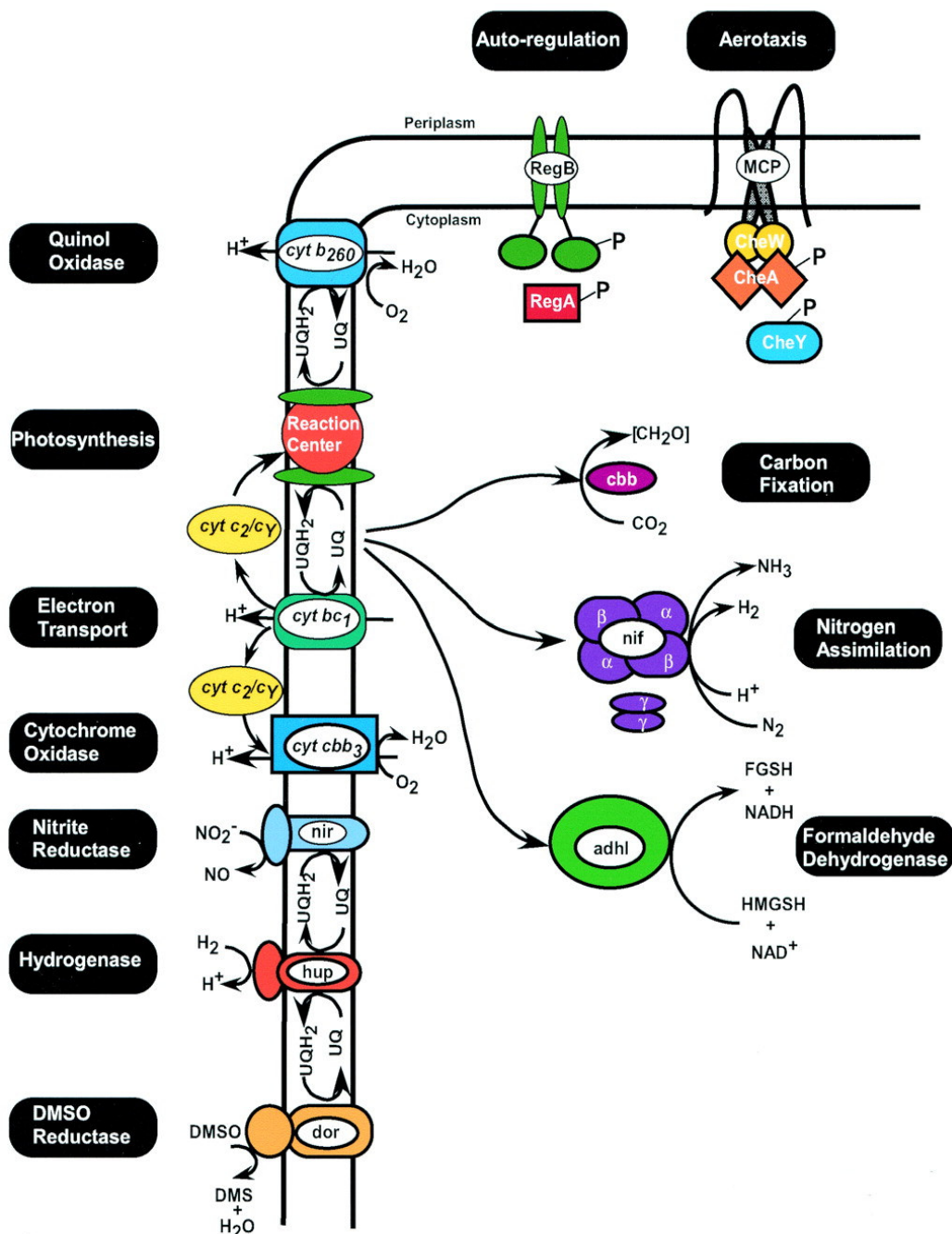


Figure 1.2. Diagram of the various RegB/RegA-controlled systems that have been identified in *R. capsulatus* and *R. sphaeroides*. UQH₂, reduced ubiquinol; UQ, oxidized ubiquinone; FGSH, *S*-formylglutathione; HMGSH, hydroxymethylglutathione; DMS, dimethyl sulfate (Elsen et al., 2004).

1.2.3. Respiratory and Photosynthetic Growth of *R. capsulatus*

When light is unavailable, *Rhodobacter* species use alternate energy transduction pathways to ascertain their growth both in the presence or absence of molecular oxygen (O_2). Under aerobic growth conditions electrons are transferred via respiratory ETC from respiratory dehydrogenases to the Q pool, the cyt bc_1 complex, and again using soluble or membrane bound electron carriers to the terminal oxidases that ultimately convert O_2 to H_2O (Koch et al., 1998) (Figure 1.3). The bacterial respiratory system is usually branched and comprises several terminal oxidases, allowing bacteria to grow at different environment. The respiratory electron transfer pathways of *R. capsulatus* are branched after the quinone pool and contain two different terminal oxidases, cyt c oxidase and quinol oxidase (Zannoni et al., 1976). The cyt c oxidase branch is similar to the mitochondrial electron transfer chain in that it depends on the cyt bc_1 complex, and a c -type cyt acting as an electron carrier. The quinol oxidase branch is independent from the cyt bc_1 complex and electrons are transferred directly from the quinone pool to reduce O_2 to H_2O . *R. capsulatus* contains only one form of cytochrome (cyt) c oxidase, which has been identified as a cbb_3 -type cyt c oxidase. However *R. sphaeroides* and *P. denitrificans* contain an additional mitochondrial-like aa_3 type cyt c oxidase. The cbb_3 -type cytochrome c oxidases belong to the heme–copper oxidase superfamily, and encoded by the *ccNOQP* operon. The *ccN*, *ccO*, and *ccP* gene products are essential for both the activity and the assembly of the functional cbb_3 oxidase. The *ccN* product is the catalytic subunit and contains the binuclear center consisting of the B-type high-spin heme and CuB. *CcoO* and *CcoP* are membrane-bound mono- and diheme cytochromes c , respectively, and transfer the electrons from cyt c_2 to *CcoN* (Mouncey and Kaplan 1998). The *CcoQ* of *R. capsulatus* is a small membrane-bound polypeptide consisting of 58 amino acids and has no apparent effect on the assembly or activity of the cyt cbb_3 oxidase (Zufferey et al., 1996). However it has been demonstrated that the *CcoQ* protein is involved in conveying a signal derived from reductant flow through the cyt cbb_3 terminal oxidase to the RegB/RegA regulatory pathway (Oh and Kaplan, 1999).

In *R. capsulatus* under the light, anoxygenic photosynthesis is driven by the cyclic electron transfer process between the RC and the cyt *bc*₁ complex. The electrons are transferred between these complexes via the lipid soluble quinone (Q) pool and the electron carriers cyt *c*₂ (soluble) or cyt *c*_y (membrane bound) (Jenney and Daldal, 1993). The photosynthetic reaction centre consists of three integral membrane proteins called H (heavy), M (medium) and L (light), and a number of pigment molecules associated with the central core of RC which is formed by L and M subunits (Debus et al., 1985). Photosynthetic pigments are composed of one carotenoid molecule, two bacteriochlorophylls, one ubiquinone as primary electron acceptor Q_A, one non-heme iron, and another ubiquinone as secondary electron acceptor Q_B. The pigments form two branches, one active (A) and more closely associated with L subunit, and another inactive (B) branches. The two branches start with the bacteriochlorophylls D_a and D_b constituting the primary electron donor (special pair) (Hoff, 1988). During photosynthesis, light induced oxidation of the RC bacteriochlorophyll dimer (P⁺) reduces a Q molecule to hydroquinone (QH₂), which is subsequently oxidized by the cyt *bc*₁ complex (Amesz and Knaff., 1988). The Ubiquinone cyt *c* oxidoreductase (cyt *bc*₁) complex consists of three subunits; a di-heme cyt *b*, cyt *c*₁, and an iron-sulfur protein known as the Rieske protein. The cyt *bc*₁ complex is similar to the cyt *b*₆*f* complex of chloroplast, but the cyt *b* subunit of the cyt *bc*₁ complex is split into two subunits(cyt *b*₆ and subunit IV)in the cyt *b*₆*f* complex (Saribas et al., 1999). Moreover another difference is that the axial ligands of covalently attached *c*-type heme in cyt *c*₁ are histidine and methionine but two nitrogenous ligands in cyt *f* subunit of the cyt *b*₆*f* complex (Saribas et al., 1999). The cyt *b* subunit of the cyt *bc*₁ complex is a transmembrane protein with two heme groups which noncovalently bind to apoprotein. These hemes are the b_L (low redox potential) near the periplasm and b_H (high redox potential) more central in the membrane, and are spectrally distinguishable. The cyt *b* subunit also forms two active sites; Q_o located on the periplasmic side of the membrane for ubihydroquinone (QH₂) oxidation and Q_i located on the cytoplasmic side of the membrane for ubiquinone (Q) reduction. The covalently-attached heme of cyt *c*₁ and 2Fe-2S cluster of Rieske iron-sulfur

protein are near the electropositive surface of the membrane (Darrouzet et al., 1999; Darrouzet et al., 2000). The cyt *bc*₁ complex directs a quinone cycle, in which the endergonic transport of protons across the membrane is coupled to the exergonic transport of electrons. In these electron transfer reaction one electron of the oxidized QH₂ is conveyed to a high-potential chain constituted by the [2Fe2S] cluster and *c*₁ heme eventually reduces cyt *c*₂ and cyt *c*_y, while the other electron is transferred to a low-potential chain composed of the *b*_L and *b*_H hemes eventually reduces a quinone at the Q_i site

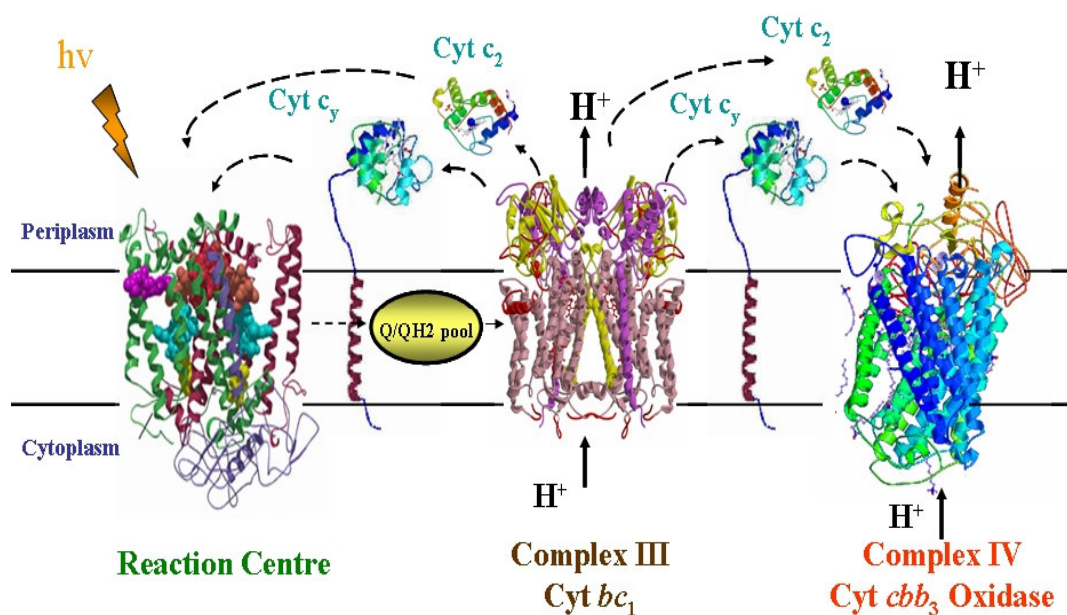


Figure 1.3. *R. capsulatus* has two different electron carrier cyts; soluble cyt *c*₂ and membrane-attached cyt *c*_y that operate between the reaction center (RC) and the cyt *bc*₁ complex during the cyclic photosynthesis, and between the cyt *bc*₁ complex and cyt *cbb*₃ oxidase during the respiration (Jenney and Daldal, 1993) (3D pictures of proteins were adopted form Protein Data Bank).

(Gennis et al., 1993). Reduced soluble or membrane bound electron carrier proteins cyt c_2 and cyt c_y transfer electrons back to oxidized reaction centre to convert P^+ to its ground state so that it can be available for the subsequent reactions (**Figure 1.3**). The end result of this cyclic electron transfer chain reaction is the conversion of light energy into a transmembrane proton electrochemical gradient used for ATP production.

1.2.4. Inter-protein electron transfer during the photosynthetic growth.

The cyclic photosynthetic electron transfer in *R. capsulatus* involves the electron transfer from electron carrier cyts c_2 and cyt c_y to photo-oxidized bacterial reaction center (RC) (Jenney and Daldal, 1993). For efficient inter-protein electron transfer form electron carrier cyts to RC, these proteins must interact together to form temporarily encounter complex. The efficient operation of this molecular machinery requires specific binding of the electron carriers and orientation of the cofactors into a position favorable for electron transfer. By this way, the redox cofactors are close enough for the electron transfer reaction to proceed and fast enough so that rapid association and dissociation rates do not limit the cyclic electron flow (Gong et al. 2003).

So far inter-protein electron transfer between the bacterial RC and its physiological electron donor, cyt c_2 from *R. sphaeroides* was studied extensively by using the chemical and genetic modification (site directed mutagenesis) of amino acids and by using the determined X-ray crystal structure of the cyt c_2 -RC complex (Axelrod et al. 2002). For the general mechanism of the binding process, a two-step mechanism has been proposed (Camacho and Vajda, 2001). The first step is diffusional association to form an encounter complex. Following the first step, the second step is rearrangement to form the fully bound complex. Short-range interactions such as van der Waals interactions are important at this stage. The X-ray crystal structure of the complex between the cyt c_2 and RC shows the

cyt *c*₂ docked with the heme edge contacting Tyr L162 directly above the bacteriochlorophyll dimer providing close contact for a strong tunneling pathway for electron transfer (Axelrod et al. 2002) (**Figure 1.4**). The binding interface between the two proteins can be divided into two regions: a short-range interaction domain and a long-range interaction domain. The short-range domain includes residues immediately surrounding the tunneling contact region around the heme and Tyr L162 that display close intermolecular contacts optimized for electron transfer.

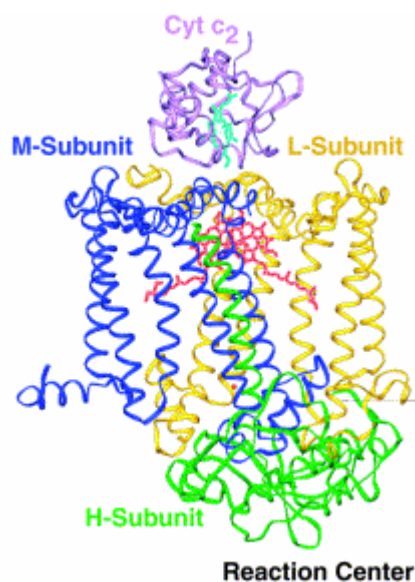
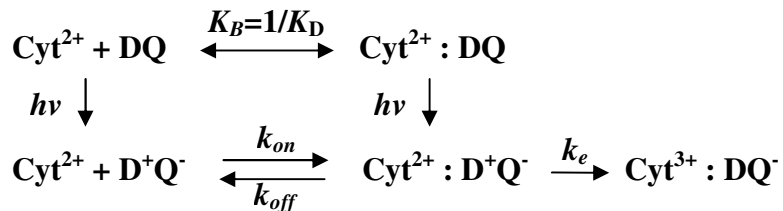


Figure 1.4. The cyt *c*₂:RC complex from *R. sphaeroides* showing the location of the bound cyt *c*₂ (lavender), the heme prosthetic group (turquoise), the RC L subunit (yellow), the RC M subunit (blue), the RC H subunit (green), the RC primary donor (red), and non-heme Fe atom (red) (Carson, M., 1997; Axelrod et al., 2002).

These include a small number of hydrophobic interactions, hydrogen bonds, and a pi-cation interaction. This domain contributes to the strength and specificity of cyt *c*₂ binding. The long-range interaction domain consists of solvated complementary charged residues; positively charged residues from the cyt and negatively charged residues from the RC that provide long range electrostatic interactions that

contribute to the dynamics of the docking process and can steer the two proteins into position for rapid association. Changes to charge-surface groups near the binding interface by using chemical modification (Long et al., 1989) and site-directed mutagenesis (Tetreault et al., 2002) were shown to change the association rate. Some mutational studies show that the most important interactions are between Asp M184 and Lys C103, and between Asp L261 and Lys C99. Moreover, X-ray crystal structure shows that there is ample space to solvate the charges. The solvation has important functional implications: it can enhance the rates of association of reduced cyt c_2 and dissociation of oxidized cyt c_2 , ensuring that cyt c_2 turnover is not the bottleneck in the photosynthetic electron-transfer cycle (Axelrod et al. 2002).

The binding and electron transfer rates of isolated cyt c_2 and the RC have been extensively studied using laser pulse kinetic measurements (Moser et al., 1988; Tetreault et al., 2001). The reduction of oxidized donor D $^+$ by reduced cyt c_2 shows two kinetic phases following a single laser flash: a fast first-order phase (independent of cyt c_2 concentration) due to electron transfer from bound cyt c_2 to the photo-oxidized donor of the RC and a slower second-order phase (dependent on cyt c_2 concentration) due to the binding and subsequent electron transfer of free cyt c_2 . The observed biphasic kinetics can be explained by the following scheme (Tetreault et al., 2001).



K_D is the dissociation constant, k_{on} is the association rate constant, k_{off} is the dissociation rate constant, and k_e is the electron transfer rate constant in the bound

state. The equilibrium between bound and free cyt c_2 is achieved in the dark. Following a laser flash, the re-reduction of D^+ by cyt c_2^{2+} is biphasic. RCs with a bound cyt c_2 undergo rapid electron transfer with a rate constant k_e ($\approx 10^6 \text{ s}^{-1}$) (Overfield et al., 1979). RCs without a bound cyt c_2 undergo slower diffusion-limited electron transfer with an observed second-order rate constant k_2 ($\sim 10^9 \text{ s}^{-1} \text{ M}^{-1}$). Since $k_e \gg k_{\text{off}}$, the observed second-order rate constant is the association rate ($k_2 \sim k_{\text{on}}$). The fraction of RCs with a bound cyt c_2 can be determined by the ratio of the fast and slow phases. The dissociation constant K_D can be determined from a plot of the fraction of RCs with bound cyt c_2 versus the free cyt c_2 concentration (Gong et al. 2003). The importance of electrostatic interactions for binding and electron transfers between cyt c_2 and the RC has been established by the ionic strength dependence of k_2 (Prince et al., 1974).

In addition to the kinetic studies of soluble cyt c_2 with RC in *R. sphaeroides*, the microsecond time range electron transfer kinetics of membrane bound cyt c_y of *R. capsulatus* were studied by light-activated time-resolved absorption spectroscopy using a mutant strain lacking cyt c_2 (Myllykallio et al., 1998). In intact cells and in isolated chromatophores of this mutant, only 30% of the RCs had their photooxidized primary donor rapidly rereduced by cyt c_y . About half of these 30% were reduced with a half-time of $\sim 5 \mu\text{s}$ and the other half with a half-time of $\sim 40 \mu\text{s}$. The two kinetic phases of P^+ (D^+) reduction by cyt c_y , with half-times of approximately 5 and $40 \mu\text{s}$ show striking differences. The fast phase (half-time of $\sim 5 \mu\text{s}$) is attributed to electron donation within a “proximal” complex between the RC and cyt c_y since its rate and amplitude not depend on the viscosity of the medium. Moreover, this fast phase was also observed in the absence of the cyt bc_1 complex with smaller amplitude. This indicates that the formation of a “proximal” RC-cyt c_y complex does not appear to depend on the presence of the cyt bc_1 complex. However, the second phase (half-time of $\sim 40 \mu\text{s}$) was slowed both in the absence of the cyt bc_1 complex and upon addition of glycerol (in viscose environment), indicating a molecular movement as a rate-limiting process. This is interpreted as cyt c_y moving from cyt bc_1 complex site

into the “proximal” position before fast electron donation to P^+ . Furthermore, using two flashes separated by a variable time interval, it was shown that the fast electron donating complex was reformed in about 60 μ s, a time span probably reflecting electron transfer from cyt c_1 to cyt c_y . In conclusion, *R. capsulatus* electron transfer from the cyt bc_1 complex to the RC via the membrane-attached cyt c_y is a fast process which functions efficiently during multiple turnovers of the cyclic electron-transport chain to sustain adequate Ps growth even in the absence of the soluble electron carrier cyt c_2 (Myllykallio et al., 1998).

1.3. Cytochromes as electron carriers

Electron carrier cytochromes functioning in a large number of different redox processes may have one or more heme groups, and are classified according to their heme iron coordination, sequence similarities and heme type (NC-IUB, 1989; Kiel, 1995). The names of cytochromes generally tend to reflect the kinds of hemes they contain. For example, cyt a contains a a type heme, cyt c contains a c type heme, and cyt b contains a b type heme (**Figure 1.5**). An example of a heme-containing protein that has heme a is the cyt c oxidase. *Heme a* differs from heme b in that a methyl side chain is oxidized into a formyl group, and one of the vinyl side chains has been replaced by an isoprenoid chain (**Figure 1.5 A**). Like heme b , heme a is not covalently bound to the apoprotein in which it is found. Cyt b has one or two heme b groups noncovalently bound to the protein (**Figure 1.5 B**). The fifth heme iron ligand is always provided by a histidine residue (**Figure 1.5 D**). Cyt c has also one or several heme c groups (**Figure 1.5C**), bound to the protein by two, thioether bonds involving sulphhydryl groups of cysteine residues and the fifth heme iron ligand is always provided by a histidine residue (Pettigrew and Moore, 1987; Moore and Pettigrew, 1990).

The soluble cyt c of mitochondria, soluble cyt c_2 and membrane attached cyt c_y of bacteria are the member of class I cyt c , and contain low-spin hemes

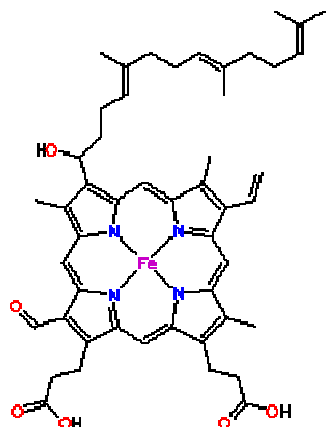
(Hexa-coordinated Fe atom of heme) (Ambler, 1991). These cyts includes the highly conserved heme attachment site **Cys-X-Y-Cys-His** towards the N-terminus, and their sixth ligand is provided by a methionine residue towards the C-terminus (**Figure 1.5 D**). The proteins consist of several helices and three of them are most conserved and form a basket around the heme group with one heme edge exposed to the solvent. The electron carrier cyts *c* in respiratory and photosynthetic pathways are among the best characterized small monomeric proteins in respect to their structure, folding, and stability (Sauder et al., 1996).

1.3.1. Electron carrier cytochromes of *R. capsulatus*

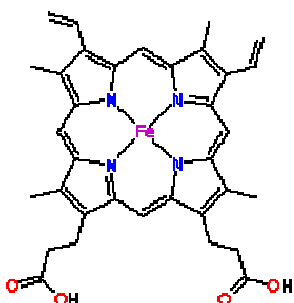
1.3.1.1. Cyt *c*₂ of *R. capsulatus*

The soluble cyt *c*₂ of *R. capsulatus* is encoded by the *cycA* gene, and has an amino (N)-terminal signal sequence of 21 amino acid residues long, which is processed during its translocation to its operation site, the periplasm. The functional mature cyt *c*₂ is a 116 amino acid protein (13 kDa) and contains covalently bound heme *c* as a prosthetic group attached to a conserved Cys-X-Y-Cys-His sequence (**Figure 1.6**). It is functionally analogous to the plastocyanin of chloroplast and has a thermodynamically favorable redox midpoint potential (E_{m7}) of +350mV, which is the value for electron transfer from the cyt *bc*₁ complex to the RC during Ps and from cyt *bc*₁ complex to the cyt *c* oxidase during Res (Moore and Pettigrew, 1990). Under some conditions it is also known that cyt *c*₂ is able to donate electrons to other periplasmic enzymes such as the nitrous oxide reductase (Ferguson et al., 1987). The lysine residues located around the water exposed edge of heme group is used for reversible binding to its physiological electron donor and acceptor complexes by charge complementary (Cramer and Knaff, 1990).

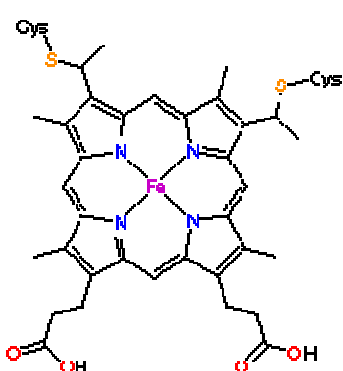
A)



B)



C)



D)

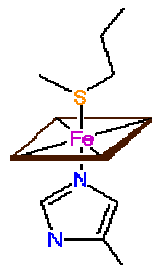


Figure 1.5. Heme is a metal-containing cofactor that consists of an iron atom contained in the center of a large heterocyclic organic ring called a porphyrin. **A)** *a* type heme noncovalently bound to protein. **B)** Like heme *a*, *b* type heme also noncovalently bound to protein. **C)** *c* type heme covalently bound to protein by two thioether bonds involving sulphhydryl groups of cysteine residues and two vinyl groups of protoporphyrin IX. **D)** Low-spin heme (Hexacoordinated Fe atom of heme), 5th and 6th ligand of Fe atom is provided by His and Met residues respectively.

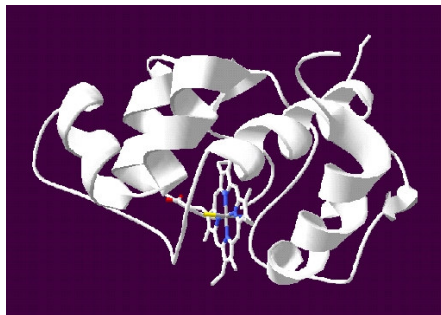


Figure 1.6. The three dimensional structure of *R. capsulatus* cyt *c*₂ (PDB ID: 1C2R). Three most conserved ‘core’ helices form a ‘basket’ around the heme group with one heme edge exposed to the solvent (Benning et al., 1991).

1.3.1.2. Cyt *c*_y of *R. capsulatus*

The membrane-bound cyt *c*_y of *R. capsulatus* is encoded by *cycY* gene and it is 199 amino acid protein (calculated molecular mass of 20.6 kDa) (Jenney and Daldal, 1993). Its first 28 residues form a prokaryotic signal sequence-like motif, which is not processed during its translocation into the periplasm, and connected to the cyt *c* domain by a 70 amino acid long flexible alanine rich linker region. Cyt *c*_y is anchored to the membrane by a putative membrane-spanning helix, between residues 7 and 28 overlapping with its signal sequence, leaving a short N-terminal extension in the cytoplasm (Myllykallio et al., 1997). The carboxyl terminal 99 residues of cyt *c*_y (cyt *c* domain) has the Cys-X-Y-Cys-His heme-binding motif and its sixth ligand of the heme iron is provided by a distal methionine residue towards the C-terminus. The cyt *c* domain of cyt *c*_y is translocated to the periplasm, where it interacts with its counterparts during electron transfer and homologous to cyt *c* of plant mitochondria (**Figure 1.7**). Characterization of the purified cyt *c*_y indicated that its spectral and thermodynamic properties are similar to other *c*-type cytochromes. The redox midpoint potential of cyt *c*_y (E_{m7}) is around +365 and its optical spectra is very similar to those of the soluble cyt *c*₂ (Zannoni and Daldal, 1993; Zannoni, 1995).

The *R. capsulatus* mutant, lacking cyts *c*₂ and *c*_y, can not grow photosynthetically, but can be complemented to Ps⁺ by either cyt *c*₂ or cyt *c*_y in the absence of the other. This indicated that there are two distinct ETC operate during Ps in *R. capsulatus* one via the soluble cyt *c*₂ and the other via the membrane-associated cyt *c*_y. In addition, flash induced electron transfer kinetics have shown that electron transfer from the *bc*₁ complex to the RC in *R. capsulatus* is accomplished by two pathways that exhibit different kinetics for RC reduction and cyt *c* oxidation (Jenney et al., 1994) and cyt *c*_y mediates fast electron transfer from the cyt *bc*₁ complex to the RC during multiple turnovers of the cyclic electron flow (Myllykallio et al., 1998). Moreover, the presence of respiratory electron transport in chemoheterotrophic growth of double mutant (cyt *c*₂⁻, Q_{ox}⁻) indicates the presence of additional electron carriers capable of replacing cyt *c*₂ in the respiration. Sensitivity patterns of this mutant (cyt *c*₂⁻, Q_{ox}⁻) to inhibitors, respiratory rates in the presence of specific inhibitors and oxidation-reduction kinetics of *c*-type cyts demonstrated that cyt *c*_y transfers electrons from cyt *bc*₁ complex to the cyt *c* oxidase during respiration as in the case of cyt *c*₂ (Hochkoeppler et al., 1995).

Several bacterial species including *R. sphaeroides*, *Bacillus subtilis* and *Paracoccus denitrificans*, have structural homologies of cyt *c*_y. The structural gene of *R. sphaeroides* cyt *c*_y (*cycY*^{*Rs*}) is highly homologous to *R. capsulatus* cyt *c*_y gene (*cycY*^{*Rc*}) but major differences are seen in the linker regions connecting the membrane anchor to the cyt *c* subdomain. For example, the linker portion of cyt *c*_y of *R. capsulatus* is considerably longer than that of *R. sphaeroides* because of the 15- and 7-residue insertions located between positions 45–60 and 84–91 of cyt *c*_y *R. capsulatus*, respectively (Myllykallio et al., 1999). The cyt *c*_y of *R. sphaeroides* is functionally unable to participate in photosynthetic electron transfer, but it is active in respiratory electron transfer in that it is able to carry electrons efficiently from the cyt *bc*₁ complex to either the cyt *cbb*₃ or the cyt *aa*₃ terminal oxidase (Daldal et al., 2001). Chimeric constructs between these cyts have shown that the photosynthetic incapability of cyt *c*_y *R. sphaeroides* is caused, at least in part, by its

redox active subdomain, which carries the covalently bound heme *c*. Therefore, this domain may interact differently with distinct redox partners, like the photochemical reaction center and the cyt *c* oxidase, and allows the bacteria to funnel electrons efficiently to various destinations under different growth conditions (Myllykallio et al., 1999).

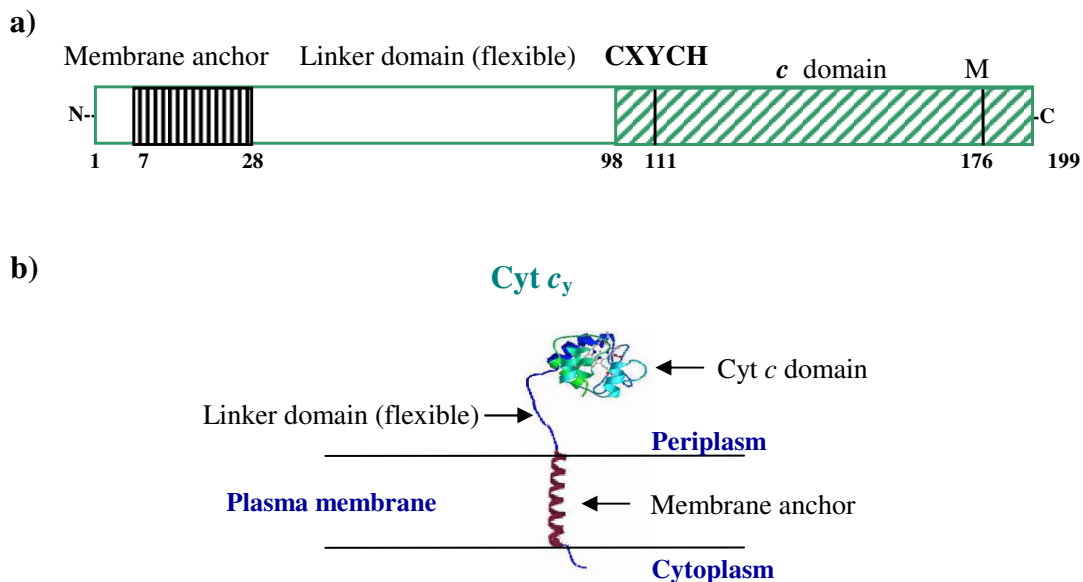


Figure 1.7. a) Primary structure of cyt *c_y* (Jenney and Daldal, 1993). It consists of three domains, signal sequence like membrane anchor domain (1-28 residues), flexible linker domain rich in alanine, and the carboxy-terminal heme binding cyt *c* domain (98 residues). Cyt *c* domain contains CXYCH heme binding site and methionine as a sixth ligand of heme iron. b) Hypothetical 3 D structure of cyt *c_y* in plasma membrane.

1.3.2. Hybrid versions of cyt *c₂* and cyt *c_y*

1.3.2.1. Membrane- attached form of cyt *c₂* (cyt MA-*c₂*)

The membrane-attached form of cyt *c₂* (Cyt MA-*c₂*) was constructed by swapping the N-terminal anchor-linker part of cyt *c_y* and the C-terminal portions of

cyt c_2 . For this swapping experiment the *EcoRI* restriction site, which is naturally found in cyt c_2 , was engineered in an appropriate region of cyt c_y (Myllykallio et al., 1997) (**Figure 1.8**).

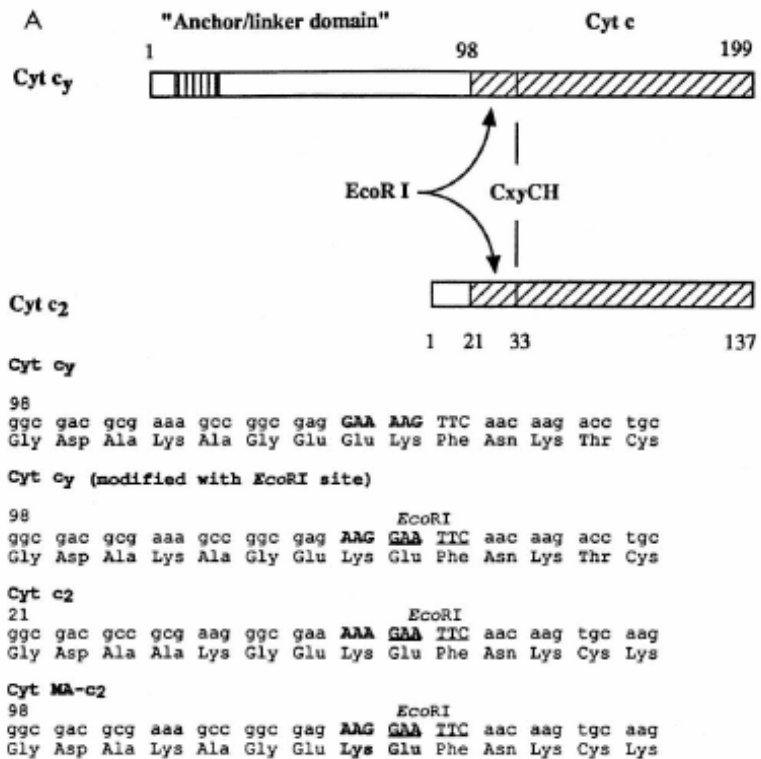


Figure 1.8. The membrane attached cyt MA-*c*₂ was constructed by fusing anchor linker domain of cyt *c*_y with *c* domain of cyt *c*₂. The partial amino acid sequences of cyts *c*_y, *c*₂, and MA-*c*₂ at the fusion joint are shown (Myllykallio et al., 1997).

The chimeric cyt, MA- c_2 , which is formed of the N-terminal extension of cyt c_y and the mature form of cyt c_2 , remains membrane-attached and supports Ps and Res growth as efficiently as its soluble wild-type counterpart does (Myllykallio et al., 1997). These findings indicated that the N-terminal domain of *R. capsulatus* cyt c_y is also sufficient to anchor the periplasmic cyt c_2 to the membrane and allow the comparison of electron transfer properties of a given electron carrier when it is anchored to the membrane or is freely diffusible in the periplasm.

1.3.2.2. Soluble versions of cyt c_y (cyt S- c_y)

In a previous study (Öztürk et al., 2001), a soluble form of cyt c_y (cyt S- c_y) was constructed by fusing genetically the signal sequence of cyt c_2 to the cyt c domain of cyt c_y by using the *EcoRI* restriction site, which was also used for construction of cyt MA- c_2 (**Figure 1.9**). The obtained chimeric soluble cyt S- c_y , was initially unable to support Ps growth of a *R. capsulatus* strain that lacks both the cyt c_2 and cyt c_y (cyt c_2^- , c_y^-). However, this mutant yielded frequently two distinct classes of photosynthetically functional (Ps⁺) revertants in both minimal and enriched media. Several of them were isolated and analyzed by molecular genetic, biochemical and biophysical methods in these study. Analyses of these revertants revealed for the first time an important property of membrane-anchored electron carrier cyt c_y , that is, it does not form tight binary complexes with the RC, unlike its freely diffusing homologues like cyt c_2 , to facilitate efficient ET during multiple turnovers.

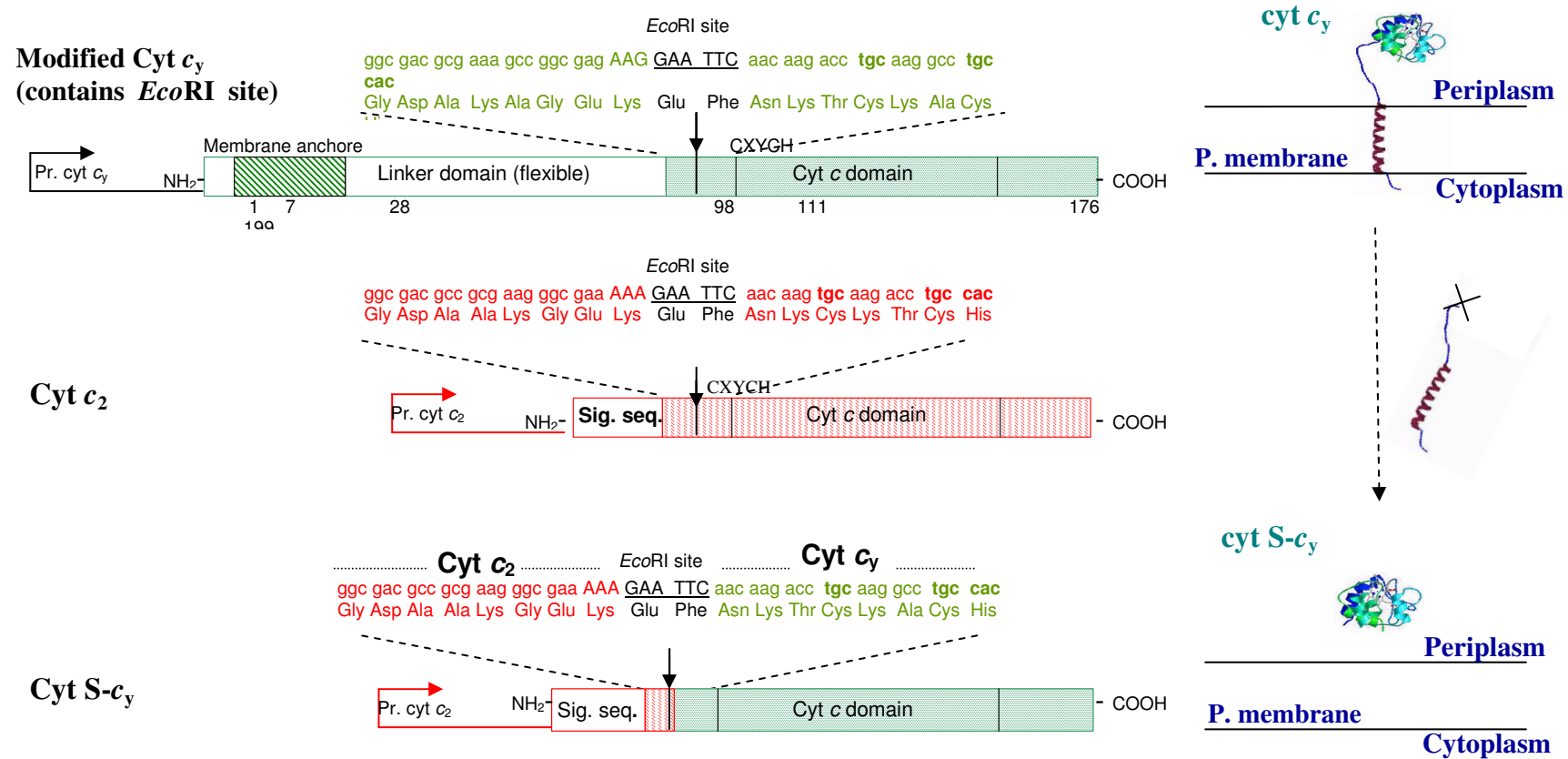


Figure 1.9. Domain swapping between cyt c_2 and reverted cyt c_y . The soluble cyt S- c_y was constructed by fusing signal sequence of cyt c_2 with c domain of cyt c_y (Öztürk et al., 2001).

1.4. Biological hydrogen production

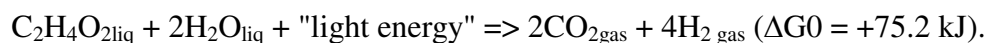
Dependence on fossil fuels brings two kinds of problems, the loss of petroleum and coal resources and the unacceptable level of pollution for life such as global climate change, environmental degradation, and health problems (Bockris J.M, 2002). Concerning these kinds of problems hydrogen, as clean fuel (it only produces water when burned with oxygen) is recognized as the fuel of the future and offers tremendous potential as a clean, renewable energy source (Goltsov and Veziroglu, 2002). Hydrogen may be produced by a number of processes, including electrolysis of water, thermocatalytic reformation of hydrogen-rich organic compounds, and biological processes. Biological production of hydrogen, using micro organisms, is an exciting new area of technology development that offers the potential production of usable hydrogen from a variety of renewable resources. Biological systems provide a wide range of approaches to generate hydrogen, and include direct biophotolysis, indirect biophotolysis, photo-fermentations, and dark-fermentation (Das D. and Veziroglu N., 2001; Hallenbeck P and Benemann JR, 2002). The first evidence that phototrophic bacteria could produce hydrogen appeared in 1949 (Gest and Kamen, 1949). Photoautotrophic organisms, microalgae and cyanobacteria are unique organisms with the ability to produce hydrogen by water photolysis with light as the energy source (Hall et al., 1995), but with very low conversion efficiencies. Beside these photosynthetic organisms there are also phototrophic bacteria able to produce hydrogen from organic substrates, as well as other anaerobic bacteria which can drive dark fermentative hydrogen production from low-cost substrates and wastes (Zajic et al., 1978). The last substances are quite interesting and provide the possibility to associate energy production with the reduction of organic pollutant. From an economic point of view, it is difficult to expect in the near future that hydrogen produced by biological ways can compete with chemical synthesis of hydrogen. However, from a global point of view, where waste treatment and production of by-products are also significant, then this issue becomes much more important.

Photobiological production of hydrogen can be performed by photoautotrophic (light as the energy source and carbon dioxide as sole carbon source) or photoheterotrophic organisms (light as the energy source and organic carbon as the carbon source) (Das D. and Veziroglu N., 2001). Microalgae and cyanobacteria (photoautotrophic microorganisms) are able to use sunlight to metabolize carbon dioxide (CO_2) into energy-rich organic compounds $[\text{C}_n(\text{H}_2\text{O})_n]$, with water (H_2O) as an additional substrate. Normal photoautotrophic microalgal growth follows; $\text{CO}_2 + \text{H}_2\text{O} + \text{"light energy"} \Rightarrow [\text{C}_n(\text{H}_2\text{O})_n] + \text{O}_2$.

Under anaerobic conditions, microalgae can produce H_2 , by water photolysis, using light as the energy source. The catalyst is a hydrogenase, an enzyme that is extremely sensitive to oxygen, a by-product of photosynthesis. The H_2 production reaction is;



The N_2 fixing photosynthetic bacteria (photoheterotrophic microorganisms) catalyze the reduction and assimilation of atmospheric N_2 to ammonia by the nitrogenase enzyme. Under photoheterotrophic growth with a nitrogen limiting source, the nitrogenase enzyme produces H_2 by the oxidation of organic acids (malate, acetate, and lactate). The conversion of the organic substrate (acetate in the example below) into hydrogen demands energy and this is obtained from light (Stam et al., 1987).



The nitrogenase enzyme is also highly sensitive to oxygen, and is inhibited by ammonium ions (Reith et al., 2003)

1.4.1. Photoheterotrophic hydrogen production by *R. capsulatus*

Under the ammonia-free environment the nitrogen fixation (nitrogenase) system of *R. capsulatus* (and of most phototrophic bacteria) is activated and enables this bacterium to grow under conditions in which N_2 is the sole source of assimilated nitrogen. The cells catalyze the reduction and assimilation of

atmospheric N₂ to ammonia, accompanied by the reduction of protons to molecular hydrogen. Nitrogen fixation process requires large amount of reducing power and energy in the form of ATP (Hallbeck and Benemann 2001). Besides the role of nitrogenase system in nitrogen metabolism, it serves as a redox-balancing system during photoheterotrophic growth with a nitrogen limiting source (like, glutamate) (Joshi and Tabita, 1996). Under this condition, the nitrogenase system is activated and the excess reducing equivalents generated by the oxidation of organic acids (malate, acetate, lactate) are consumed by the reduction of protons and consequent evolution of molecular hydrogen by a hydrogenase-like activity of the nitrogenase system (Vignais et al., 1985). It has been shown that, in this way, many organic acids can be transformed into hydrogen gas (H₂) under the photosynthetic nitrogen limiting growth condition (Hillmer and Gest 1977). On the other hand, like many phototrophic bacteria, *R. capsulatus* has membrane-associated respiratory uptake hydrogenase that recycles the H₂ produced by nitrogenase. The enzyme uptake hydrogenase enzyme is essential under the photoautotrophic and chemoautotrophic growth in which CO₂ serves as the primary carbon source and molecular hydrogen as the reductant.

1.4.2. Electron transfer chain and hydrogen production in *R. capsulatus*

The facultative photosynthetic bacterium, *R. capsulatus* has only one photosystem (PS) and water is not split into hydrogen and oxygen in this system (anoxygenic photosynthesis). In *R. capsulatus* anoxygenic photosynthesis is driven by the cyclic electron transfer between the reaction center and the cyt *bc*₁ complex via the lipid soluble ubiquinone pool and the electron carriers; soluble cyt *c*₂ or membrane bound cyt *c*_y (Jenney and Daldal, 1993). Under anaerobic photosynthetic condition, these bacteria are able to use simple organic acids, like acetate, malate and lactate as electron donor (Vignais et al., 1985). The oxidation of organic acids under photoheterotrophic growth conditions can result in overreduction of the ubiquinone pool (McEwan, 1994). Cyclic photosynthesis

requires oxidized ubiquinone as an electron acceptor. Therefore the excess reducing equivalents, at the level of the reduced ubiquinone pool must be removed by redox-balancing systems (Ferguson et al., 1987). In nonsulfur purple bacteria, redox homeostasis is achieved by the coordinate control of redox-balancing systems; the Calvin-Benson-Bassham (CBB), nitrogenase and dimethyl sulfoxide (DMSO) reductase systems in the presence of external electron acceptor. (Tichi et al., 2001) (**Figure 1.2**). Under the photoheterotrophic growth condition, the excess reducing equivalents are transferred from ETC to activated nitrogenase enzyme by ferridoxin, and consumed for reduction of protons and consequent evolution of molecular hydrogen in conjunction with the CBB cycle (Vignais et al., 1985) (Jee et al., 1987). This allows the cell to balance its intracellular redox potential (Joshi and Tabita, 1996). Moreover, periplasmically oriented membrane-associated uptake hydrogenase of *R. capsulatus* is connected to the electron transport chain by its cyt *b* subunit. The cyt *b* subunit of the uptake hydrogenase is encoded by the third gene (*hupC*) of the *hupSLC* operon. The electrons from H₂ are transferred to the quinone pool of the membrane via this cyt *b* subunit. The cyt *b* is not merely a redox carrier, but also is an anchor for the binding of the uptake hydrogenase to the periplasmic side of the membrane. Thus, the oxidation of H₂ results in a release of protons into the periplasmic compartment (Dross et al., 1992).

The respiratory electron transfer pathways of *R. capsulatus* are branched after the ubiquinone pool, and contain two different terminal oxidases, the cyt *cbb₃* oxidase and quinol oxidase. The quinol oxidase branch is independent from the cyt *bc₁* complex, and electrons are transferred directly from the ubiquinone pool to reduce O₂ to H₂O (Amesz and Knaff, 1988). The cyt *cbb₃* oxidase branch is similar to the mitochondrial electron transfer chain in that it depends on the cyt *bc₁* complex, and electron carrier cytochromes; cyt *c₂* and cyt *c_y* (Koch et al., 1998). In *R. sphaeroides* it was shown that the cyt *cbb₃* terminal oxidase possesses extensive regulatory activities under both aerobic and anaerobic conditions by effecting RegB/RegA (PrrB/PrrA) global regulatory system (Kaplan et al., 2005). The cyt *cbb₃* oxidase can generate an inhibitory signal sufficient to shift the equilibrium of

the PrrB kinase/phosphatase activity in the direction of phosphatase activity even in the absence of O₂ (Oh et al., 2004). Inactivation of the cyt *cbb₃* oxidase in *R. sphaeroides* through mutations of the *ccNOQP* operon brings about increased expression of the RegB/RegA regulon under both aerobic and anaerobic conditions (Zeilstra-Ryalls et al., 1996) (Oh and Kaplan, 2000). In *R. capsulatus* it is demonstrated that the RegB/RegA system indirectly activates the synthesis of nitrogenase by activating expression of the *nifA2* gene, which encodes one of the two functional copies of the NifA transcriptional activator of the nitrogenase structural genes. It was also demonstrated that RegA directly represses uptake hydrogenase structural gene expression by binding to the *hupSLC* promoter (Elsen et al., 2000) (**Figure 1.10**). In addition to the cyt *cbb₃* oxidase, redox state of the cyclic photosynthetic Electron Transfer Chain (ETC) also serves as a signal that is in part mediated by the AppA–PpsR system controls the transcription rate of the *puc* operon in *Rhodobacter* (Roh et al., 2004).

1.4.3. Enzyme systems for hydrogen metabolism in *R. capsulatus*

The main enzymes of *R. capsulatus* involved in hydrogen metabolism are nitrogenase and uptake hydrogenase.

1.4.3.1. Nitrogenase

1.4.3.1.1. Genetics, structure and activity of nitrogenase

Most of anoxygenic phototrophic bacteria conduct very important specialized metabolic process nitrogen fixation (*nif*), the reduction of N₂ to ammonia (NH₃). Nitrogen fixation is catalyzed by the enzyme nitrogenase (a molybdenum-containing enzyme) whose expression and activity are highly regulated. In *R. capsulatus* two major clusters of *nif* genes coding up to 34 genes

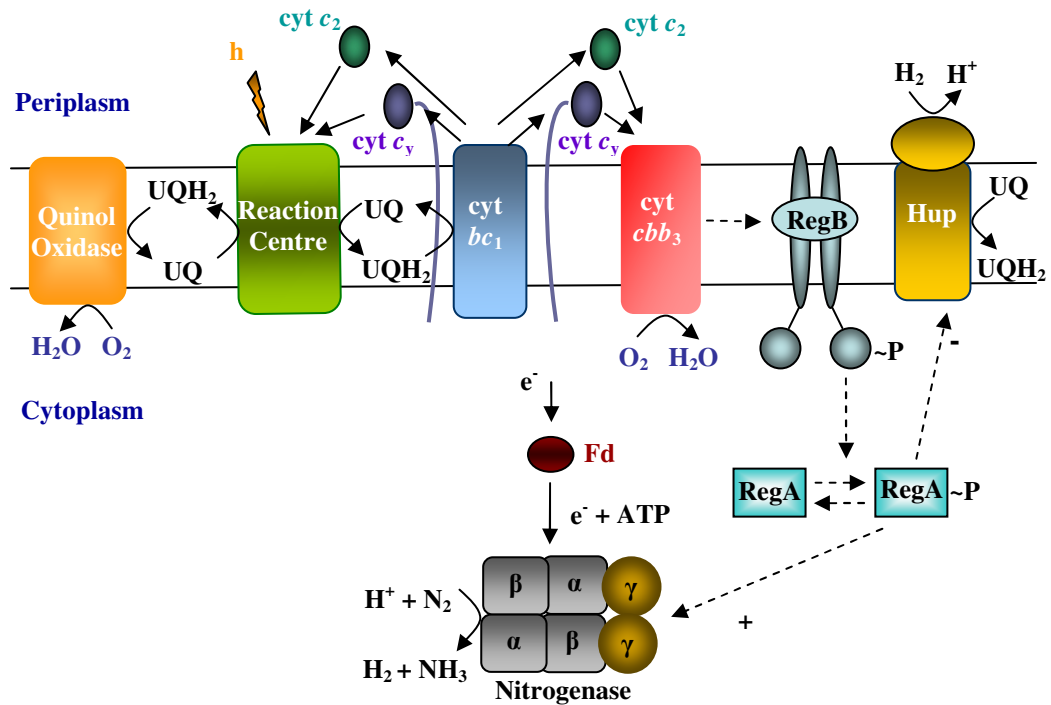


Figure 1.10. Respiratory and photosynthetic electron transport pathways in *R. capsulatus* and model for redox sensing and signal transduction through the *cbb*₃-RegBA signal transduction pathway. Electron flow through the *cbb*₃ oxidase generates an inhibitory signal which shifts the equilibrium of RegB activity from the kinase-dominant mode to the phosphatase-dominant mode, leading to dephosphorylation of RegA. The solid and dotted arrows demonstrate the electron and signal flows, respectively. The '+' and '-' signs indicate the activation and inactivation of genes respectively. Abbreviations: UQH₂-UQ, ubiquinone pool; cyt *bc*₁, cytochrome *bc*₁ complex; cyt *c*₂, soluble cytochrome *c*₂; cyt *c*_y, membrane-bound cytochrome *c*_y; cyt *cbb*₃, *cbb*₃-type cytochrome *c* oxidase; *h*_v, light; Hup, uptake hydrogenase; Fd, ferridoxin.

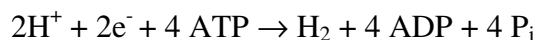
products, are involved in nitrogen fixation. Non-regulatory genes include a) structural genes *nifHDK*, b) MoFe cofactor synthesis genes *nifE*, *nifN*, *nifX*, *nifV* and *nifB*, c) nitrogenase MoFe protein component processing genes *nifY*, *nifU* and *nifS* d) Mo processing gene *nifQ*. Some of the orfs at the *nifENX* cluster encode ferridoxin-like proteins. Three genes within the two *nif* clusters are involved in transcriptional regulation: *nifA1*, *nifA2* and *rpoN*. Two other loci encode the regulatory genes *glnB*, *ntrB* and *ntrC* which are also take part in regulation. In addition to molybdenum-containing nitrogenase enzyme, *Rhodobacter capsulatus* contains an alternative nitrogen fixation (*anf*) gene system, encodes a nitrogenase containing neither Mo, V nor any other heterometal atom, and has been designated as the Fe nitrogenase or Fe-only nitrogenase (Merrick, 1993).

Nitrogenase systems consist of two-component proteins, the dinitrogenase component (MoFe protein of Mo nitrogenase, Fe-Fe protein of Fe only nitrogenase) and the dinitrogenase-reductase component (also termed Fe protein) (Eady, 1996; Smith, 1999). While the MoFe protein consists of four subunits forming a $\alpha_2\beta_2$ tetramer, the dinitrogenase proteins of the alternative Fe-only nitrogenase, contain an additional small 13–15 kDa subunit to form an $\alpha_2\beta_2\delta_2$ hexameric structure. The dinitrogenase component of nitrogenases contains two types of unique metal clusters, the M-cluster (FeMo cofactor in Mo nitrogenase, FeFe cofactor in Fe only nitrogenase), which represents the site of substrate reduction, and the P-cluster, whose function is likely to transfer electrons as well as protons to the cofactor. The Fe-only nitrogenase components that has been isolated and purified as intact and catalytically active proteins, has relatively high specific activities for N_2 reduction (350 nmol of NH_3 formed per min per mg protein), acetylene reduction as well as very high activities ($1300 \text{ nmol } H_2 \cdot min^{-1} \cdot mg^{-1}$ in an N_2 atmosphere) for the evolution of molecular hydrogen. Particularly in the simultaneous presence of a second substrate (N_2 , C_2 or H_2 in addition to H^+), the H_2 production rates were distinctly higher than the respective activities of the Mo nitrogenase (~ six fold) (Hawks et al., 1984).

Nitrogenase catalyses the ATP and reductant dependent reduction of N₂ to ammonia as shown in following reaction (Miyake *et. al.*, 1982):



The simultaneous evolution of hydrogen along with nitrogen reduction seems to be an inherent property of the nitrogenase (Hall *et al.*, 1995). When the natural substrate is absent, nitrogenase catalyses the reduction of protons that is the primary product:



So, under the conditions of nitrogen limitation and light as an energy source, nitrogenase reduces protons to hydrogen. Nitrogenase can also catalyse the reduction of some other substrates, like acetylene. The reduction of acetylene to ethylene by the action of nitrogenase can be easily measured by gas chromatography (Madigan *et. al.*, 2000).

1.4.3.1.2. Regulation of nitrogenase

Nitrogenase enzyme is irreversibly inactivated by the oxygen so the nitrogen fixation possible only under anaerobic conditions in *R. capsulatus* and other anoxygenic photosynthetic bacteria (Hall *et al.*, 1995). Moreover nitrogen fixation process is cost expensive (requires significant reductant and energy) and involves large number of proteins (at least 34). Therefore *R. capsulatus* and other anoxygenic phototrophic bacteria have developed specific nitrogen and oxygen-sensing systems that activate transcription of *nif* genes under condition of limiting nitrogen and oxygen (Kranz *et al.*, 1990). Uridyltransferase (UTase) is proposed to sense the ratio of glutamate to 2-ketoglutarate, compounds that reflect endogenous levels of fixed nitrogen. Under conditions of nitrogen limitation (low glutamine/high 2-ketoglutarate), UTase inactivates *GlnB* by the covalent addition of uridylmonophosphate (UMP). Uridylated *GlnB* would no longer interact with *NtrB*, which is consequently functioning only as a kinase. The *NtrB* protein phosphorylates *NtrC* a proposed transcriptional activator. The *NtrC* protein has

three domains: An N-terminal regulatory domain, a central ATP-binding activation domain, and a C-terminal helix-turn-helix domain that is shown to bind to DNA over 100 bp upstream of the *nifA1* and *nifA2* promoters. Phosphorylated *NtrC* is proposed to activate transcription of the *nifA* and *nifA2* genes resulted in the increase in NifA protein. NifA protein acts as a transcriptional activator of all other *nif* genes, including *nifHDK*. The transcriptional activation of *nif* genes by NifA additionally requires an RNA polymerase (RNAP) alternative sigma factor called RpoN. Expression of the *R. capsulatus rpoN* gene is autoactivated (by RpoN and NifA) at a secondary promoter upstream of *nifU2*. This secondary promoter results in a more rapid and higher (maximal) induction of other *nif* genes. Although oxygen regulation is not as well understood as nitrogen control, the NifA protein itself may be oxygen sensitive, and that additional oxygen-sensing controls may be mediated through DNA supercoiling (Merrick, 1992).

In addition to specific regulations, molybdenum nitrogenase biosynthesis is under the control of the RegB-RegA two-component regulatory system in *R. capsulatus*. Footprint analyses and in vivo transcription studies showed that RegA indirectly activates nitrogenase synthesis by binding to and activating the expression of *nifA2*, which encodes one of the two functional copies of the *nif*-specific transcriptional activator, NifA. Expression of *nifA2* but not *nifA1* is reduced in the *reg* mutants up to eightfold under derepressing conditions and is also reduced under repressing conditions. Thus, although *NtrC* is absolutely required for *nifA2* expression, RegA acts as a coactivator of *nifA2* (Elsen et al., 2000). Post-translational regulation of nitrogenase is also present in *R. capsulatus*. To prevent unproductive nitrogen fixation during energy-limiting or nitrogen-sufficient conditions, the nitrogenase complex is rapidly, reversibly inactivated by ADP-ribosylation of Fe protein. ADP-ribosylation of dinitrogenase is catalyzed by dinitrogenase reductase ADP-ribosyl transferase (DRAT) and the removal of ADP-ribose is performed by dinitrogenase reductase activating glycohydrolase (DRAG). These enzymes encoded by *draT* and *draG* respectively (Ludden add Roberts, 1989).

1.4.3.2. Uptake hydrogenase

1.4.3.2.1. Genetics, structure and activity of uptake hydrogenase

Hydrogenases (H_2 ases) catalyze the reversible oxidation of molecular hydrogen ($H_2 \leftrightarrow 2H^+ + 2e^-$) and play an important role in microbial energy metabolism. They are usually committed to catalyze either hydrogen uptake or evolution in vivo, depending on the demands of the host organism. Various microorganisms can use H_2 as an electron source either aerobically or anaerobically. Nitrogen fixers like *R. capsulatus* usually contain uptake H_2 ases that recycle the H_2 produced by nitrogenase. Different cellular localizations are often associated with the functions of them, e.g. hydrogen evolution is most often cytosolic, whereas hydrogen uptake is usually periplasmic or membrane-localized. Some bacteria contain two or more different H_2 ases, localized in different cell compartments. They can be classified into three classes: the [Fe]- H_2 ases, the [NiFe]- H_2 ases, and the metal-free H_2 ases (Vignais et al., 2001). The vast majority of known H_2 ases belong to the first two classes. Compelling evidence from sequence and structure analyses indicates that the [NiFe]- and [Fe]- H_2 ases are phylogenetically distinct classes of proteins. The *R. capsulatus* uptake hydrogenase belongs to membrane-associated respiratory uptake [NiFe]-hydrogenases. They are periplasmically oriented hydrogenases, and are connected to the electron transport chain (Meyer, 1978). In *R. capsulatus*, the *hup/hyp* gene cluster, localized on the chromosome, comprises 21 genes and some of these products are necessary for maturation of the enzyme, some for Ni insertion to the active site, and some for regulation of the hydrogenase gene expression (Colbeau, et al., 1993). These genes include the regulatory/biogenesis genes: *hupTUV* operon, *hupR*, *hupD*, *hupA*, and the structural genes: *hupSLC*. In *R. capsulatus*, *hupS* is capable of encoding a protein of 34,256 Da with 13 Cys residues, and the *hupL* gene can encode a protein of 65,839 Da containing 10 Cys residues. These proteins share a high degree of identity with the [Nife] hydrogenases (Colbeau et al., 1993). The *hupS* gene is preceded by a sequence capable of encoding a signal peptide of 45 amino acids,

which contain a strictly conserved "RRXFXK" consensus element (twin-arginine element), the completely folded SL heterodimer is translocated through the cytoplasmic membrane by the Tat translocation pathway (Sargent, 1998). The third gene of the *hupSLC* operon is the *hupC* gene encoding a cytochrome *b* which links the hydrogenase to the respiratory chain.

The X-ray structure of the [NiFe]-H₂ases showed that the two H₂ase subunits interact extensively through a large contact surface and form a globular heterodimer (Volbeda, 1995). The bimetallic NiFe center of the active site is located in the large subunit and is deeply buried inside the protein. The small subunit contains up to three Fe-S clusters, which conduct electrons between the H₂-activating center and the physiological electron acceptor or donor of H₂ase. The [4Fe-4S] cluster that is proximal to the active site is essential to H₂ activation in [NiFe]-H₂ases (Albracht, 1994). Hydrophobic channels expanding through both subunits linking the active site to the surface of the molecule were suggested to facilitate gas access to the active site (Montet, 1997). H₂ oxidation is linked to reduction of various electron acceptors such as O₂, NO₃⁻, SO₄⁻², fumarate or CO₂. The electrons from H₂ are transferred to the quinone pool of the membrane via a cyt *b* encoded by the third gene of the structural operon *hupC*. This gene is necessary for growth on H₂ of *R. capsulatus* cells by photoautotroph.

1.4.3.2.2. Regulation of uptake hydrogenase

In nitrogen-fixing bacteria, uptake [NiFe]-Hydrogenases are induced when nitrogenase is synthesized and produces molecular hydrogen. The control is exerted at the transcriptional level (Richaud et al., 1991). *R. capsulatus* uses a regulatory system involving the specific H₂-sensing HupUV hydrogenase to regulate the synthesis of the HupSLC. The *hup-hyp* cluster comprises the *hupTUV* operon, the products of which exert a negative control on *hupSL* gene expression. The HupUV protein complex can catalyze the hydrogen-deuterium (H-D) exchange reaction in the presence of D₂ gas and was suggested to function as a

cellular H₂ sensor (Vignais et al., 1997). The *hupT* gene product is a protein histidine kinase (Elsen et al., 1997). With the response regulator HupR, it forms the two-component HupT-HupR system, which regulates the synthesis of HupSL hydrogenase in *R. capsulatus*. In the absence of H₂, HupT represses the transcription of hydrogenase (*hupSL*) genes by phosphorylating HupR (Dischert et al., 1999). The HupR protein is a transcriptional activator and shows the typical three domain organization of the response regulators of the *NtrC* subfamily (Richaud et al., 1991). The N-terminal receiver domain contains conserved residues (D10, D11, D54, K105) capable of forming an active phosphorylation site, and in its C-terminal domain, which is the DNA-binding domain, a stretch of conserved amino acids is able to form a helix–turn–helix structure (Toussaint et al., 1997).

In addition to specific H₂-sensing HupUV regulatory system, in *R. capsulatus* the global RegB/RegA regulatory system, which responds to the redox status of the cell, controls the transcription of the hydrogenase *hupSLC* genes and the regulatory *nifA* gene (Elsen et al., 2000). A major DNA-binding site of RegA was shown to be located close to the -35 promoter recognition sequence, with a second, lower-affinity RegA-binding site overlapping the IHF DNA-binding region which is another regulatory factor required for *hupSLC* expression (Dischert et al., 1999). At that location, RegA could prevent either the RNA polymerase or the IHF protein, or both, from binding to the *hupSLC* promoter. It was demonstrated that in *reg* mutants, [NiFe] hydrogenase synthesis and activity are increased up to six fold (Elsen et al., 2000). Interestingly, a deletion in RegB can be suppressed by addition of multiple copies of the sensor kinase HupT presumably due to increased amounts of HupT phosphorylating RegA in the absence of RegB (Gomelsky et al., 1995).

1.4.4. Genetic studies for hydrogen production in *R. capsulatus*

Depression of the synthesis of hydrogenase, which recycles the H₂ produced by nitrogenase, through a certain mutation may give the ability to mutant bacteria to produce more hydrogen in photoheterotrophic cultures. To demonstrate the role of *R. capsulatus* uptake hydrogenase in H₂ photoproduction, the Hup⁻ mutants of *R. capsulatus* B10 growing in lactate- and glutamate-containing medium were tested for their efficiency to photoproduce H₂. Two Hup⁻ mutants, JP91 (which has an *IS21* element inserted between the *hupS* and *hupL* genes) and RS 13 (contains a point mutation in *hypF*), which are devoid of hydrogenase, produced 10-20% more H₂ and at higher rates than did the wild-type strain B10. On the other hand, the *HupT* mutant BSE8, which is derepressed for hydrogenase biosynthesis, showed a decreased rate and yield of H₂ production (Zorin et al., 1996). In addition, *R. capsulatus ST410*, a mutant of the wild strain B100 lacking hydrogenase activity, evolved a larger amount of hydrogen than the parent strain B 100. *R. capsulatus ST410* converted 60 mM malate to hydrogen at a yield of 68%, calculated as a percentage of the stoichiometric maximum for the complete conversion of the carbon source to H₂ and CO₂. On the other hand, when the wild strain was used under the same conditions, the yield was only 25% (Ooshima et al., 1998). In another mutant of *R. capsulatus*, the *hupL* gene encoding the large subunit of the uptake hydrogenase was mutated by insertion of an interposon. The mutant neither synthesized an active hydrogenase nor grew photoautotrophically. Under conditions of nitrogen (N) limitation, photoheterotrophic cultures of the wild type and the mutant evolved H₂ by activity of the nitrogenase enzyme complex. When grown with glutamate as an N source and either D,L-malate or L-lactate as carbon sources, the efficiency of H₂ production by the HupL mutant was higher than 90%, whereas wild-type cultures exhibited efficiencies of 54% (with D,L-malate) and 64% (with L-lactate), respectively (Jahn et al., 1994).

1.5. Scope of the work

The aim of the first part of this study is to obtain a functional soluble version of cyt c_y (cyt S- c_y), and to demonstrate the effect of anchor-linker and cyt c domain of cyt c_y on protein-protein interactions and inter-protein electron transfer process with its physiological partner reaction centre (RC) during the photosynthetic electron transport. By this way, the effects of structural difference of membrane attached cyt c_y and soluble cyt c_2 on electron transfer process can be analyzed by constructing its hybrid versions.

In the second part of this study, hydrogen production of various *R. capsulatus* strains harboring the genetically modified electron carrier cyt and respiratory oxidase deficient strains have been compared with the wild type *R. capsulatus* species to observe these genetic modifications on hydrogen production metabolism through the effecting redox signaling pathway and the redox state of the photosynthetic ETC. In addition, recycling of the produced H₂ was prevented by chromosomal inactivation of the uptake hydrogenase to increase the hydrogen production efficiency of wild type, Qox and cyt cbb_3 oxidase deleted strains of *R. capsulatus*.

CHAPTER 2

MATERIALS AND METHODS

2.1. Materials

2.1.1. Bacterial strains and plasmids

The bacterial strains and plasmids used in this work are described in **Table 2.1**. All *R. capsulatus* strains used in this thesis are the derivatives of MT1131 which is referred to as a wild type strain with respect to its cyt c profile and growth properties. *E. coli* strains XL-1 BLUE and HB101 were used for genetic studies as competent host cells for pBSII KS⁺ (high copy plasmid) and pRK415 (low copy, broad host range plasmid) plasmid vectors respectively (**Appendix F**). The small size pBSII KS⁺ (3 kb) plasmid was used for molecular genetic studies such as initial cloning experiments and site directed mutagenesis. The broad host range plasmid pRK415 (10.6 kb) was used to mobilize the cloned genes from *E. coli* HB101strain to different *R. capsulatus* strains by triparental mating.

2.1.2. Bacterial growth mediums and culture conditions

MPYE (Mineral, Peptone, Yeast Extract) enriched medium (Daldal et al., 1986) or Sistrom's minimal medium A (Med A) (Sistrom, 1960) supplemented with 10 µg of kanamycin or 2.5 µg of tetracycline per ml, were used for chemoheterotrophic (Res) or photoheterotrophic (Ps) growth of *R. capsulatus* strains at 35° C (**Appendix A**). Liquid cultures grown under Res conditions were shaken at 150 rpm in the dark, while Ps cultures on solid media were incubated under saturating light intensity in anaerobic jars containing H₂ and CO₂ generating gas packs (BBL 270304, Becton Dickenson and Co.), as described earlier (Jenney and Daldal, 1993). *E. coli* strains were grown on Luria broth (LB), and cultures were supplemented with ampicillin, kanamycin, or tetracycline antibiotics at final concentrations of 100, 50, or 12.5 µg per ml, respectively as needed (Daldal et al., 1986) (**Appendix B**). Equipments used in this study are listed in **Appendix H**.

2.1.3. Growth mediums and culture conditions for hydrogen production

For hydrogen production experiments, the minimal medium of Biebl and Pfennig (1981), supplied with C/N sources (15mM/2mM for malate/L-glutamate and 10mM/2mM for glucose/L-glutamate) without ammonium chloride and yeast extract (**Appendix A**), was used under the condition of starting pH: 6.8-7.0, temperature: 30-33° C, light Intensity: 250 W/m², atmosphere: anaerobic, bioreactor volume: 55 ml, inoculation amount: 2-5 %.

Table 2.1. Bacterial strains, and plasmids used in this work

Strain	Genotype	Phenotype	Reference
<i>E. coli</i>			
HB101	F ⁻ proA2 hsdS20 (rB ⁻ mB ⁻) recA13 ara-14 lacY1 galK2 rpsL20 supE44 rpsL20 supE44 proA2 xyl-5 mtl-1		Sambrook et al., 1989
XL1-Blue	recA1 endA1 gyrA96 thi-1 hsdr-17 supE44 relA1 lac [F9 proAB lacI q Δ M15 Tn10]	Tet ^R	Stratagene
<i>R. capsulatus</i>			
MT-1131 ^a	crtD121 Rif ^R	Wild type	Scolnik et al., 1980
Y262	Overproducer of gene transfer agent		Yen et al., 1979
FJ1	crtD121, Δ(cycY::spe)	Cyt c _y ⁻ Ps ⁺ Res ⁺	Jenney and Daldal, 1993
FJ2	crtD121, Δ(cycA::kan) Δ(cycY::spe)	Cyt c ₂ ⁻ c _y ⁻ Ps ⁻ Res ⁺	Jenney and Daldal, 1993
FJ2-R4	crtD121, Δ(cycA::kan) Δ(cycY::spe), cycR4	Cyt c ₂ ⁻ c _y ⁻ Ps ⁻ Res ⁺	This work
GK-32	crtD121, Δ(ccoNO::kan)	Kan ^R , cyt cbb ₃ ⁻ Ps ⁺ Res ⁺	Koch et. al., (1998)

KZ1	<i>crtD121</i> , $\Delta(cydAB::spe)$	Spe ^R , Qox ⁻ Ps ⁺ Res ⁺	Previous work
YO3	<i>crtD121</i> , $\Delta(hupSL::gen)$	Gen ^R , hup ⁻ , Ps ⁺ , Res ⁺	This work
YO4	<i>crtD121</i> , $\Delta(hupSL::gen)$, $\Delta(ccoNO::kan)$	Gen ^R , Kan ^R , cyt <i>cbb₃</i> ⁻ hup ⁻ , Ps ⁺ , Res ⁺	This work
YO5	<i>crtD121</i> , $\Delta(hupSL::gen)$, $\Delta(cydAB::spe)$	Gen ^R , Spe ^R , Qox ⁻ , hup ⁻ , Ps ⁺ , Res ⁺	This work
Plasmid			
pBSII	pBluescriptII (KS ⁺)	Amp ^R	Stratagene
pRK2013		Kan ^R , helper	Ditta et al., 1985
pRK415		Tet ^R	Ditta et al., 1985
pFJ631	<i>CycY</i> on a 1.2-kb <i>Bam</i> HI/ <i>Hind</i> III fragment in pRK415	Tet ^R Cyt <i>c_y</i>	Myllykallio et al., 1997
pHM14	<i>cycA</i> on a 1.25-kb <i>Bam</i> HI/ <i>Hind</i> III fragment in pRK415	Tet ^R	Myllykallio et al., 1999
pYO12	0.8-kb <i>Eco</i> RI fragment of pRKE12 ⁺ ligated to 3.5-kb <i>Eco</i> RI fragment of pHM5	Amp ^R Cyt S- <i>c_y</i>	Öztürk et al., 2001
pYO100	1.2-kb <i>Kpn</i> I/ <i>Bam</i> HI fragment of pYO12 on pRK415 <i>cycA₉::cycY₁₀₈</i>	Tet ^R Cyt S- <i>c_y</i>	Öztürk et al., 2001

pYO103	H53Y reversion of Cyt S- <i>c_y</i> , on pRK415 <i>cycA₉::cycY₁₀₈</i> H53Y	Tet ^R Cyt S- <i>c_y</i> R3	Öztürk et al., 2001
pYO105	K19R reversion of Cyt S- <i>c_y</i> , on pRK415 <i>cycA₉::cycY₁₀₈</i> K19R	Tet ^R Cyt S- <i>c_y</i> R5	This work
pYO16	0.7-kb <i>HindIII/PstI</i> fragment of pYO103 on pBSII,	Amp ^R Cyt S- <i>c_y</i> R3	Öztürk et al., 2001
pYO26	1.2 kb <i>KpnI/BamHI</i> fragment of pYO105 on pBSII	Amp ^R Cyt S- <i>c_y</i> R5	This work
pYO27	Site directed mutation of H53Y in Cyt S- <i>c_y</i> R5 gene on pYO26 <i>cycA₉::cycY₁₀₈</i> H53Y& K19R	Amp ^R Cyt S- <i>c_y</i> R35	This work
pYO135	1.2 kb <i>KpnI/BamHI</i> fragment of pYO27 on pRK415	Tet ^R Cyt S- <i>c_y</i> R35	This work
pYO39	4.1 kb PCR product containing <i>hupSLC</i> operon cloned to <i>KpnI/XbaI</i> site of pBSII	Amp ^R , <i>hupSLC</i>	This work
pYO40	4.1 kb PCR product containing <i>hupSLC</i> operon cloned to <i>KpnI/XbaI</i> site of pRK415	Tet ^R , <i>hupSLC</i>	This work
pYO41	2.3 kb <i>BalI/BamHI</i> fragment of pYO39 replaced with the 1.2 kb Gentamicin resistance cassette.	Amp ^R , Gen ^R , <i>hupSL::gen</i>	This work
pYO42	3 kb <i>KpnI/XbaI</i> fragment of pYO41 cloned to pRK415	Tet ^R , Gen ^R , <i>hupSL::gen</i>	This work

^a*R. capsulatus* MT-1131 (Rif^r *crtD*) is referred to as wild type, since it is wild type with respect to its cytochrome c profile and growth properties. MT-1131 was originally isolated as a green derivative of *R. capsulatus* SB1003 (Scolnik et al., 1980)

2.1.4. Chemicals, restriction endonucleases and DNA modifying enzymes

The chemicals used in the preparation of solutions were all commercially available from Merck, Sigma, Duchefa, Oxoid and Fluka (**Appendix D**). The name and catalog no of restriction endonucleases and DNA modifying enzymes (from MBI Fermentas) used in molecular biology studies are listed at **Appendix E**. All of the solutions were prepared by using distilled water.

2.2. Methods

2.2.1. Molecular genetic techniques

2.2.1.1. Plasmid DNA isolation

Miniprep plasmid DNA isolation was performed by using different plasmid isolation kits (Promega Wizard® Plus SV Miniprep cat no: A1330, Qiagen Qiaprep Spin Miniprep cat.no: 27104, Macherey Nagel NucleoSpin® Plasmid). 5-10 ml culture of each sample was prepared for plasmid isolation (grow at 37°C, with shaking for 12-16 hrs). Protocols of manufacturer were followed as indicated. For cloning experiment, 10 ml culture of *E. coli* HB101 strains containing low copy pKR415 derivative plasmids and 5 ml culture of *E. coli* XL1-Blue strain containing high copy pBSII derivative plasmids were used. According to Qiagen Qiaprep Spin Miniprep protocol, after the growth of bacterial cells, the samples were centrifuged for 10 min at 4000 rpm at 4°C and supernatants (all trace of medium) were discarded. The pelleted bacterial cells were resuspended in 250 µl Buffer P1 and transferred into a microcentrifuge tube. 250 µl Buffer P2 was added and mixed gently, thoroughly by inverting the tube 4–6 times. 350 µl Buffer N3 was added mixed immediately and thoroughly by inverting the tubes 4–6 times. The solution should become cloudy.

Samples were centrifuged for 10 min at 13,000 rpm (~17,900 x g) in a table-top microcentrifuge. The supernatants were transferred to QIAprep spin column by pipetting and centrifuged for 1 min. at 13,000 rpm. For *endA*⁺ strains such as HB101 and its derivatives, or any wild-type strain, it is recommended to wash QIAprep spin column by adding 0.5 ml buffer PB and centrifuging for 1 min. at 13,000 rpm. The flow through liquid was discarded flow through and QIAquick column was placed back in the same collection tube. To wash the QIAquick column, 750 µl PE buffer was added to QIAquick column and centrifuged for 1 min at 13,000 rpm. After the liquid was discarded, the QIAquick column was centrifuged for additional 1 min at 13,000 rpm to remove the residual ethanol. QIAquick column was placed in a clean 1.5 ml microfuge tube. To elute DNA, 50 µl EB buffer (10 mM Tris-HCl, pH 8.5) or H₂O was added to the center of the QIAquick membrane and centrifuged for 1 min at 13,000 rpm.

2.2.1.2. Chromosomal DNA isolation

Chromosomal DNA isolation was performed by Qiagen DNeasy Tissue Kit cat no: 69504 and MN NucleoSpin® Tissue isolation systems. 1-5 ml culture of *R. capsulatus* samples were prepared by growing at respiratory growth condition at 35° C for 18-24 hrs. Protocols of manufacturer were followed as indicated. The chromosomal DNA samples were dissolved in 100 µl ddH₂O of final volume and concentrations of samples were determined by measuring at OD₂₆₀ (Biorad, SmartSpect™ 3000) and by running samples on 0.7 % agarose gel. According to MN NucleoSpin® Tissue isolation kit protocol, 1 ml culture of *R. capsulatus* strains were centrifuged up to for 5 min at 13,000 rpm and supernatants were removed. The pellets were resuspended in 180 µl buffer T1 by pipetting up and down. 25 µl proteinase K was added and samples were vortexed vigorously and incubated at 56°C until complete lysis is obtained (at least 1–3 h). Samples were vortexed occasionally during

incubation. 200 µl buffer B3 was added, vortexed vigorously, and incubated at 70°C for 10 min. The samples were vortexed briefly and 210 µl ethanol (96-100%) was added to the samples, and vortexed vigorously. For each sample, one NucleoSpin® Tissue column was placed into a 2 ml collecting tube. The samples were transferred to the column and centrifuged for 1 min at 10,000 rpm. The flow through liquid was discarded, the flow through and column was placed back in the same collection tube. To wash the columns, 500 µl buffer BW was added to column and centrifuged for 1 min at 10,000 rpm. This step was repeated for 600 µl buffer B5. After liquid was discarded, the columns were centrifuged for additional 1 min at 10,000 rpm to dry the silica membrane. Residual ethanol was removed during this step. The NucleoSpin® Tissue columns were placed into a 1.5 ml microcentrifuge tube and 100 µl prewarmed elution buffer BE (70°C) was added. The samples were incubated at room temperature for 1 min. and centrifuged 1 min at 13,000 rpm to elute the chromosomal DNA. The DNA samples were stored at -20° C.

2.2.1.3. Enzyme digestion

For the control of cloned insert fragment, ~200 ng plasmids DNA were digested with 0.5 µl of restriction enzymes (5 u) in a reaction mixture containing related enzyme buffers in 1X final concentration. Reaction mixture was completed to 15 µl of final volume with ddH₂O and incubated at 37° C for 1 hr for complete digestion. For cloning experiment, ~500 ng plasmid DNA were digested with 1 µl of restriction enzymes (10 u) in 60 µl reaction mixture containing related enzyme buffers in 1X final concentration and incubated at 37° C for 1-2 hrs for complete digestion.

2.2.1.4. Purification and concentration of digested DNA samples

The digested plasmid DNA, alkaline phosphatase treated plasmid DNA and PCR products were purified and concentrated by either Promega clean-up system (cat # A7280), by MN NucleoSpin® Extract clean up or by Qiagen QIAquick PCR purification kit cat. no: 28704 purification system. According to Qiagen QIAquick PCR purification kit protocol, 5 volumes of buffer PB was added to 1 volume of sample and mixed (e.g. 400 µl buffer PB and 100 µl sample). Sample was transferred to the QIAquick column which was place in 2 ml collection tube, and centrifuged for 1 minute. Liquid was discarded flow through and QIAquick column was placed back in the same collection tube. To wash the QIAquick column, 750 µl PE buffer was added to QIAquick column and centrifuged for 1 min. After liquid was discarded, the QIAquick column was centrifuged for additional 1 min at 13.000 rpm to remove the residual ethanol. QIAquick column was placed in a clean 1.5 ml microfuge tube. To elute DNA, 50 µl EB buffer (10 mM Tris-HCl, pH 8.5) or H₂O was added to center of the QIAquick membrane and centrifuged for 1 min at 13.000 rpm. (According to digested plasmid amount, it can be eluted in 15-30 µl to increase DNA concentration)

2.2.1.5. Isolation of DNA fragments from agarose gel

The digested DNA samples (~500 ng plasmid DNA in 40-60 µl volume) were loaded on 1% agarose gel and the gel was run to separate DNA fragments. Agarose gel band containing the desired DNA fragment was excised (minimization of UV exposure is required to protect DNA). The approximate volume of gel slice was determined by its weight (100 mg equals approximately 100 µl) and placed into 1.5 ml eppendorf tube. The QIAGEN QIAquick® Gel Extraction Kits (cat. #: 28704) and MN NucleoSpin® Extract gel purification kits were used according to the manufacturer's suggestions to isolate DNA fragments from the agarose gel.

According to QIAGEN QIAquick^R Gel Extraction Kit protocol, 3 volumes of buffer QG to one volume of the gel (300 μ l buffer QG for 100 μ l (\approx 100 mg) gel) was added and incubated at 50 °C for 10 minutes to dissolve agarose. To help dissolve gel, it was mixed by vortexing the tube every 2-3 min during the incubation. After the gel slice was dissolved completely, one gel volume of isopropanol was added to the sample and mixed. (This step increase the yield of DNA fragments \leq 500 bp and \geq 4 kb). To bind DNA, sample was then transferred to the QIAquick column, which was placed in collection a tube, and centrifuged for 1 minute. Liquid was discarded flow through and QIAquick column was placed back in the same collection tube. To wash the QIAquick column, 750 μ l PE buffer was added to QIAquick column and centrifuged for 1 min. After the liquid was discarded, the QIAquick column was centrifuged for additional 1 min at 13.000 rpm to remove the residual ethanol. QIAquick column was placed in a clean 1.5 ml microfuge tube. To elute DNA, 50 μ l EB buffer (10 mM Tris-HCl, pH 8.5) or H₂O was added to center of the QIAquick membrane and centrifuged for 1 min at 13.000 rpm. (Sometimes to increase DNA concentration, it was eluted in 30 μ l of elution buffer).

2.2.1.6. Ligation reaction

MBI Fermentas T4 ligase (cat # EL0334) was used. Concentration of the vector and insert DNA are determined by either OD_{260nm} measurement or by comparing with a marker on agarose gels. Vector and insert amounts in pmoles can be calculated by amounts in pmol = $1.52 \text{ pmol} \times \mu\text{g of DNA}/\text{kb of DNA}$ equation. Ligation reaction mixture should contain an equal or higher (generally 4-fold is used) concentration of foreign DNA than that of vector x pmol vector, 2 μ l 10x ligation buffer, 4x pmol insert and 4u T4 ligase were combined and final volume are completed to 20 μ l with ddH₂O. The ligation mixture was incubated at 22 °C for 1-2 hrs.

2.2.1.7. DNA sequencing

The DNA sequences of various cyt S-*c_y* revertants were determined by automated DNA sequencing with the BigDye terminator cycle sequencing kit (Applied Biosystems Inc.), according to the protocols provided by the manufacturers. The M13 universal primer and the following *cycY* internal primers, FR1 (5'-CAGAGTGGCGATGGCGG-3'), FR4 (5'-GC GGCCGATCACCCCGT-3'), FF2 (5'-ATGGCAAGAACGCCGT), YOR1 (5'-GGCTGACCAAGATAGATG-3'), YOF1 (5'-GCGACCGCAAAGCCGGC-3) and YOF2 (5'-TTGGCCCCGGCTCCAGA-3), were used as sequencing primers as appropriate.

The DNA sequences of *hupSL*::gentamicin construct were determined by Automated DNA sequencing with the big dye terminator cycle sequencing kit (AmpliTaq FS, Applied Biosystems) was performed as specified by the manufacturer, Iontek, Istanbul. The following primers were used for sequencing.

Hup F: 5`-CCAGACTTGGTACCATGACGCGAAATTCCCTGCC-3`

Hup R: 5`-CCCAAATTCTAGAACCTTGTACCACTTATAAGG-3`

2.2.1.8. PCR based site-directed mutagenesis

The Quick Change site-directed mutagenesis kit was used to make His 53 Tyr mutations on cyt S-*c_y*R5 gene to get double mutant Cyt S-*c_y*R35. The QuikChange site-directed mutagenesis method is performed using *PfuTurbo*® DNA polymerase and a temperature cycler. *PfuTurbo* DNA polymerase replicates both plasmid strands with high fidelity and without displacing the mutant oligonucleotide primers. The

basic procedure utilized a supercoiled double-stranded DNA (dsDNA) vector with an insert of interest and two synthetic oligonucleotide primers containing the desired mutation. The oligonucleotide primers each complementary to opposite strands of the vector, are extended during temperature cycling by *PfuTurbo* DNA polymerase. Incorporation of the oligonucleotide primers generates a mutated plasmid containing staggered nicks. Following temperature cycling, the product is treated with *Dpn* I. The *Dpn* I endonuclease (target sequence: 5'-Gm⁶ATC-3') is specific for methylated and hemimethylated DNA and is used to digest the parental DNA template and to select for mutation-containing synthesized DNA. DNA isolated from almost all *E. coli* strains is dam methylated (methylation at the N⁶ position of adenine in GATC sequence by Dam methylase) and therefore susceptible to *Dpn* I digestion. The nicked vector DNA containing the desired mutations was then transformed into XL1-Blue competent cells. The synthetic oligonucleotide primers containing the mutation His 53 Tyr were

YO3 (5'-CCGCGATGAAGAACTATGTCGGCAACTGGACGC-3') and
 YO4 (5'-GCGTCCAGTTGCCGACATAGTTCTTCATCGCGG-3'). Primers were synthesized at Nucleic acid facility at University of Pennsylvania Cancer Centre.

Reaction Condition of Site-Directed mutagenesis

	Sample Reaction	Control Reaction
• Template DNA (50 ng/μl)	1μl	1μl
• ddH ₂ O	40μl	41μl
• Primers (Forward, 125 ng/μl)	1μl	1μl
• Primers (Reverse, 125 ng/μl)	1μl	1μl
• Buffer (10X <i>Pfu</i> pol. Buf.)	5μl	5μl
• Enzyme (<i>Pfu</i> DNA pol. 5 u/μl)	1μl	1μl
• dNTP Mix (5 mM)	2μl	2μl
Total reaction volume	50μl	50μl

Cycling Parameters for the Quick Change Site-Directed Mutagenesis Method

	Temperature	Time
• Initial denaturation	95 °C	1 min.
• Denaturation	95 °C	30 sec
• Annealing	55 °C	1 min.
• Extension	68 °C	10 min.
• Cycle number:	25	

Template DNA: pYO26, size: 4.2 kb.

2.2.2. Bacterial genetic techniques.

2.2.2.1. Competent cell preparation and CaCl₂ transformation

For *E. coli* HB101 and XL1-Blue competent cells, 50 ml LB and LB+Tet in a 500 ml flask were inoculated with 500µl over night culture of *E. coli* HB101 and XL1-Blue strains respectively. The inoculated cultures were incubated at 37°C with shaking until OD_{600 nm}= 0.4-0.5 (it takes nearly 2 hrs) and than cells were taken on ice. From this point, the cells must be on ice until heat shock step. Cells were centrifuged for 10 min at 4000 rpm at 4°C. Supernatant was discarded and the pellet was resuspended in 25 ml (1/2 of the culture volume) of ice-cold 100 mM CaCl₂ and incubated on ice for 30 min. Cells were centrifuged for 10 min at 4000 rpm at 4°C. Supernatant was discarded and pellet was resuspended in 2.5 ml (1/20 of the culture volume) of ice-cold 100 mM CaCl₂. Competent cells were aliquoted 100 µl into eppendorf tubes. For stock competent cells glycerol was added (final conc. 10%). 5-500 ng DNA was added to 100 µl competent cells and competent cells were incubated on ice for 45 min. Heat shock was applied to the sample for 5 min at 37°C. 1 ml LB was added and cells were incubated for 1 hr at 37°C with shaking. Cells were

centrifuged for 1 min at 4000 rpm at room temperature and resuspend in 100 µl LB. Cells were plated on a selection plate and incubated for overnight (Davis et al., 1986).

2.2.2.2. Triparental mating (Conjugation)

Two days before the cross, 1 ml Med A+ Kan was inoculated with a single colony of the recipient *R. capsulatus* FJ2 strain, which lacks both the cyt *c₂* Δ(cycA::kan), and cyt *c_y*, Δ(cycY::spe), from a fresh plate and incubated over night (18-24 hrs) at 34° C with shaking. The day before the cross 1 ml culture was added to 10ml Med A+ kan and incubated overnight (16-18 hrs) at 34°C. At the same day, 2 ml LB+kan was inoculated directly from the glycerol stock of the helper strain pRK2013/HB101. 2 ml LB+Tet or kan, depending on the vector, was inoculated with the donor strain pRK derivative/HB101 from a single colony on a fresh stock plate and grown overnight (12-16 hrs) at 37° C with shaking. The required number of Med A plates (number of crosses plus a control) were dried in the incubator for 30 min. The cell density of each culture was determined by using the following conversions (Ditta et al., 1985):

$$R. caps: 7,5 \times 10^8 \text{ cells/ml at } OD_{630\text{nm}} = 1$$

$$E. coli: 5,0 \times 10^8 \text{ cells/ml at } OD_{600\text{nm}} = 1$$

It is best to take OD at 1/10 dilution so that the value is well below 1. The cells were centrifuged for 10 min at 4000 rpm at room temperature. The cells were washed twice with 1ml Med A to remove all antibiotics. The cells were resuspended in a volume of Med A that the final cell density was 10¹⁰/ml. In the middle of Med A plate, 100µl of recipient *R. capsulatus* was pipetted; to the spot 20 µl of each of helper and donor *E. coli* were added and mixed well. Plates were waited for absorption of the spot into the agar completely before placing it in the incubator for the night. The control plates

were made with just the recipient/helper and recipient/donor in the spot as the control. Approximately 24 hrs later, the cells were collected from each spot in 1 ml Med A and transferred to eppendorf tubes. The cells were centrifuged for 1 min at 13000 rpm at in microcentrifuge room temperature. The supernatant was discarded, and the cells were washed in 1 ml Med A. The cells were resuspended in 400 μ l Med A. 10 μ l and 100 μ l of the cell suspension were plated on Med A plates with appropriate antibiotic; as for the control, 100 μ l of the recipient/helper and recipient/donor were plated on a selection plate were incubated for 2-3 days. At least 4 transconjugants from each cross were purified by picking from the centre of well-separated colonies and streaked on MPYE or Med A plate with appropriate selection. If Ps phenotype is be checked, then a duplicate set of plates is made from the same colonies, and one was incubated under Res condition, the other under Ps conditions. Glycerol stocks of the transconjugants were made, and frozen at -80° C. All crosses were listed in Table 2.2.

2.2.2.3. Photosynthetic growth:

For photoheterotrophic growth on solid media, anaerobic jars and H₂+CO₂ generating gas packs from Oxoid were used. The strains were streaked on MPYE or Med A plate with appropriate selection. The petri dishes were placed in the carrier. An Oxoid anaerobic indicator (BR55) was opened and exposed 10 mm of the fabric strip. The sachet was inserted into a smaller, upper clip on the dish carrier. The corner of an Oxoid gas generating kit (BR38) was cut and 10 ml water was added to the sachet and immediately inserted in the lower clip of the dish carrier. The carrier was put into the polycarbonate base (HP11). The lid containing catalyst on the base was placed and screwed down the knurled well until tight. The pressure gauge was observed. First the pressure increased up to 0.3 bar then it fell over a period of 30-40 min to 0.1 bar. Note that the pressure will not fall in the presence of an inactive

catalyst. After 2-3 hrs, the anaerobic indicator will change from pink to incolor. Plates were incubated for 4 days at continuous illumination. To increase the rate of activity, the catalyst should be dried between uses by heating to 160° C for 90 min as advised by producer.

2.2.2.4. Photosynthetic reversion

1ml MedA+Tet and 1ml MPYE+Tet were inoculated with a single colony of the various cyt S-*c_y* derivatives from a fresh plate and incubated over night (16-18 hrs) at 34° C with shaking. The cells were transferred to eppendorf tube and centrifuged for 1 min at 13000 rpm at room temp. The cells were dissolved in 100 µl sterile distilled water. 10 µl and 90 µl of cells were plated on both MedA+Tet and MPYE+Tet. Plates were incubated around 4-5 days at anaerobic condition with continuous illumination for Ps growth. Reverted cells grow at anaerobic condition by Ps and give single colonies. Selected colonies were further purified at least twice under the selective growth conditions. Then the plasmids carrying the structural genes in the reverted *R. capsulatus* strains were isolated and re-transferred into the cyt *c₂*⁻, *c_y*⁻ double mutant FJ2 to determine the chromosome- or the plasmid-borne state of the reversion mutation. Next, the molecular nature of the mutation was defined by sequencing the entire 1.2 kb DNA fragment that carried *cycY*.

2.2.2.5. Chromosomal inactivation of uptake hydrogenase: Gene transfer agent (GTA) cross

Uptake hydrogenase (Hup) minus derivatives of *R. capsulatus* strains were obtained using the *R. capsulatus* gene transfer agent (GTA) (Yen *et al.*, 1979). For

this purpose, a $\Delta(hupSL::gen)$ insertion-deletion allele was constructed and transferred into an *R. capsulatus* GTA overproducer strain such as Y262.

GTA preparation: Many colonies of a GTA producing strain (such as Y₂₆₂ strain with a plasmid containing the desired insertion-deletion allele of the gene of interest) from MedA plate were picked and inoculated into MPYE in a 5-10 ml screw-cap tube and filled up to top. Cells were incubated for 3-5 days under photosynthetic growth conditions until slight cell lyses were visible. The samples were centrifuged at 4 K for 5 min. 5 ml of the top supernatants were taken, and filtered aseptically through a 0.45 μ , and then 0.2 μ disposable filters. The filtrates which contain GTA were kept at 4° C, and their sterility tested using MPYE plates.

GTA Cross: 10 ml of recipient *R. capsulatus* strains were grown in MPYE by photosynthesis or by respiration as required for the specific conditions of the cross. The cultures were streaked onto MPYE plate to check for contamination.

The samples were centrifuged in sterile screw-cap tube at 4.000 rpm at 20° C for 10 min and, the pellets were resuspended in 2.5 ml GTA buffer. The samples were centrifuged for 10 min at 10 K to pellet the recipient cells, and the cells were washed for two more times. At the end of the third wash cells were resuspended into 1 ml GTA buffer.

The crosses were set up as follows:

GTA control:	No cells	100 μ l GTA	200 μ l GTA Buffer
Recipient cells:	200 μ l cells	no GTA	100 μ l GTA buffer
Cross:	100 μ l cells	100 μ l GTA	100 μ l GTA buffer

The tubes were mixed gently by shaking (no vortex), and incubated at 37° C for 10 min then at 35° C for 2 hours. 3 ml MPYE top agar (0.7 % agar kept at 45° C) was added to each tube, mixed well and poured onto appropriate selective plates (i.e., MPYE with gentamicin). The plates were incubated for 2-3 days at respiratory or photosynthetic growth conditions.

2.2.3. Biochemical and biophysical techniques.

2.2.3.1. Isolation of chromatophore vesicles and membrane sheets.

Intra-cytoplasmic membrane vesicles, or chromatophores, and chromatophore supernatant fractions (containing cytoplasmic and periplasmic proteins) were prepared from *R. capsulatus* cells grown semiaerobically in MPYE, by using a French pressure cell (SML Aminco, Inc) at 18000 lb/in².

Chromatophore membrane preparation for SDS-PAGE, TMBZ analysis:

Three days before the chromatophore isolation, 1 ml MPYE+ antibiotic was inoculated with a single colony of the strains of *R. capsulatus* from a freshly streaked plate and incubated over night (18-24 hrs) at 34 °C with shaking at 150 rpm. Next day, 1 ml culture was added to 10 ml MPYE+tet and incubated overnight (16-18 hrs) at 34°C. The day before starting chromatophore isolation, 10 ml cultures were transferred to 1 L MPYE+tet medium in 1 L flasks shaking at 150 rpm and incubated overnight (24 hrs) at 34°C. The cells were centrifuged at 8000 rpm and at 4°C for 15 minutes. The supernatants were discarded, and cells were resuspended in 30 ml 50 mM MOPS (pH: 7) / 1 mM KCl buffer. Resuspended solutions centrifuged again at 10.000 rpm and 4 °C for 10 minutes and supernatants were discarded. Before breaking the cells, pellets were resuspended in 10 ml 50 mM MOPS/1mM KCl solution containing, RNase, DNase (10 mg/ml), 1 mM MgCl₂ and 1 mM PMSF (Phenylmethanesulphonyl Floride dissolved in DMSO) which was added just before breaking the cells and mixed well. Then cells were broken by passing through a French press at 18000 psi. This process was repeated one more time, and the broken cells were centrifuged to remove the cells and membrane debris at 17 000 rpm for 45 minutes. Supernatants containing chromatophore membranes and cytoplasmic soluble proteins were transferred to appropriate ultracentrifuge tubes. The chromatophore membrane fraction was obtained

by centrifuging at 45 000 rpm and 4 °C for two hours, and the supernatant containing cytoplasmic soluble proteins were kept at -20 °C. As needed, the supernatant fractions were re-centrifuged at 45 000 rpm and 4 °C for 12-16 hours to pellet small membrane fragments from the soluble cell fraction. Chromatophore membrane fragments were then washed and resuspended in 10 ml 50 mM MOPS/1 mM KCl buffer with a paint brush and then centrifuged at 45 000 rpm and 4 °C for two hours. Finally, pellet was dissolved in 1 ml 50 mM MOPS/1 mM KCl buffer containing 1 mM PMSF and kept in -80 °C (Gray *et al.*, 1994).

Chromatophore membrane preparation for light activated kinetic spectroscopy analyses: The cells were grown in 1 L MPYE (or MedA) in a 2 L flask at 35°C, 150 rpm in the dark for 25-27 hours starting from a 10 ml preculture. The cells were harvested by spinning 15 minutes at 8 000 rpm, 4°C in the JA10 rotor. The pellets were resuspended in 60 ml of cold MOPS-KCl buffer (50 mM MOPS pH 7.0, 100 mM KCl). The cells were centrifuged again 15 minutes at 8000 rpm, 4°C. The cells were washed ones more and centrifuged 20 minutes at 10K in the JA17 rotor. The cells were resuspended in 30 ml of MOPS-KCl EDTA buffer (50 mM MOPS pH 7.0, 100 mM KCl, 1 mM EDTA) for 1 L culture. DNase (50 µl of 10 mg/ml) was added to sample. Just before using the French press, PMSF from a 0.1 M solution in DMSO was added at a final concentration of 1 mM. Cells were broken by two passages through the French press at 18000 psi. The broken cells were centrifuged at 17 000 rpm, 4°C 45 minutes. The supernatant were transferred by using transfer pipettes (don't pour it). For flash kinetic experiments especially, only the 2 upper thirds were taken. The samples were centrifuged 2 hours at 45 000 rpm, 4°C. The pellets were washed 3 times in the MOPS-KCl EDTA buffer and spin 50 minutes at 45 000 rpm. At the end, the pellet was resuspended in 1 ml of MOPS-KCl EDTA buffer. The last resuspension was done carefully with a brush in order not to leave particles.

2.2.3.2 Determination of the protein amount by the Lowry assay

Chromatophore vesicle concentration was determined by the Lowry method, using BSA as a standard protein (Lowry et al., 1951). To prepare the standart BSA protein solution to be used as a standard, 1 g solid BSA (Bovin Serun Albumin) dissolved in 1 ml ddH₂O and, 20, 40, 60, 80, 100 µl protein solutions from 1µg/µl stock BSA were added into five eppendorf tubes, respectivelly and final volume completed to 200 µl by adding required amount of 1% SDS/0.1N NaOH. 10 µl chromatophore samples from each mutant was dissolved in 990 µl MOPS/KCl buffer (50 mM/ 1mM, pH:7.0). Then 50 µl and 100 µl diluted chromatophore samples from each mutants were mixed with 150 µl and 100 µl 1 % SDS/0.1 N NaOH solution respectively and than reagent E (**Appendix B**) was added to BSA standard and chromatophore memebbrane proteins and they incubated at RT for 10 minutes. Then 100 µl 1 N Folin and Ciocalteu's Phenol reagent was added to all samples, and they were incubated at RT for 30 minutes. The standard curve was made by the mesurement of the OD of the standart BSA samples at 650 nm.

2.2.3.3. Tricine SDS-PAGE (16.5 % Schägger) gel

Schägger-type Sodium dodecyl sulfate SDS-PAGE were performed using 16.5% acrylamide Tris-Tricine gel as described in (Schägger et al., 1987). Acrylamide-Bis Acrylamide mixture (49.5% T, 3%C), Gel buffer (3M Tris, 0.3% SDS, pH 8.45), Glycerol, H₂O, Ammonium persulphate (APS, 10%) and TEMED were used for separating and staking gels (**Appendix B**). First separating, running gel, was prepared then after 45 minutes, staking gel was poured. After polymerization of the gel, which takes about two hours, samples were loaded. Before loading the chromatophore samples on SDS-PAGE, equal volume of the loading dye (**Appendix C**) was added to samples and β-Mercaptoethanol (MBE) was added just prior to use

and they are incubated at 37 °C for five minutes. Usually 100 µg chromatophore proteins were loaded on 16.5 % Schägger type SDS-PAGE and run first at 30V for 1 hour than at 90-120V for 20-24 hours. To monitor the migration of the proteins on gels, Kaleidoscope Prestained Standards (BIO-RAD, # 161-0324) were used.

Schägger Gel (16,5 %)

	<u>Separating (Running gel)</u>	<u>Stacking Gel</u>
Glycerol	5.3 g	-
Acry/Bis	13.3 ml	1 ml
Gel Buffer	13.3 ml	3.1 ml
dH ₂ O	4.5 ml	8.4 ml
10% APS	0.065ml	0.1 ml
TEMED	0.01 ml	0.01 ml
Total:	40 ml	12.5 ml

2.2.3.4. TMBZ staining of c-type cytochromes

The *c*-type cyts were revealed by their heme peroxidase activity, using 3,3', 5, 5'-tetramethylbenzidine (TMBZ) and H₂O₂ (Thomas *et al.*, 1976). Schägger type SDS-PAGE gel was washed with 0.25 M Na- Acetate buffer, pH 5 for 20 minutes. Washing of the gel was repeated three times, while 45 mg TMBZ, 3, 3', 5, 5' Tetrametyl Benzidine, were dissolved in 30 ml methanol and mixed with 70 ml 0.25 M Na-Acetate (dissolving takes place 20- 30 minutes, covered with aliminium foil) Then gel was placed in TMBZ solution and washed it by shaking gently for 1 hr in dark (TMBZ percipiates on the gel as white powder). Finally, 1240 µl 30% Hydrogen peroxide, H₂O₂, was added (to 30 mM) and gel was incubated for more 10-30 minutes at room temperature. After bands appeared, the solution was poured off

and gel was covered with ioproponol and 0.25 M sodium-acetate mix (3:7 ratio), and the pictures of the gels were taken.

2.2.3.5. Spectroscopic analysis

Optical spectra were recorded on a Perkin-Elmer UV/vis spectrophotometer (Lambda 20), fitted with an anaerobic redox cuvette, as needed. The difference spectra for *c*-type cyts were obtained with samples that were first oxidized by the addition of potassium ferricyanide (to a final concentration of 20 μ M) and then reduced by using either sodium ascorbate (added to a final concentration of 1 mM), or a minimal amount of solid, fresh dithionite. Chemical oxidation-reduction midpoint potential titrations of supernatant fractions of chromatophore membranes were performed in 50 mM MOPS, 100 mM KCl pH 7.0 (Dutton et al., 1978) in the presence of the redox mediators tetrachlorohydroquinone, 2,3,5,6-tetramethyl-1,4-phenylenediamine, 1,2-naphtho quinone-4-sulfonate, 1,2-naphthoquinone, phenazine ethosulfate, phenazine methosulfate, duroquinone, pyocyanine, 2-hydroxy-1,4-naphthoquinone, and anthraquinone-2-sulfonate at concentrations of 15 to 30 μ M, (Prince et al., 1986). The optical changes that accompanied ambient redox potential change were recorded in the α -band region (500-600 nm), and the E_m values were determined by fitting normalized data to a single $n = 1$ Nernst equation.

2.2.3.6. Light-Activated absorption spectroscopy.

Light-activated, millisecond time scale kinetic spectroscopy was performed using chromatophore membranes prepared as indicated in the Materials and Methods section, in 50 mM MOPS/ 100 mM KCl pH 7 buffer. The samples were adjusted to around 20 μ M bacteriochlorophyll corresponding to around 0.2 μ M RC final

concentration and chromatophore membranes were reduced with sodium ascorbate to adjust the potential to 100 mV (the potential should be very stable before starting the experiment). The double-beam flash photolysis spectrophotometer was used as described earlier, and actinic flashes were provided by a xenon flash lamp (full width at half-height about 12 μ s) filtered through a Schott RG780 filter (Prince et al., 1986; Jenney et al., 1994). These flashes were greater than 95% saturating under the experimental conditions used. Following a flash of actinic light (eight flashes for multiple turnover ET kinetics and single flash for single turnover ET kinetics), cyt *c* re-reduction kinetics in the absence or presence the cyt *bc₁* complex inhibitor stigmatellin (2.5 μ M), and the carotenoid bandshifts in the presence of valinomycin (2.5 μ M), were monitored in the millisecond time domain at 550 – 540 nm and 490 – 475 nm, respectively, to reveal ET kinetics of various cyts to the RC.

2.2.4. Cloning strategies for cyt S-*c_yR5* (cyt S-*c_y*)

The 1.2 kb *KpnI-BamHI* fragment carrying cyt S-*c_y* Ps⁺ revertants with R5 (K19R) mutations were cloned to both pBSII and the broad host range plasmid pRK415 using the same *KpnI /BamHI* sites on multiple cloning site, to yield the plasmids pYO26 and pYO105 (cyt S-*c_yR5*) respectively (**Figure 2.1**). Plasmid pYO105 was transferred to *E. coli* for sequencing and recross into FJ2 strain.

2.2.5. Cloning strategies for double mutant cyt S-*c_yR35* (cyt S-*c_y*)

The double mutant cyt S-*c_yR35* combining the mutations R3 (H53Y) (Öztürk et al., 2001) and R5 (K19R) was constructed by site-directed mutagenesis of pYO26, carrying the cyt S-*c_yR5* allele in pBSII, using the QuikChange mutagenesis kit (Stratagene Inc.) as recommended by the manufacturer. Briefly, 25 cycles of 95° C

for 30 sec, 55° C for 1 min, and 68° C for 10 min were used with the mutagenic primers containing R3 (H53Y) mutation

YO3 (5'-CCCGCGATGAAGAACTATGTCGGCAACTGGACGC-3') and
YO4 (5'-GCGTCCAGTTGCCGACATAGTTCTTCATCGCGG-3'),

to yield pYO27. The obtained 1.2 kb *Kpn*I-*Bam*HI fragment of pYO27 was then cloned into the same restriction sites of the broad host range plasmid pRK415 to yield pYO135 (cyt S-*c*yR35) (**Figure 2.2**).

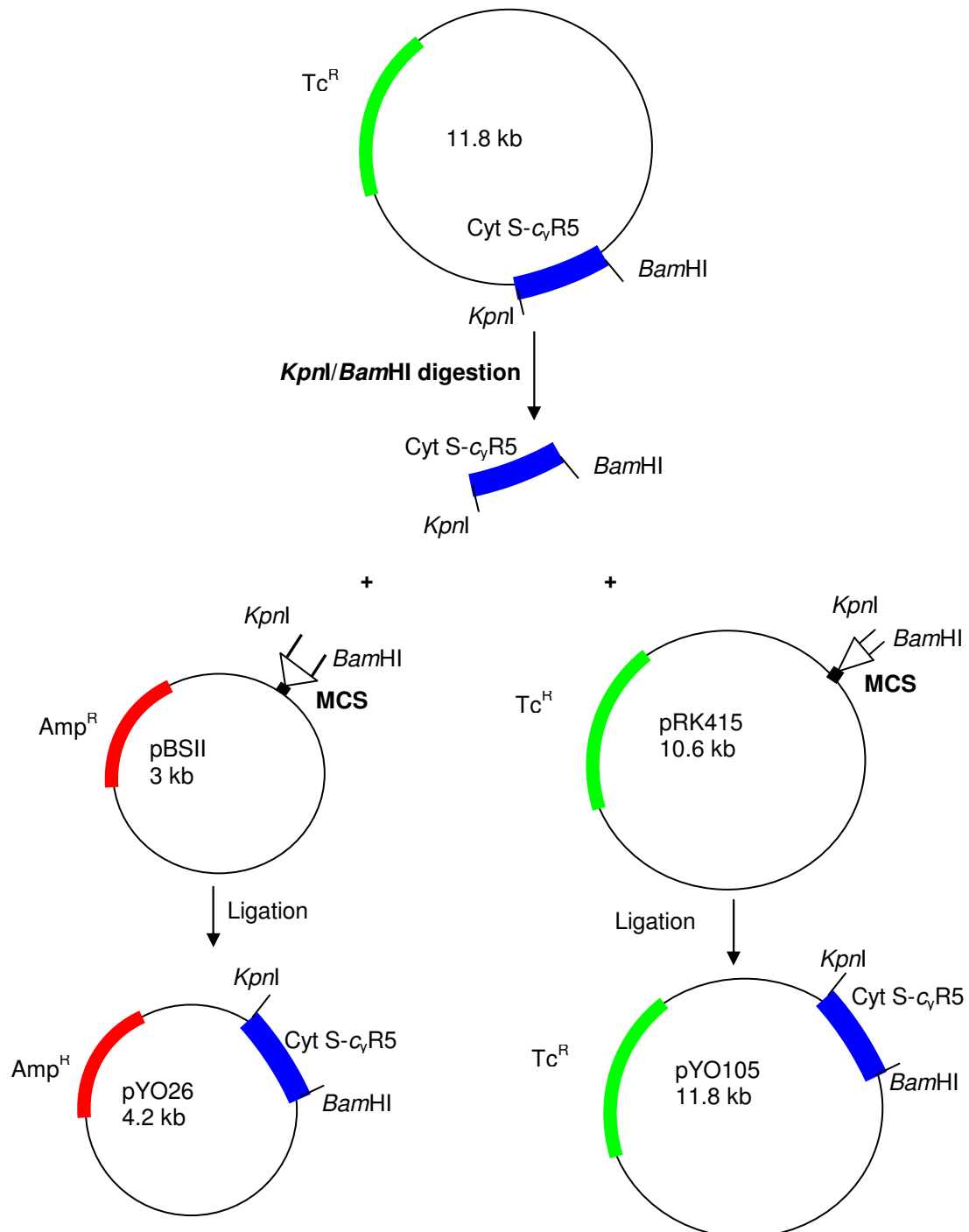


Figure 2.1. Cloning strategies for pYO26 and pYO105 in that 1.2 kb *KpnI/BamHI* fragment containing cyt S-*c_y*R5 was cloned to pBSII and pRK415.

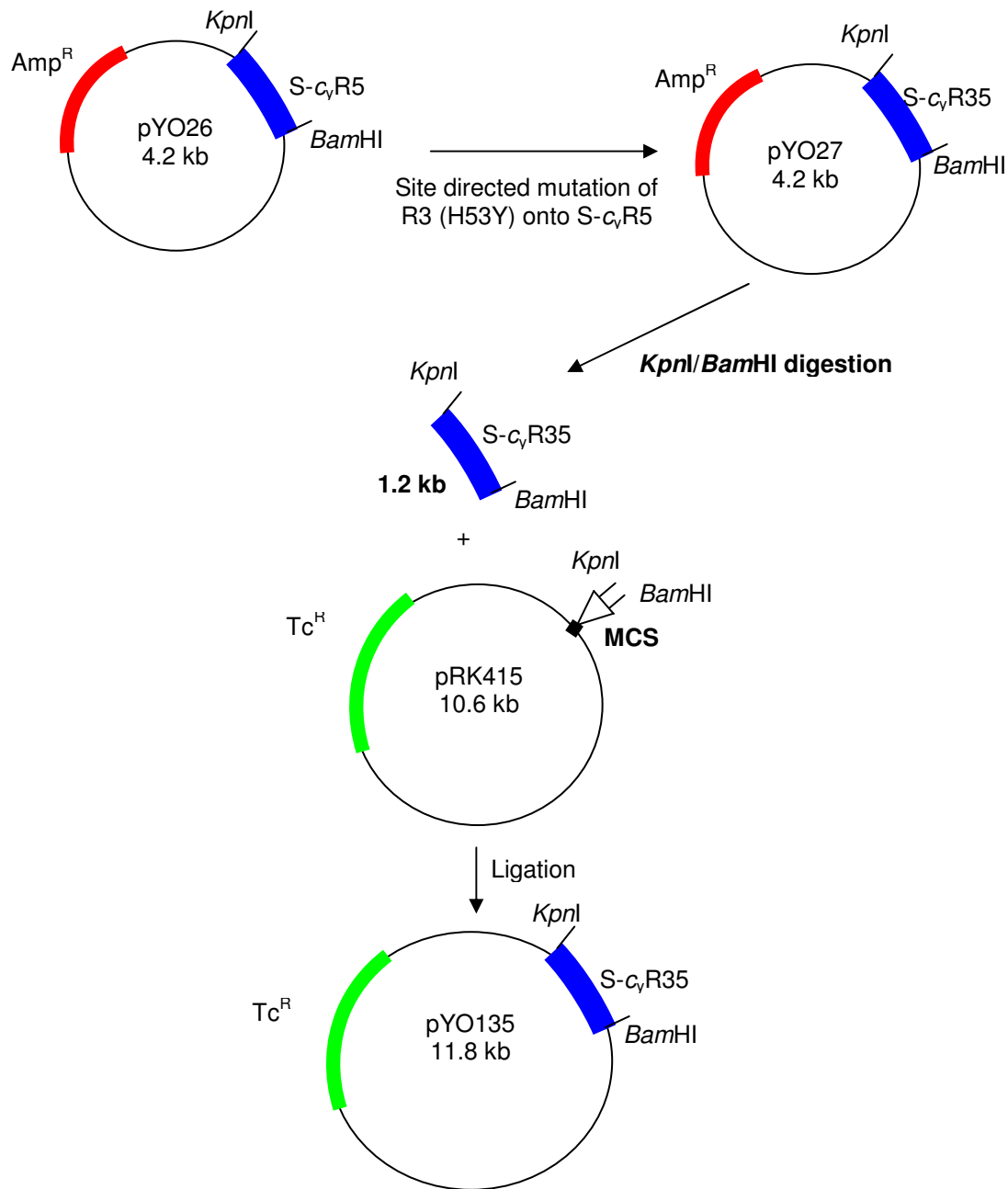


Figure 2.2. Site directed mutagenesis of R3 (H53Y) and cloning of resulted mutant cyt *S-c_yR35* to pRK415 plasmid.

2.2.6. Cloning strategies for *hupSLC*

For this cloning, mutagenic primers HupF with *Kpn*I (ggtac/c) and HupR with *Xba*I (t/ctaga) restriction enzyme sites that are not present inside the *hupSLC* operon (**Appendix F**) were used to amplify the 4.1 kb *hupSLC* operon by PCR and clone to pBSII and pRK415 (**Appendix F**) to yield pYO39 and pYO40 respectively (**Figure 2.3**). Mutagenic primers (synthesized by Iontek, Istanbul):

Hup F: 5`-CCAGACTTGGTACCATGACGCGAAATTCCCTGCC-3`

Hup R: 5`-CCCAAATTCTAGAAACCTGTTACCACTATAAGG-3`

PCR amplification:	Initial denaturation	96°C for 5 min,	
	denaturation	96°C for 1 min,	35 cycles
	annealing	65°C for 1 min,	
	extension	72°C for 8 min, 12 sec	

2.2.7. Construction of the $\Delta hupSL::gen$ insertion-deletion allele

The $\Delta(hupSL::gen)$ insertion-deletion allele was constructed by cloning the 1.2 kb *Hind*III/*Bam*HI fragment containing gentamicin structural gene driven by the *R. capsulatus cycA* promoter into the *Bal*I (blunt end) and *Bam*HI sites of the pYO39 carrying the *hupSLC*. For this cloning *Hind* III site was blunted by T4 polymerase enzyme. The 2.3 kb *Bal*I / *Bam*HI fragment covering the large portion of *hupS* and *hupL* genes was replaced by 1.2 kb gentamicin cassette and pYO41 plasmid containing $\Delta hupSL::gen$ was obtained. Then the 3 kb *Kpn*I / *Xba*I fragment of pYO41 containing $\Delta hupSL::gen$ insertion-deletion allele was cloned on pRK415 to yield pYO42 (**Figure 2.4**). The pYO42 was transferred to GTA over producer Y₂₆₂ strain by three parental conjugation and used to obtain chromosomal inactivation of the *R. capsulatus hupSL* genes by GTA cross (section 2.3.4).

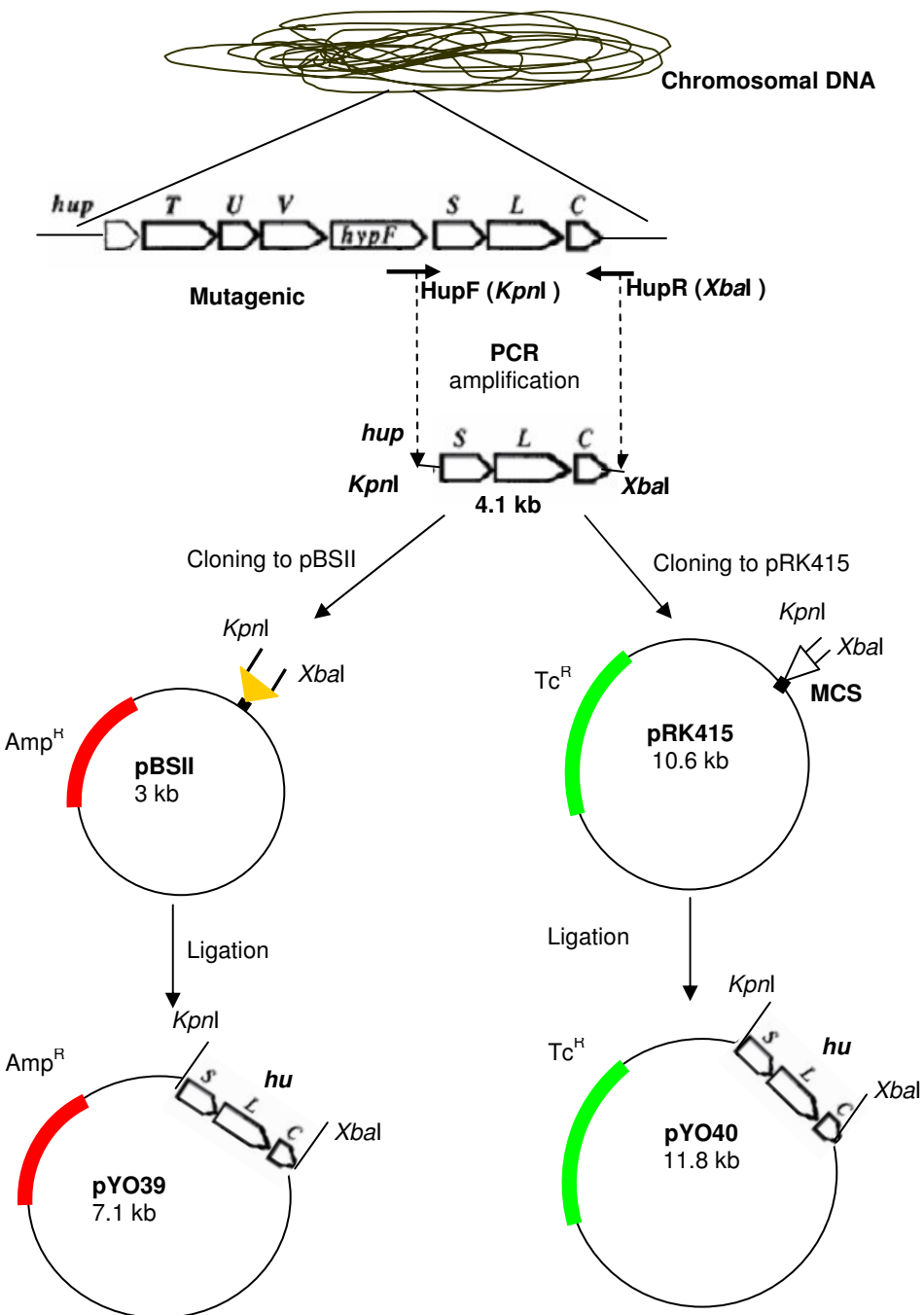


Figure 2.3. Amplification of the structural genes of uptake hydrogenase (*hupSLC*) and cloning strategy to pBSII and pRK415 plasmids. Mutagenic primers containing *KpnI* and *XbaI* Restriction Enzyme (RE) sites were used to amplify the *hupSLC* operon and to clone in pBSII and pRK415.

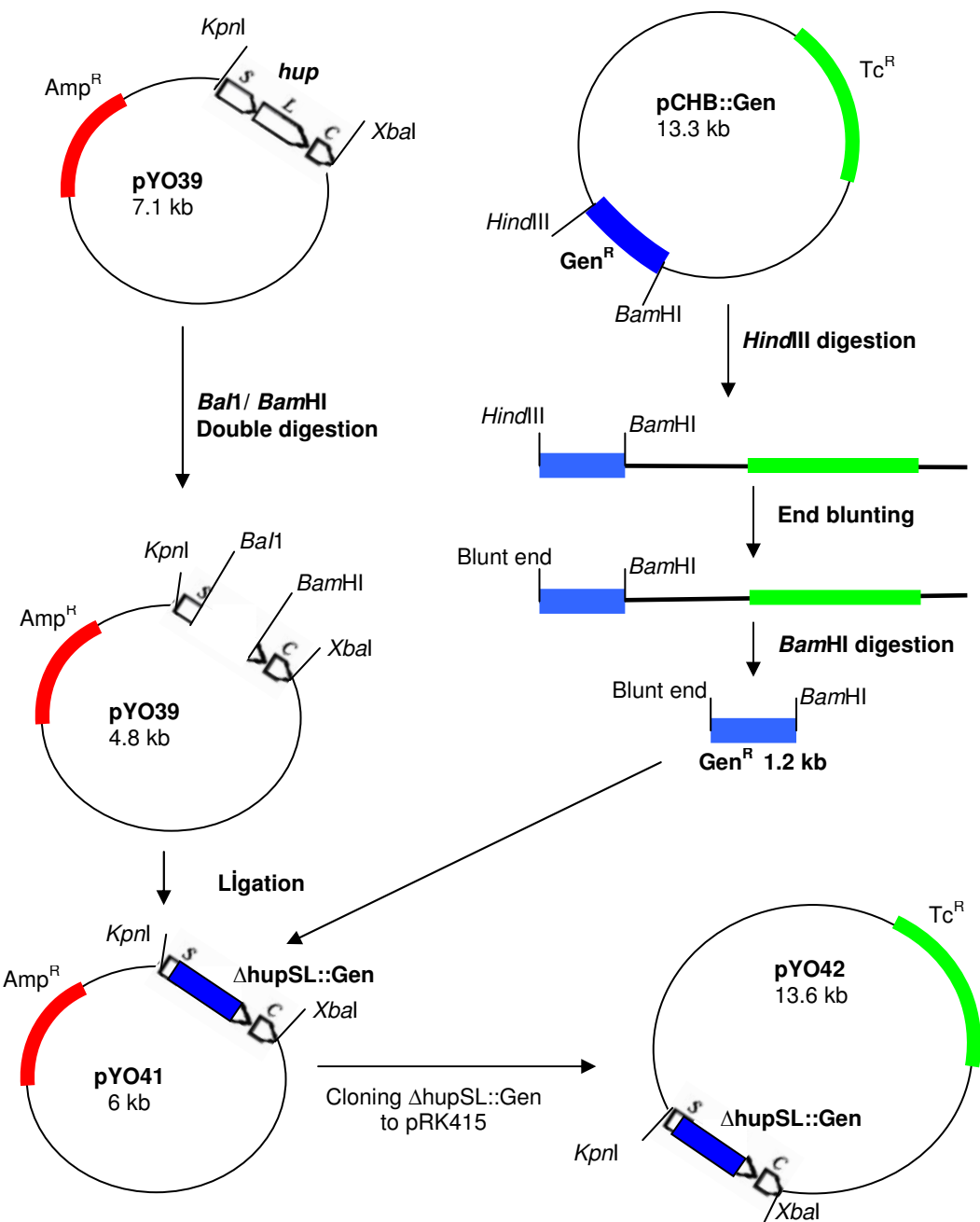


Figure 2.4. Construction of the $\Delta hupSL::gen$ insertion deletion allele and cloning of it to pRK415 plasmid.

2.2.8. Bioreactor setup for hydrogen production

2.2.8.1. Experimental setup for hydrogen production.

Hydrogen production profiles of different *R. capsulatus* mutant strains were analyzed by using 55 ml small scale glass bottle photobioreactors. Fully filled photobioreactors (anaerobic atmosphere) were connected to water filled H₂ collection tubes. The produced H₂ gas replaced the water and decreased its level which was monitored by a webcam connected to computer (**Figure 2.5**). The bioreactors containing 55 ml of BP medium supplemented with 15 mM/2 mM malate-glutamate were inoculated with 1ml pre-activated cultures under sterile conditions and incubated at 30-33°C under a light intensity of 4000 lux at the surface of the reactor. The illumination was provided by a 150 W tungsten lamp, and the initial pH values of the growth medium was about 6.8.



Figure 2.5. Bioreactor setup for hydrogen production. Photobioreactors were connected to water filled H₂ collection tubes and incubated at 30-33°C under the light intensity of 4000 lux for hydrogen production.

For activation of the bacteria, 1 ml BP cultures were inoculated with *R. capsulatus* strains from a fresh plate, and incubated over night (18-24 hrs) at 30-33° C under the light intensity of 4000 lux. The following day, a 5 ml sample tube fully-filled with BP and incubated under the same conditions for over night growth. The 1ml of pre-activated cultures were used to inoculate the 55 ml bioreactors under sterile conditions.

2.2.8.2. Sampling and analyses

Liquid samples of 1 ml were collected from the bioreactors by a sterile syringe at time intervals for the analysis of both pH and cell density. The pH of the culture was measured with a standard combination pH electrode (Mettler Toledo 3311) and an electronic transmitter (Nel pHR-1000 Transmitter). Cell concentrations were determined by measuring the optical density of the culture at 660 nm (OD_{660}). Also, dry cell weight analysis was performed in one of the experiments. The produced gas was analysed by gas chromatography. A Hewlett-Packard Series II system with a thermal conductivity detector and a Propak Q column was used. The oven, injector and detector temperatures were 30, 40 and 50°C, respectively. Nitrogen was used as the carrier gas (Koku et al., 2003)

2.2.9. Dry weight analysis

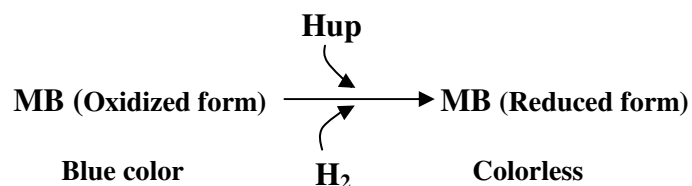
10 ml of sample cultures from 500 ml culture were taken at different time intervals. Their OD_{660} were measured and dilution is done wherever necessary (when $OD_{660}>1$), then samples were centrifuged at 4,000 rpm for 15 min. The supernatants were removed, and pellets were re-suspended in 1 ml distillated water and transferred to 1,5 ml eppendorf tubes. Samples were

centrifuged at 13,000 rpm for 2 min and pellets were dissolved in 200 μ l distilled water and transferred to small, pre-weighed aluminum cups. The pellets were dried for 5-6 hours at 50 °C in oven and cups containing the dried bacteria were weighed. The bacterial dry cell weight in g bacteria/l culture was determined by subtracting the empty cup weight from the total weight of the cup with the dried pellet. The dry weight versus OD₆₆₀ calibration was plotted from the samples corresponding to various points of the growth curve.

2.2.10. Assay of hydrogenase activity

Hydrogenase activity in whole cells was assayed by following the reduction of methylene blue (MB) linked to H₂ oxidation. The reactions were carried out in capped vials containing cell suspension in 1 ml of 20 mM Tris-HCl pH 8, and 30 μ l of 10 mM MB (final 0.15 mM) and made anaerobic by gassing with Ar. After the passing H₂ gas, the samples were incubated at 25° C (room tem) for 20-30 min. Absorbance was measured at 565 nm at (Cauvin et al. 1991).

The reaction in this assay is as follows



CHAPTER 3

RESULTS AND DISCUSSION

In this study, *Rhodobacter capsulatus* was used as a model system for understanding the role of its electron transport chain components, and the effects of these components on hydrogen production metabolism. For these purposes, functional soluble variant of membrane bound electron carrier cyt *c_y* was obtained characterized as described in sections 3.1-3.9 of this thesis. The interaction of the electron transfer chain components with hydrogen metabolism and the genetic modifications in cyt systems and uptake hydrogenase genes were also analysed and presented in sections 3.10-3.17 of this thesis.

3.1. Isolation of Ps⁺ revertants of soluble cyt S-*c_y*: cyt S-*c_yR5* and FJ2-R4 chromosomal reversion

The constructed soluble cyt S-*c_y* was initially unable to support photosynthesis of FJ2 strain (cyt *c₂*⁻ cyt *c_y*⁻) (Öztürk et. al., 2001). However the strains, harboring cyt S-*c_y*, produced Ps⁺ revertants frequently in both minimal and enriched media (at a frequency of 10⁻⁶ to 10⁻⁷ on MPYE medium), and several of them were isolated. The obtained Ps⁺ revertants were tested several times on growth mediums with appropriate antibiotics under the photosynthetic conditions to confirm the reversion phenotype.

In order to define the molecular nature of the mutations in the Ps⁺ revertants, the plasmids that they harbored were isolated, sequenced and re-crossed

into the strain FJ2 to test their ability to confer the Ps⁺ growth phenotype. The data indicated that the mutations responsible of the Ps⁺ phenotype were plasmid-borne in the case of Reversion 3 (R3) yielding cyt S-*c_y*R3 (His53Tyr) (Öztürk et al., 2001) and Reversion 5 (R5) yielding cyt S-*c_y*R5 (Lys19Arg), and was located on the chromosome in the case of Reversion 4 (R4).

The plasmid of revertant R4 (had a chromosomal mutation) was cured of by successive subcultures on MPYE medium without any antibiotic selection to yield FJ2-R4. Although the determination of the molecular nature of this chromosomal mutation was out of the scope of this work, nonetheless, this mutant turned out to be useful for subsequent work because of its ability to better support Ps⁺ growth of cyt S-*c_y* variants.

3.2. Sequence analysis of the Ps⁺ revertants

The plasmids from R4 and R5 were isolated and transferred to *E. coli* HB101 strain for further cloning and DNA sequencing. DNA sequence determination revealed that R5 (cyt S-*c_y*R5) contained A to G base pair substitutions resulted in K19R mutation in cyt *c* domain of cyt S-*c_y*R5 (**Figure 3.1**). DNA sequencing of plasmid from R4 indicated that it did not contain any mutation in *cycY* but contained mutation on its chromosome.

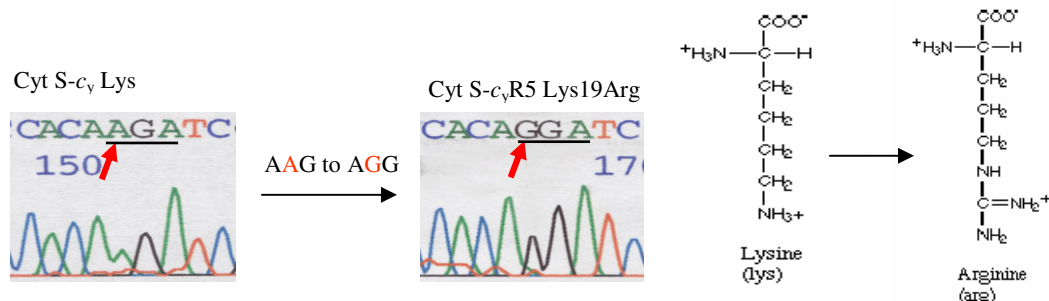


Figure 3.1. DNA sequence of the R5 mutation on cyt S-*c_y*R5 (AAG to AGG - Lys19Arg).

3.3. Cloning of the Ps⁺ revertant cyt S-c_yR5

For molecular and bacterial genetic studies, the 1.2 kb *KpnI/BamHI* fragment of the plasmid which was isolated from R5 carrying the mutation K19R was cloned to both pBSII and the broad host range plasmid pRK415 by using the same *KpnI /BamHI* restriction enzyme sites as described in Materials and Methods (**Figure 2.2 and 3.2**). The insert of resulted plasmids pYO26 and pYO105 respectively were controlled by the digestion of these plasmids by *KpnI* and *BamHI* enzymes, and the corrections of obtained plasmids were confirmed. (**Figure 3.2 B and D**).

3.4. Construction of double mutant cyt S-c_yR35

3.4.1. Site directed mutagenesis for double mutant cyt S-c_yR35

To combine the effect of R3 (His53Tyr) and R5 mutations on the same cyt S-c_y, the mutation R3 was created on pYO26, carrying the cyt S-c_yR5 (Lys19Arg), by site-directed mutagenesis as described in Materials and Methods (**Figure 2.3**). Following temperature cycling, the PCR product of the sample reaction was seen on agarose gel (**Figure 3.3 A**). Remaining PCR products were treated with *DpnI*, specific for methylated and hemimethylated DNAs, to digest the parental template DNA and to select mutated and PCR synthesized DNA. Following *DpnI* treatment, PCR product was transformed into *E. coli* XL-1 blue strain to select the double mutant. Four of the transformants were selected to determine mutation by sequencing (**Figure 3.3 B**). The obtained plasmid pYO27 carrying double mutant cyt S-c_yR35 (H53Y and K19R) was sequenced to confirm the both H53Y and K19R mutations (**Figure 3.4**).

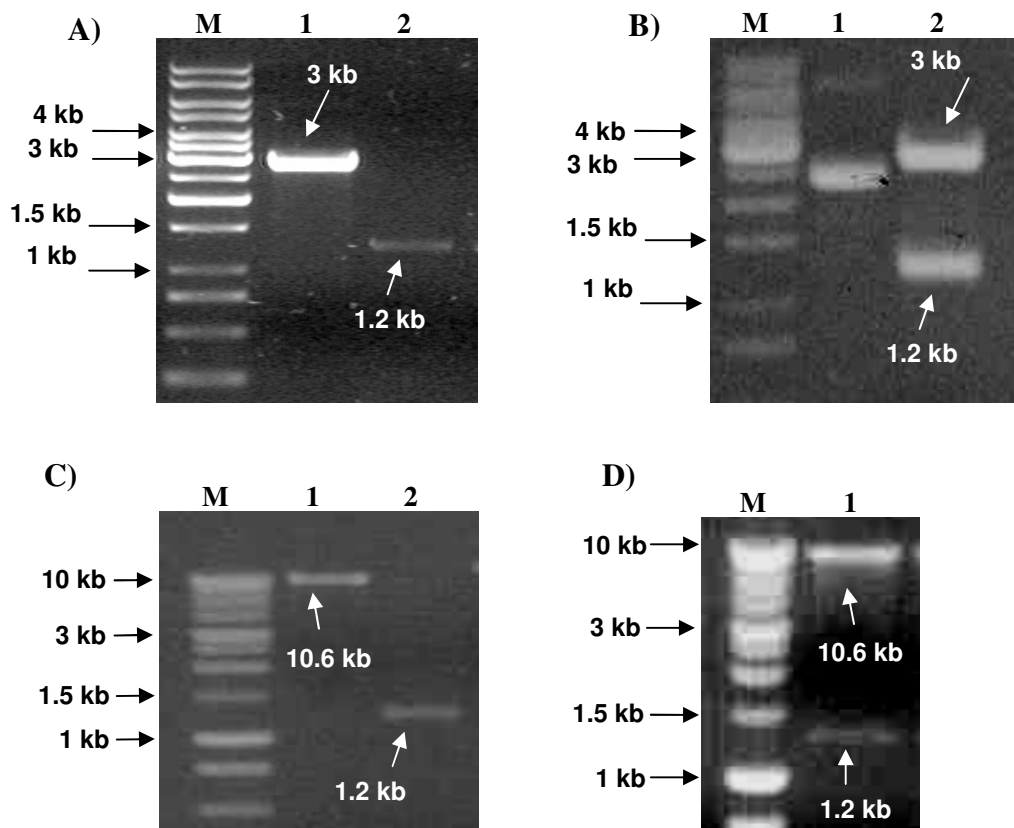


Figure. 3.2. Agarose gel (1%) electrophoresis results for the cloning of cyt S-*c_y*R5 on pBSII and pRK415. **A:** The 1.2 kb *Kpn*I/*Bam*HI fragment carrying the S-*c_y*R5 gene (line 2) was cloned to 3 kb pBSII vector (line 1) and pYO26 was obtained. **B:** Control enzymatic digestion of pYO26. Line 1; uncut pYO26 plasmid, line 2; *Kpn*I/*Bam*HI digestion of pYO26. **C:** The 1.2 kb *Kpn*I/*Bam*HI fragment carrying the S-*c_y*R5 gene (line 2) was cloned to 10,6 kb pRK415 vector (line 1) and pYO105 was obtained. **D:** Control enzymatic digestion of pYO105 with *Kpn*I/*Bam*HI (line 2). M; represents 1 kb DNA ladder marker (MBI Fermentas).

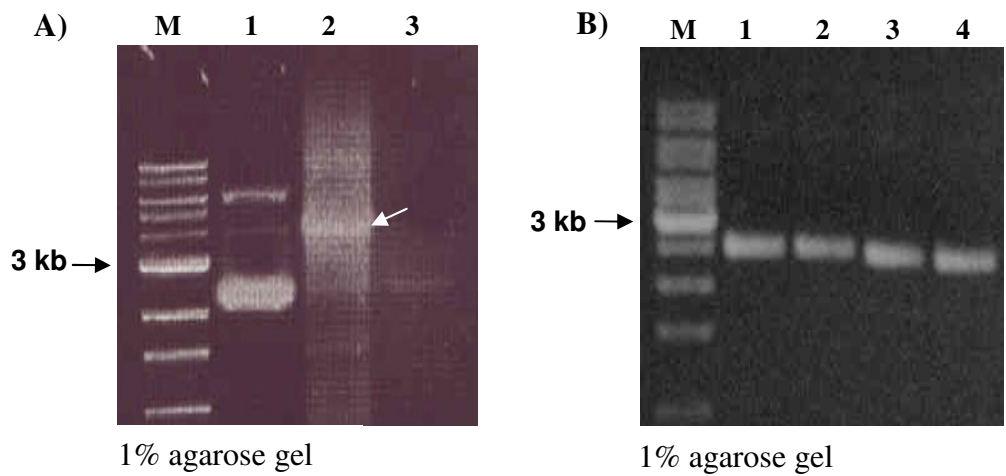


Figure. 3.3. Agarose gel electrophoresis result of PCR based site directed mutagenesis for double mutant cyt S-*c_y*R35. **A:** PCR products after the thermal cycling for site-directed mutagenesis. Line 1; Template plasmid pYO26, line 2; 10 μ l of sample reaction for site-directed mutagenesis, line 3; control reaction (no *pfu* polymerase enzyme). Arrow indicates the linear form of amplified mutation containing PCR products. **B:** Four of the transformants were selected and sequenced for confirmation of mutation. M; marker.

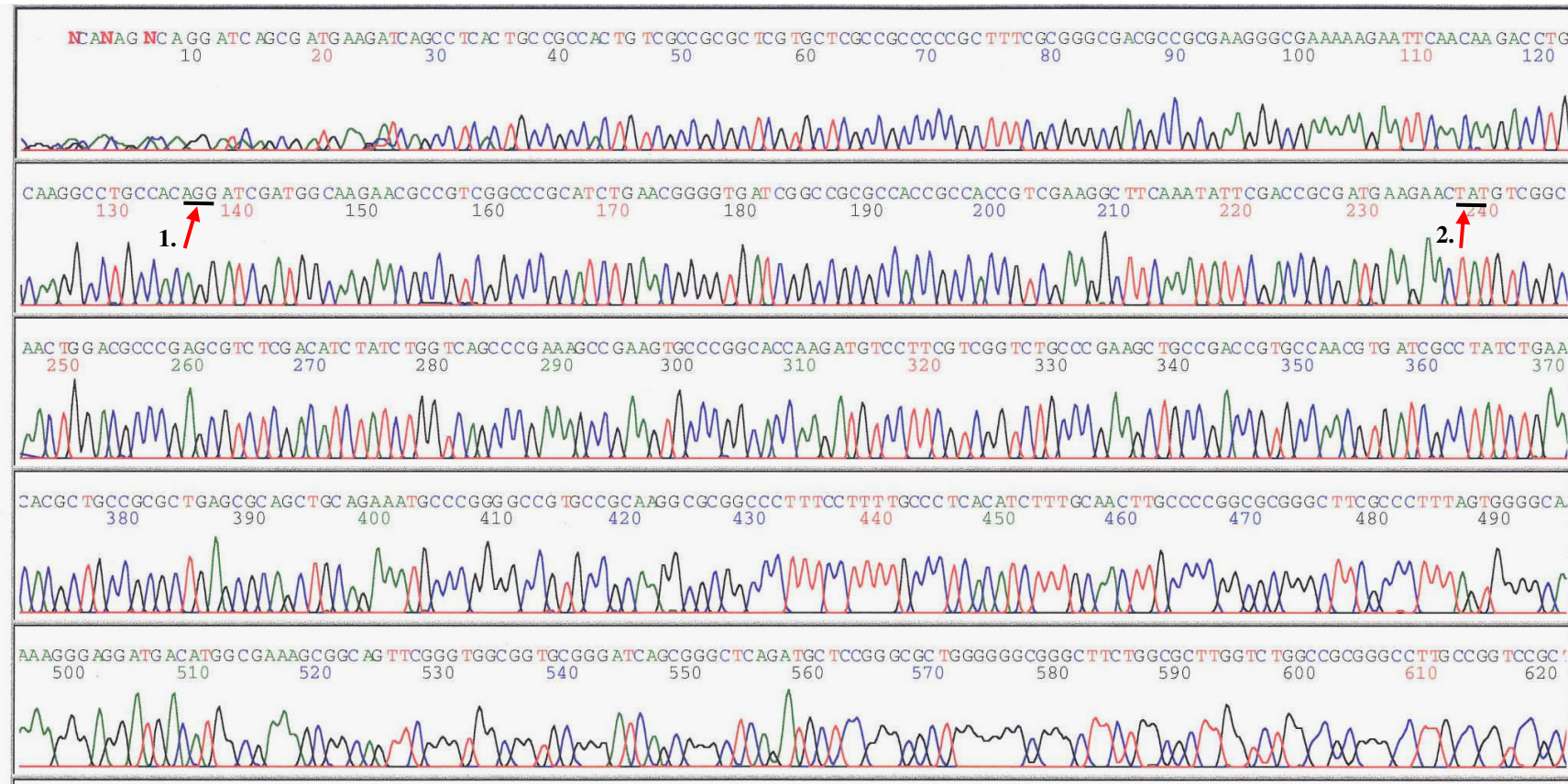


Figure 3.4. Sequencing analysis of pYO27 carrying the double mutant S-cyR35. 1st arrow indicates the **AAG** to **AGG** (Lys19Arg) Mutation and 2nd arrow indicates **CAT** to **TAT** (His53Tyr) mutation that was engineered on cyt S-cyR5 gene.

3.4.2. Cloning of double mutant cyt S-*c_y*R35

After the confirmation of mutations, the 1.2 kb *KpnI/BamHI* fragment of pYO27 was cloned into the same restriction sites of the broad host range plasmid pRK415 to yield pYO135 which was transferred to FJ2 and FJ2-R4 strains to test the Ps phenotype of double mutant cyt S-*c_y*R35 (**Figure 3.5**).

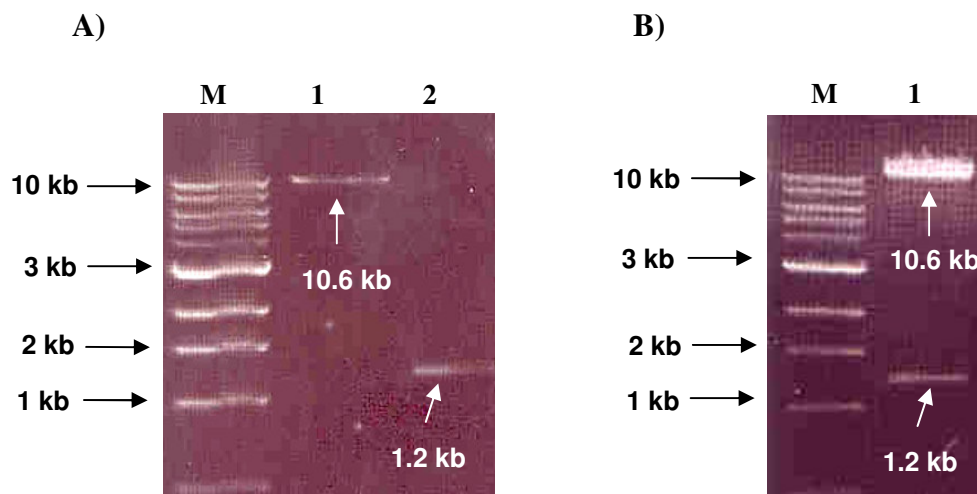


Figure. 3.5. Agarose gel (1%) electrophoresis result for the cloning of double mutant cyt S-*c_y*R35. **A:** The 1.2 kb *KpnI/BamHI* fragment of pYO27 carrying the S-*c_y*R35 gene (line 2) was cloned to 10.6 kb pRK415 vector (line 1). **B:** Control enzymatic digestion of the resulted plasmid pYO135 with *KpnI/BamHI* restriction enzymes gave the 1.2 kb insert fragment (line 1). M; represents 1 kb DNA ladder marker (MBI Fermentas).

3.5. Ps growth properties of Ps⁺ revertants

In order to estimate the Ps⁺ growth abilities of revertants of cyt S-*c_y* the average size of the colonies that they formed were measured under Ps growth conditions on MPYE enriched medium in both FJ2 and FJ2-R4 backgrounds (**Table 3.1**). The data indicated that in the FJ2 background cyt S-*c_y*, cyt S-*c_y*R3 (H53Y) and S-*c_y*R5 (K19R) conferred Ps⁻, Ps^{+/-} (Ps slow) and Ps⁺ phenotypes, respectively (**Figure 3.6 A**). Moreover, the double mutant cyt S-*c_y*R35 exhibited a Ps⁺ phenotype as vigorous as a wild type *R. capsulatus* strain, and remarkably, Ps growth phenotypes of all mutants were further improved by the FJ2-R4 background, to the point that even cyt S-*c_y* conferred Ps^{+/-} growth (**Figure 3.6 B**).

Table 3.1. Photosynthetic growth properties of soluble S-*c_y* and its Ps⁺ revertants in FJ2 and FJ2-R4 strains.

Plasmids	Cytochromes	In FJ2		In FJ2-R4	
		Phenotype ^a	Colony size in Ps (mm) ^b	Phenotype	colony size in Ps (mm)
pYO100	Cyt S- <i>c_y</i>	Ps ⁻	NG	Ps ^{+/-}	1.1
pYO103	Cyt S- <i>c_y</i> R3	Ps ^{+/-}	1.2	Ps ⁺	1.5
pYO105	Cyt S- <i>c_y</i> R5	Ps ⁺	2.1	Ps ⁺	2.1
pYO135	Cyt S- <i>c_y</i> R35	Ps ⁺	2.4	Ps ⁺	2.4

^a Ps⁺ indicates the ability to grow under photosynthetic and respiratory growth condition, respectively . Ps^{+/-} and Ps⁻ are refer to slow and no photosynthetic growth respectively.

^b Average colony diameter measured after 3 days of incubation under the Ps growth condition.

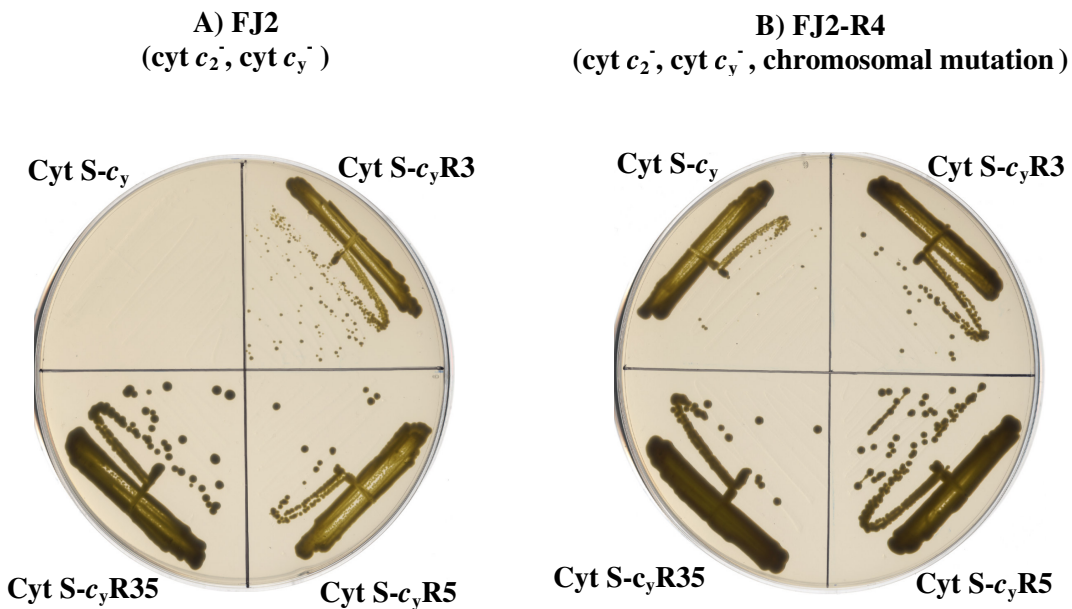


Figure 3.6. Photosynthetic phenotypes of strains carrying the soluble derivatives of *cyt c_y* in FJ2 (**A**) and in FJ2-R4 (**B**) under anaerobic condition with saturated light on MPYE medium.

3.6. Characterization of cyt S-*c*_y produced by various Ps⁺ revertants.

The *c*-type cyt profiles of Ps⁺ revertants, grown under respiratory conditions in MPYE enriched medium, were examined by SDS-PAGE/TMBZ analysis and reduced *minus* oxidized optical difference spectra.

3.6.1. SDS-PAGE/ TMBZ heme staining of *c* type cytochromes

As expected, the membrane bound cyt *c*_y was absent in chromatophore membranes of FJ2 (cyt *c*₂⁻, cyt *c*_y⁻) and FJ2-R4 (cyt *c*₂⁻, cyt *c*_y⁻, R4 chromosomal mutation) while the amounts of the cyt *c*₁, cyt *c*_o and cyt *c*_p were unchanged (**Figure 3.7 A**). In supernatants cell fraction from FJ2 derivatives, cyt S-*c*_y was not detectable but cyt S-*c*_yR5 (K19R), cyt S-*c*_yR3 (H53Y) and cyt S-*c*_yR35 (K19R and H53Y) were readily visible (**Figure 3.7 B**), and their amounts further increased in the FJ2-R4 background (**Figure 3.7 C**). This mutant was used for subsequent work instead of FJ2, because it enhanced production of cyt S-*c*_y variants and improved their Ps⁺ growth phenotypes (**Figure 3.6**). The sizes of cyt S-*c*_y derivatives were slightly smaller (about 10 kDa) than those of cyt *c*₂ and cyt *c'* (about 12 kDa), they were readily distinguished.

3.6.2. Difference spectra (Red_{Ascorbate}- Ox_{Ferricyanide}) of supernatant fraction of S-*c*_y and its Ps⁺ revertants.

Further estimation of the amounts of cyt S-*c*_y derivatives by using reduced *minus* oxidized optical difference spectra of chromatophore supernatants (**Table 3.2**) indicated that cyt S-*c*_yR5 and cyt S-*c*_yR35 were produced in FJ2-R4 at approximately 1/3 and equal amounts, respectively, to that of the cyt *c*₂ found in *R. capsulatus* wild type strain MT1131, or in its cyt *c*_y⁻ derivative FJ1 (**Figure 3.8**). The availability of mutants producing high amounts of cyt S-*c*_y allowed us to

determine its redox mid point potential (E_m) using chromatophore membrane supernatants.

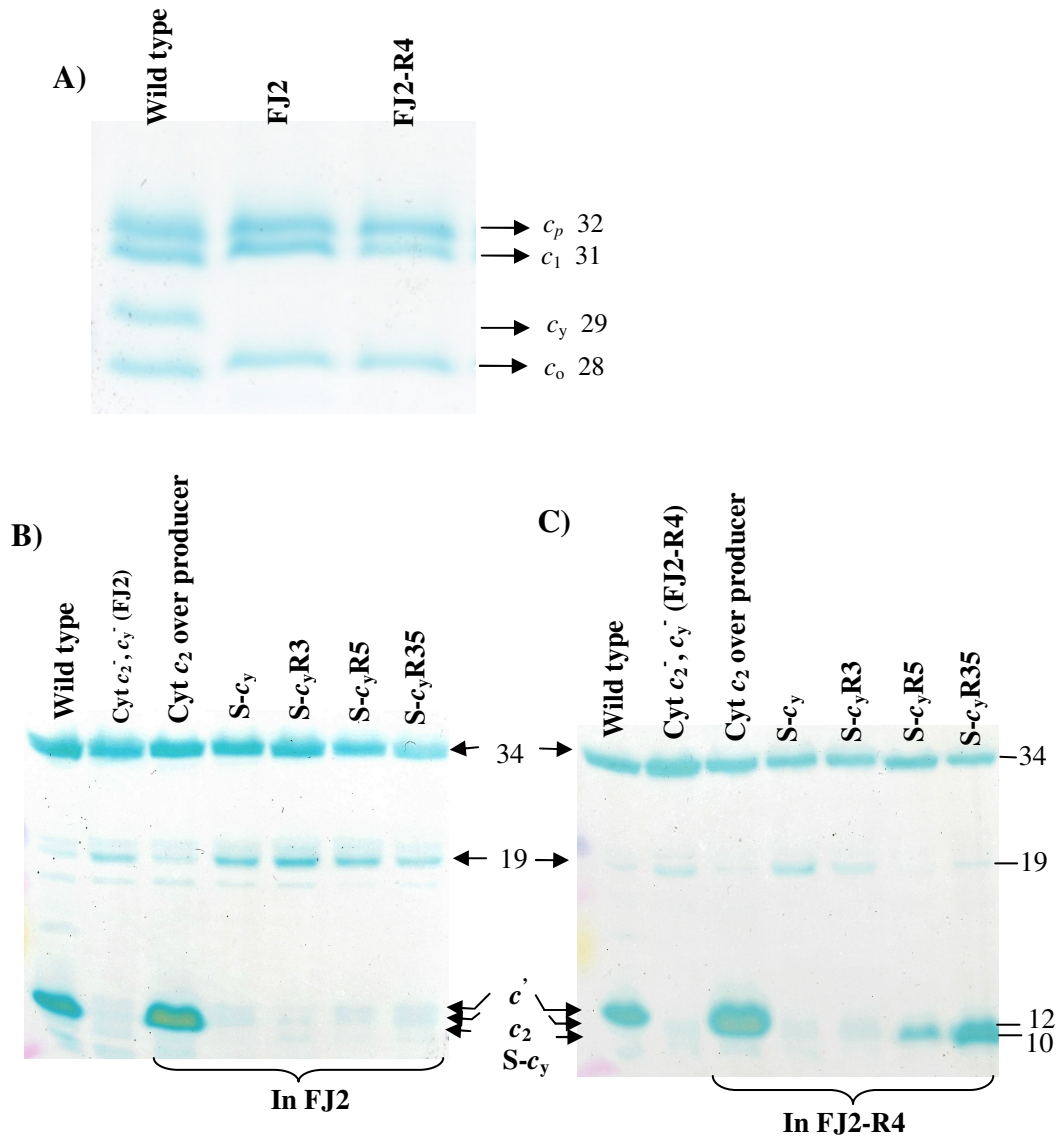


Figure 3.7. SDS-PAGE/ TMBZ heme staining of c type cytochromes from different *R. capsulatus* strains. 50 µg protein for chromatophore membranes and 80µg protein for supernatant fractions were loaded in each lane of a 16.5% SDS-polyacrylamide gel. Chromatophore membranes of wild type, FJ2 and FJ-R4 (A). Supernatant cell fractions of the different samples: MT1131, FJ2, soluble cyts in FJ2 (B), and MT1131, FJ2-R4, soluble cyts in FJ2-R4 (C).

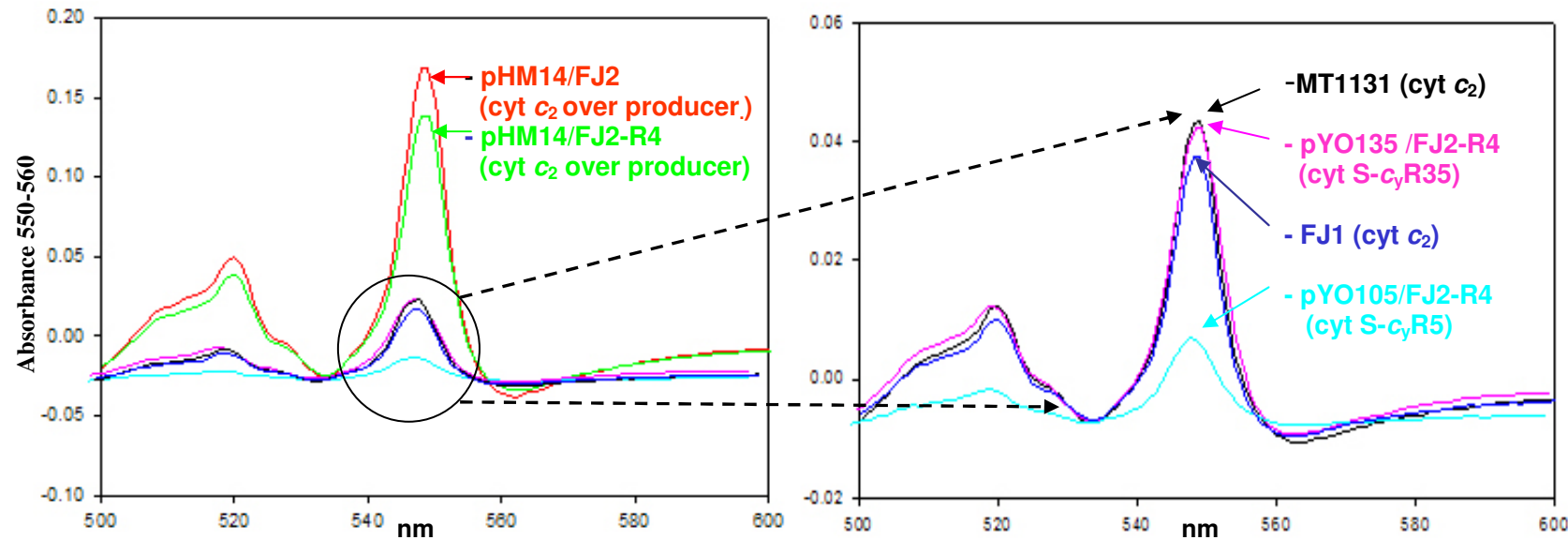


Figure 3.8. Difference spectra ($\text{Red}_{\text{Ascorbate}} - \text{Ox}_{\text{Ferricyanide}}$) of supernatant fraction of S-*c*_y and its Ps^+ revertants.

Table 3.2. Difference spectra ($\text{Red}_{\text{Ascorbate}} - \text{Ox}_{\text{Ferricyanide}}$) of supernatant fraction of $S-c_y$ and its Ps^+ revertants in FJ2 and FJ2-R4 strains.

Strains	Cytochromes	Phenotype ^a	$A_{550-535}$ (mOD) ^b
MT1131	Cyt c_2	Ps^+	50.8
FJ1	Cyt c_2	Ps^+	44.2
pYO100/ FJ2	Cyt S- c_y	Ps^-	1.45
pYO103/ FJ2	Cyt S- c_y R3	$\text{Ps}^{+/-}$	1.24
pYO105/ FJ2	Cyt S- c_y R5	Ps^+	1.57
pYO135/ FJ2	Cyt S- c_y R35	Ps^+	2.49
pHM14/ FJ2	Cyt c_2	Ps^+	198.4
pYO100/ FJ2-R4	Cyt S- c_y	$\text{Ps}^{+/-}$	4.48
pYO103/ FJ2-R4	Cyt S- c_y R3	Ps^+	5.22
pYO105/ FJ2-R4	Cyt S- c_y R5	Ps^+	14.12
pYO135/ FJ2-R4	Cyt S- c_y R35	Ps^+	49.2
pHM14/ FJ2-R4	Cyt c_2	Ps^+	163.2

^a Ps^+ indicates the ability to grow under photosynthetic and respiratory growth condition, respectively . $\text{Ps}^{+/-}$ and Ps^- are refer to slow and no photosynthetic growth respectively.

^b Amplitude of absorption pick at 550-535 nm of the ascorbate reduced minus ferricyanide oxidized spectra for 1.52 mg/ml protein.

3.7. Midpoint potential of soluble cyt $S-c_y$ variants

The redox chemical dark titrations of cyt $S-c_y$ R35 indicated that its midpoint potential (E_{m7} value) is around +338 mV, which is similar to that of its membrane-attached form (365 mV) (Figure 3.9). Thus, neither rendering cyt c_y soluble, nor the K19R and H53Y mutations that apparently increased its steady-state amounts affected drastically its E_{m7} value.

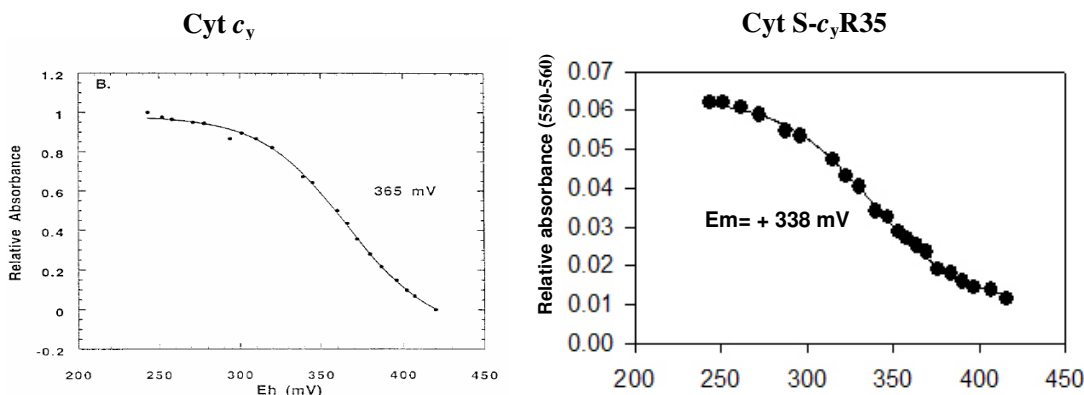


Figure 3.9. Redox midpoint potentials of cyt S-*c_y*R35 was performed in 50 mM MOPS/100 mM KCl pH 7 buffer as described in methodology. The data were fit to a Nernst equation for a one-electron couple. The midpoint potential of cyt S-*c_y*R35 is are +338 mV that is very close to Em of wild type cyt *c_y* (+365).

3.8. Multiple turnover ET kinetics of cyt S-*c_y* variants.

ET kinetics exhibited by cyt S-*c_y*R35 to the RC were examined by light activated, millisecond time resolved, optical difference spectroscopy. As expected, cyt *c* oxidation and re-reduction kinetics monitored at 550 - 540 nm wavelengths indicated no detectable ET activity to the RC either in FJ2 (Jenney et al., 1994) or FJ2-R4 backgrounds, although the previously established ET features of cyt *c_y* were readily seen in the control strains MT1131 (cyt *c₂*, cyt *c_y*), FJ1 (cyt *c₂*) and pFJ631/FJ2 (cyt *c_y*) (**Figure 3.10**). In addition, pHM14/FJ2-R4, which overproduced cyt *c₂* exhibited kinetics similar to but more amplified than MT1131 kinetics because of its increased cyt *c₂* pool size. The strains pYO135/FJ2 or pYO135/FJ2-R4 harboring different amounts of cyt S-*c_y*R35 exhibited various levels of cyt *c* re-reduction activities in parallel with their Ps⁺ phenotypes (**Figure 3.10, left column**). In all cases the full extent of cyt *c* oxidation was revealed by

addition of the cyt bc_1 complex inhibitor stigmatellin, which blocked cyt c re-reduction (**Figure 3.10, middle column**). Of a train of eight flashes used in each case, complete cyt c oxidation required a different number of flashes according to different cyt c pool sizes in different strains. For example, when FJ1 containing wild type levels of cyt c_2 compared with cyt c_2 overproducers pHM14/FJ2-R4, extra flashes were needed for complete oxidation of pHM14/FJ2-R4 in the presence of stigmatellin. In respect to electron transfer properties of cyt S- c_y R35, the data established clearly that cyt S- c_y R35 was able to transfer electrons from the cyt bc_1 complex to the RC upon its light activation and exhibited different mode of ET than that of either cyt c_y or cyt c_2 . Furthermore, carotenoid band-shifts monitored at 475 – 490 nm wavelengths confirmed ET events of cyt S- c_y R35 between the physiological partners (**Figure 3.10, right column**). The slower phases of the carotenoid band shifts were proportional to the extents of the ET activities seen in each case, demonstrating that trans-membrane charge separation occurred upon establishment of the cyclic ET pathway between the cyt bc_1 complex and the RC via the cyt S- c_y R35 (**Figure 3.10**).

3.9. Comparison of single turnover ET kinetics mediated by different electron carrier cys.

In order to further examine the kinetic differences between cyt c_2 , cyt c_y and cyt S- c_y R35, single turnover cyt c oxidation kinetics were monitored in the presence of stigmatellin (**Figure 3.11**). As observed previously, the oxidation of cyt c_y is very fast and has no readily detectable slower phase at the millisecond time scale but cyt c_2 exhibits an equally fast phase oxidation followed by a slower phase of oxidation indicating fast electron transfer by bound cyt c_2 to RC and slower electron transfer by unbound cyt c_2 to RC, respectively. The differences between the ET kinetics exhibited by the membrane-anchored cyt c_y and the water-soluble cyt c_2 are attributed to their restricted or free diffusion abilities, respectively (Jenney et al., 1994; Myllykallio et al., 1998; Vermeglio et al., 1998). On the other hand, cyt c oxidation kinetics of cyt S- c_y R35 were composed of a

barely perceptible fast oxidation phase, followed by a very prominent slower oxidation phase (**Figure 3.11**). According to these results, it appears that a remarkable consequence of converting the diffusion-restricted cyt c_y to a freely diffusible cyt S- c_y R35 is to slow down appreciably its fast ET abilities to the RC. The quasi-absence of the fast phase in cyt S- c_y R35 kinetics suggests that, unlike cyt c_2 , it does not associate tightly with the RC.

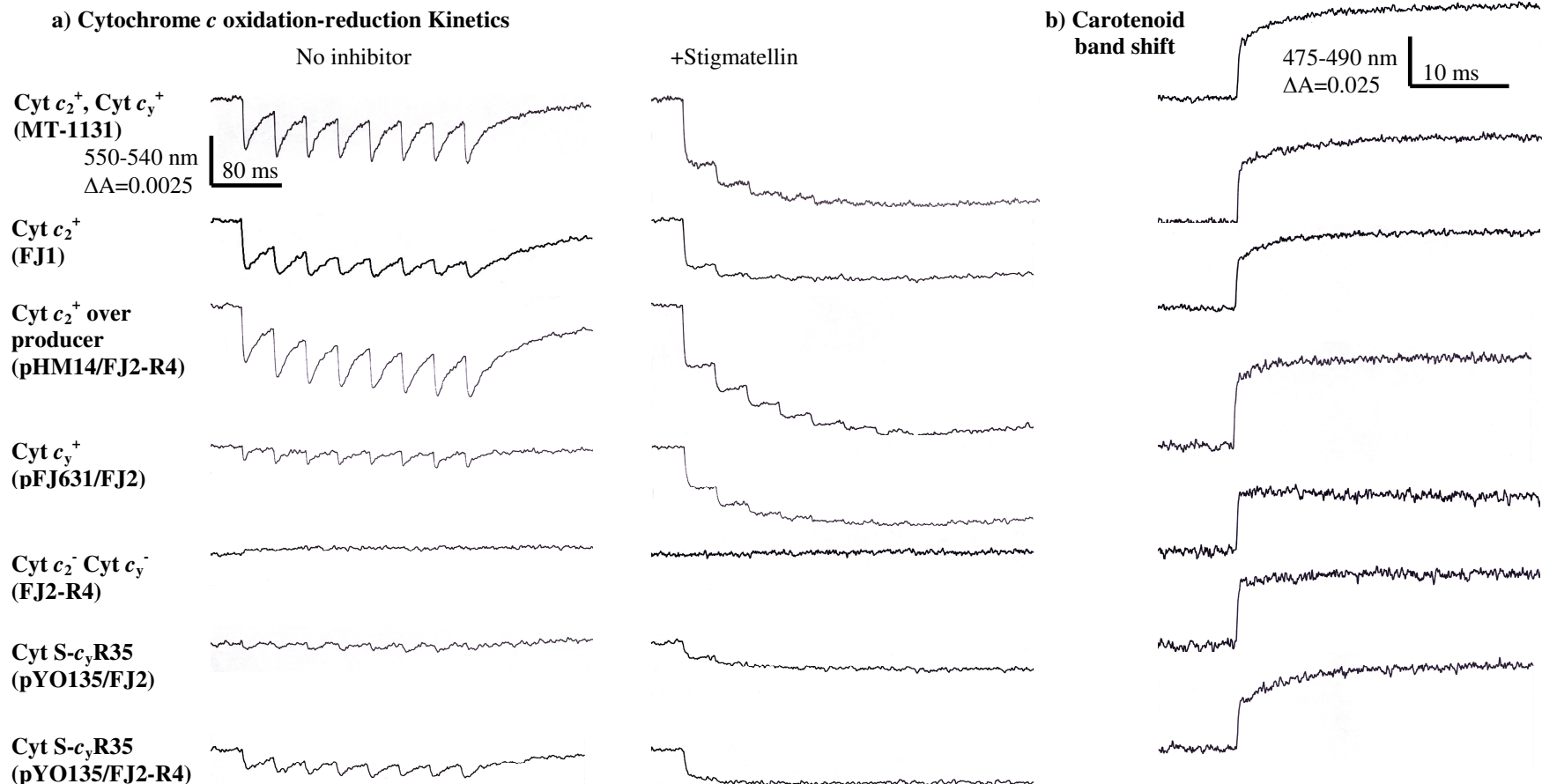
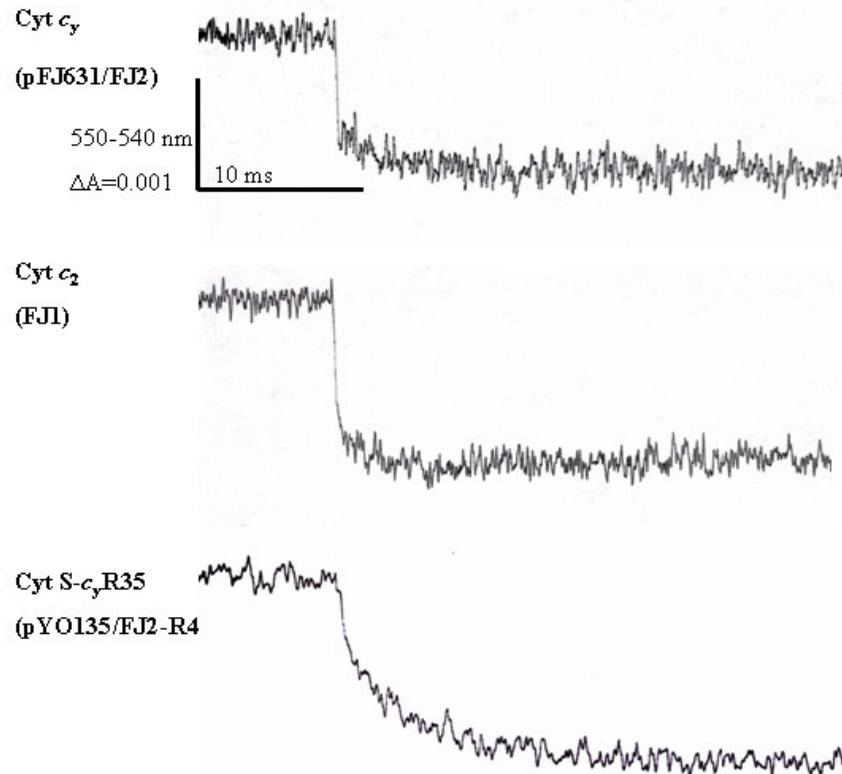


Figure 3.10. Transient kinetics of the flash induced oxidation and reduction of the cyt *c* components were followed at 550-540 nm for cyt *c* (A.) and at 490-475 nm for carotenoid band shift (B). The traces obtained with no inhibitor and stigmatellin by train of eight flashes.

Cyt *c* oxidation kinetics in the presence of stigmatellin



Photosynthetic electron transfer pathways
mediated by

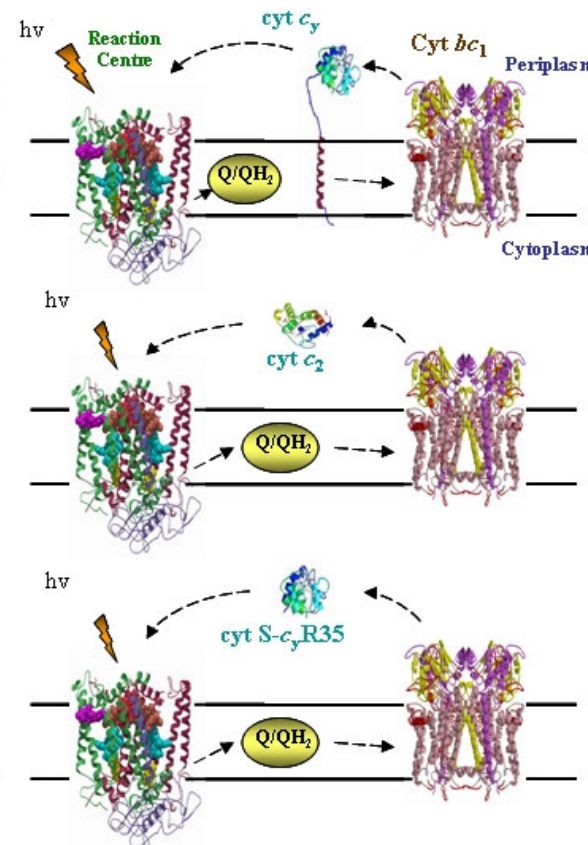


Figure 3.11. Flash-induced electron transfer kinetics of the pFJ631/FJ2 ($\text{cyt } c_y^+$), pHM14/FJ2-R4 ($\text{cyt } c_2^+$), and pYO135/FJ2-R4 ($\text{cyt } S\text{-}c_y\text{R35}$) strains were followed at 550-540 nm in the presence of stigmatellin.

3.10. Cloning of *hupSLC* operon

For the cloning of uptake hydrogenase genes, first the 4.1 kb *hupSLC* operon (Appendix F), structural genes of uptake hydrogenase, was amplified by using the mutagenic primers HupF (containing *Kpn*I site) and HupR (containing *Xba*I site). Chromosomal DNA of *R. capsulatus* MT1131 was used as a template for this amplification (**Figure 3.12 A**). After the amplification of 4.1 kb *hupSLC* operon, it was first cloned to pBSII plasmids by using *Kpn*I and *Xba*I sites of this plasmid in the multiple cloning site (**Figure 3.12 B**).

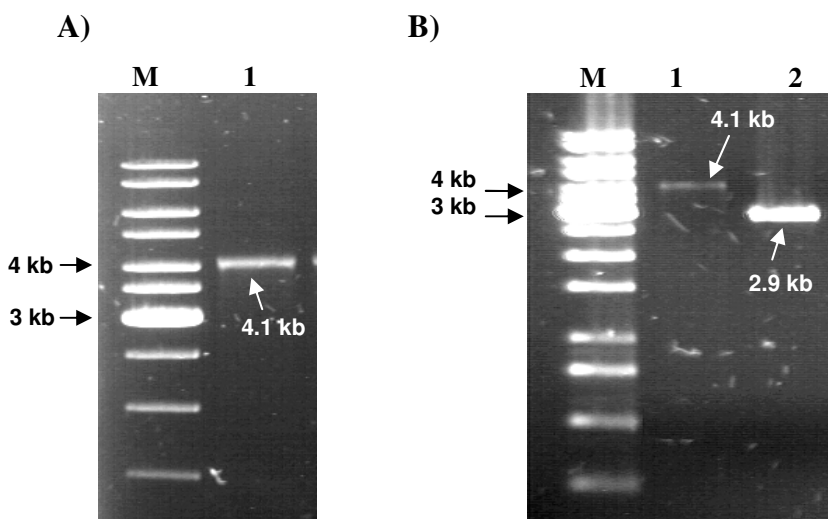


Figure 3.12. **A:** PCR amplification of 4.1 kb *hupSLC* operon by mutagenic primers (line 1). **B:** Cloning of 4.1 kb *Kpn*I / *Xba*I digested *hupSLC* operon (line 1) to 2.9 kb pBSII vector (line 2).

The correct clone pYO39 (*hupSLC* in pBSII) was selected by restriction enzyme digestions of operon with several restriction enzymes (**Figure 3.13**). The 4.1 kb *KpnI* / *Xba*I fragment of pYO39 was cloned to pRK415 plasmid to yield pYO40 (*hupSLC* in pRK415) (**Figure 3.14**). The plasmid pYO39 was used to construct $\Delta hupSL::\text{gen}$ insertion-deletion allele for chromosomal inactivation of uptake hydrogenase.

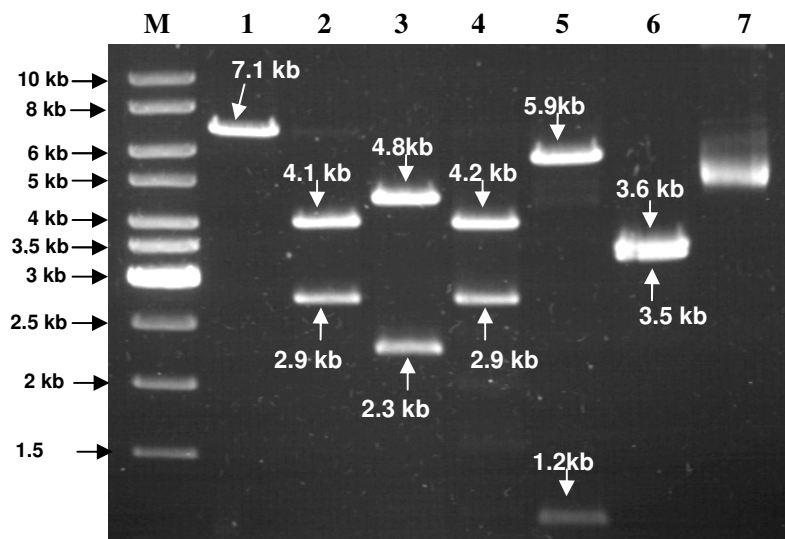


Figure. 3.13. Control enzymatic digestion of pYO39 with different restriction enzymes. Line 1; *Bam*HI digestion, line 2; *Kpn*I/ *Xba*I digestion, line 3; *Bal* I/ *Bam* HI digestion, line 4; *Kpn*I/ *Bam* HI digestion, line 5; *Bam* HI/ *Xba*I digestion, line 6; *Bal* I / *Xba*I digestion, line 7; uncut pYO39 plasmid.

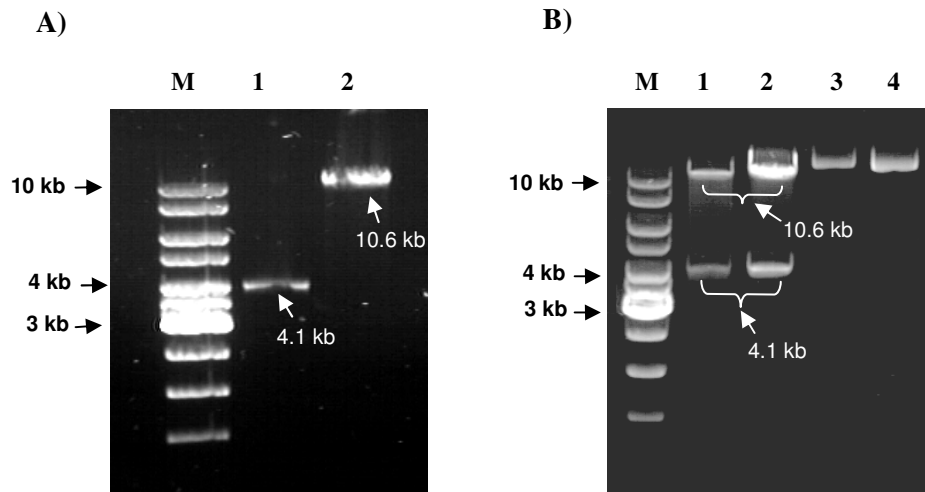


Figure. 3.14. A: Cloning of 4.1 kb *KpnI* / *XbaI* fragment (*hupSLC* operon) of pYO39 to 10.6 kb pRK415 vector. **B:** The correct clone was selected by digestion of two transformants with *KpnI* / *XbaI* double digestion (line 1 and line 2). Line 3 and line 4; uncut plasmid of two transformants. The obtained plasmid was named pYO40.

3.11. Construction of $\Delta hupSL$::gen deletion-insertion allele

The $\Delta hupSL$::gen insertion-deletion allele was constructed by replacing 2.3 kb *BalI*/ *BamHI* fragment of *hupSLC* on pYO39 plasmid with the 1.2 kb gentamicin resistance cassette (**Figure 2.8 in Material and Method**) . The correct clone pYO41 was selected by the restriction enzyme digestions (**Figure 3.15**) and confirmed by DNA sequencing (**Figure 3.16 and Figure 3.17**).

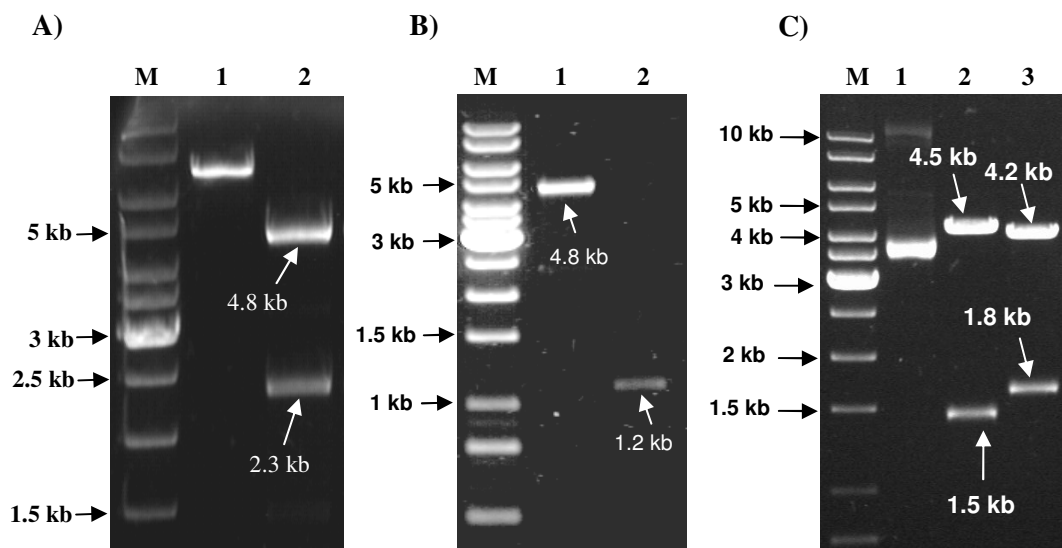


Figure 3.15. The $\Delta hupSL::gen$ deletion-insertion allele was constructed by replacing the 2.3 kb *BalI* / *BamHI* fragment of *hupSLC* in pYO39 (**A**, line 2) by 1.2 kb gentamicin cassette (**B**, line 2). The 4.8 kb *BalI* / *BamHI* fragment containing the rest of *hupSLC* operon in pBSII plasmid was used as a template for cloning of pYO41 (**A**, line 2 and **B**, line 1). **C:** The correction of $\Delta hupSL::gen$ deletion-insertion allele in resulted plasmid pYO41 was controlled by restriction enzyme digestion. Line 1; uncut pYO41, line 2; *BglIII*/ *XbaI* digestion of pYO41, line 3; *KpnI* / *Bam HI* digestion of pYO41.

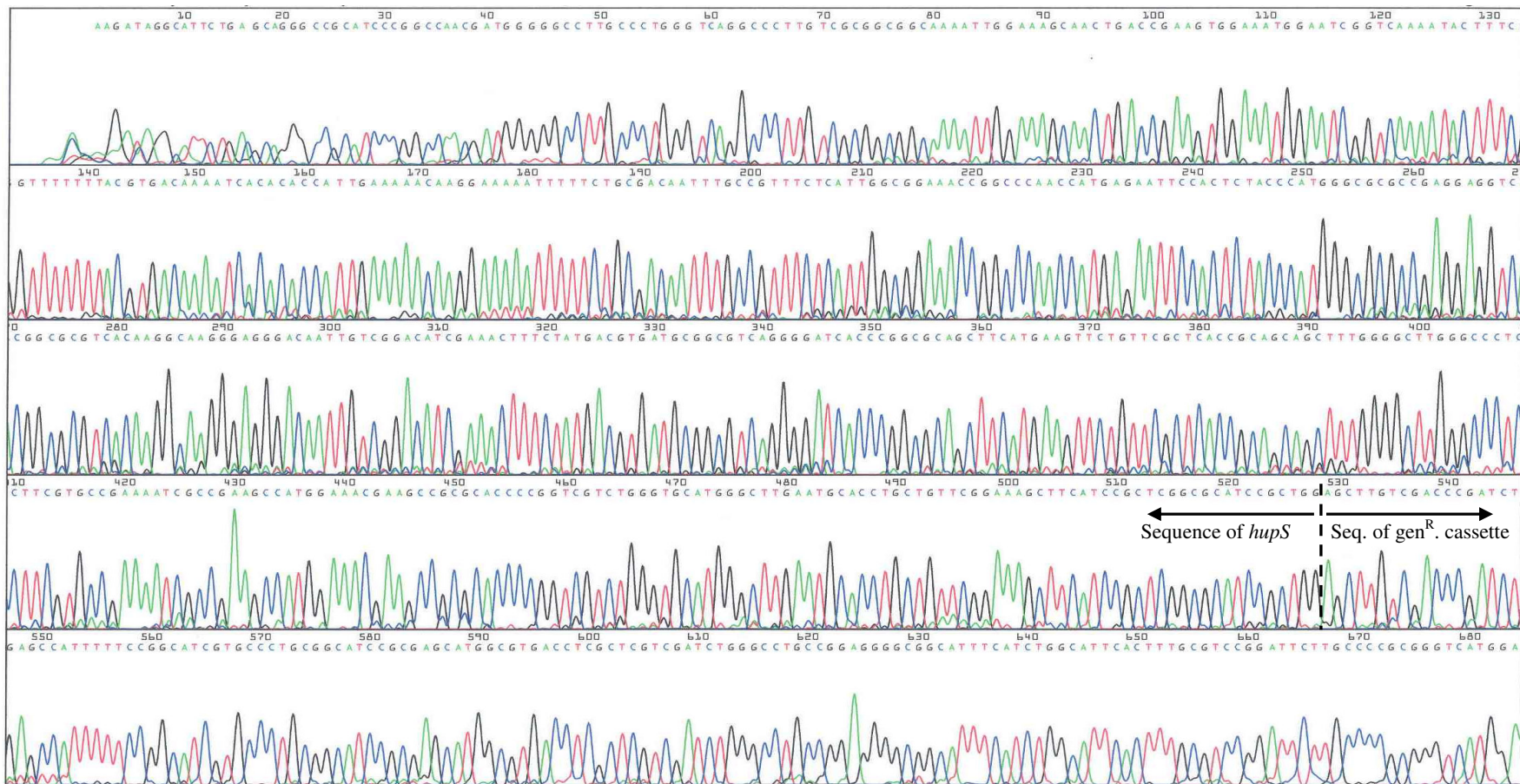


Figure 3.16. Sequencing analysis of pYO41 carrying the $\Delta hupSL::gen$ deletion-insertion cassette with hupF forward primer. Arrows indicate the parts of $\Delta hupSL::gen$ deletion-insertion cassette.

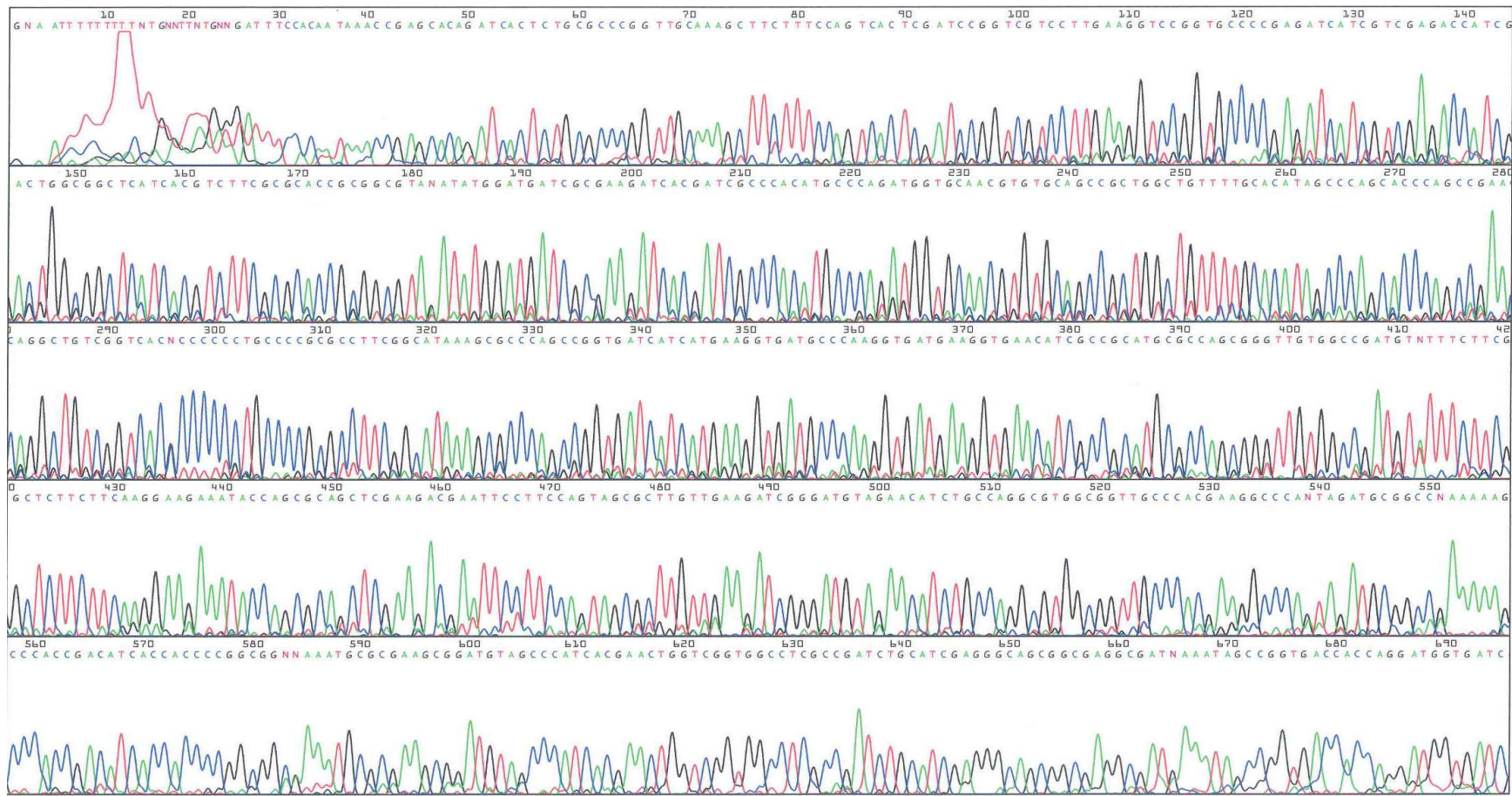


Figure 3.17. Sequencing analysis of the 3' extension of the $\Delta hupSL::gen$ cassette on pYO41 (reverse sequence of *hupC*) with *hupR* reverse primer.

The 3 kb $\Delta hupSL::gen$ insertion-deletion allele located on *KpnI/XbaI* fragment of pYO41 was cloned to broad-range plasmid pRK415 for mobilization of it to *R. capsulatus* strains (the resulting clone was named pYO42) (**Figure 3.18**).

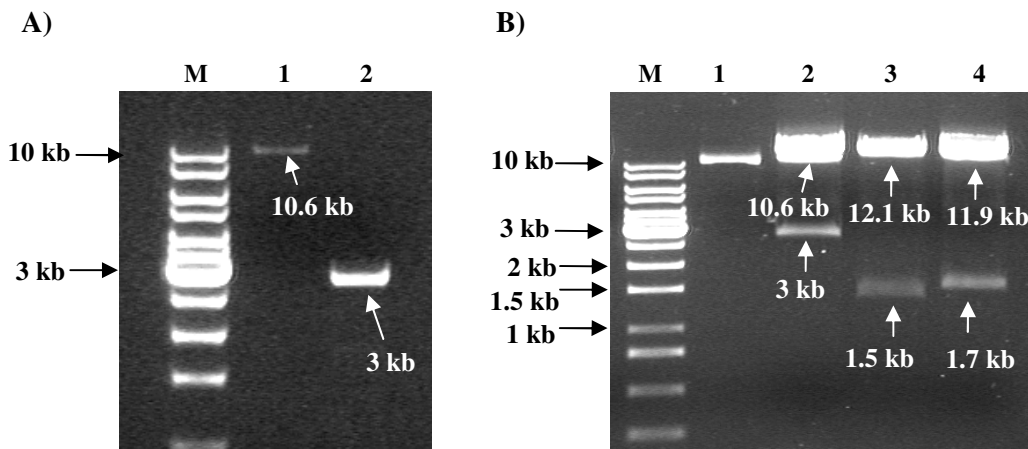


Figure 3.18. **A:** Cloning of $\Delta hupSL::gen$ insertion-deletion allele located on 3 kb *KpnI/XbaI* fragment of pYO41 (line 2) to 10.6 kb pRK415 vector (line 1). **B:** Control enzymatic digestion of pYO42. Line 1; uncut pYO42 plasmid, line 2; *KpnI/XbaI* digestion, line 3; *BglIII/XbaI* digestion, line 4; *KpnI/BamHI* digestion.

3.12. Generation of the knock-out uptake hydrogenase mutant strains of *R. capsulatus*.

In order to increase the hydrogen production efficiency, the uptake hydrogenase of MT1131 (wild type), GK-32 (cyt *cbb3⁻*) and KZ1 (Qox⁻) strains were deleted from their chromosomes by interposon mutagenesis. For interposon mutagenesis, the plasmid pYO42 containing $\Delta (hupSL::gen)$ insertion-deletion allele was transferred to GTA over-producer *R. capsulatus* Y₂₆₂ strain by three parental conjugation (**Figure 3.19**). The GTA particles were isolated from pYO42/Y₂₆₂ strain and used for GTA cross to obtain Hup⁻ strains by homologous

recombination between the *hupSLC* operon and $\Delta hupSL::gen$ insertion-deletion allele. The Hup⁻ strains YO3, YO4 and YO5 derived from MT1131 (wild type), GK-32 (cyt *cbb3*⁻) and KZ1 (Qox⁻) strains respectively were selected on the gentamicin containing MPYE plates (**Figure 20**, **Figure 21**, **Table 3.3**).

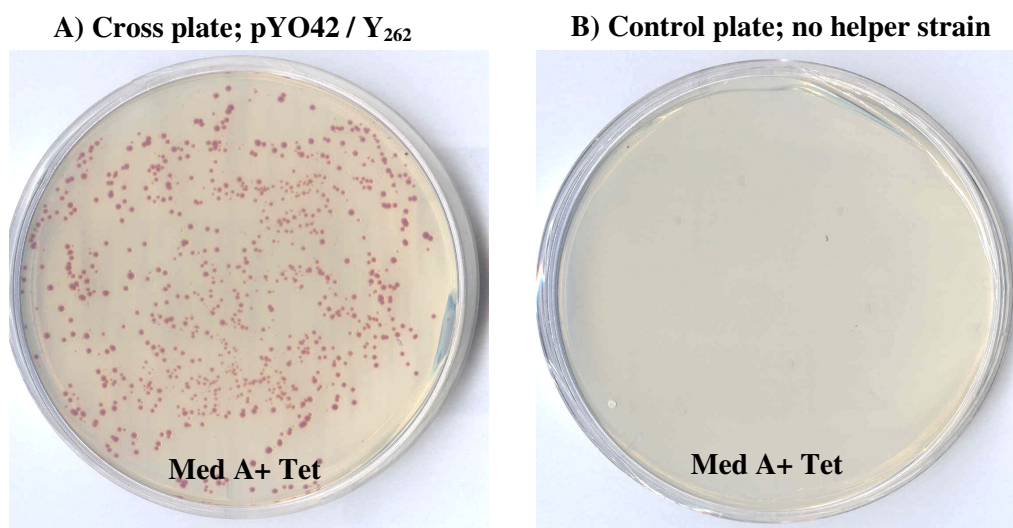


Figure 3.19. The plasmid pYO42 carrying $\Delta hupSL::gen$ insertion-deletion allele was transferred from *E. coli* HB101 strain to *R. capsulatus* Y₂₆₂ strain (GTA over-producer strain) by three parental conjugation. *R. capsulatus* Y₂₆₂ strain that transformed with pYO42 bearing TetR gene gave colonies on Med A+ Tet plate (A). No colonies grown on control plate that helper strain pRK2013/HB101 was not used (B).

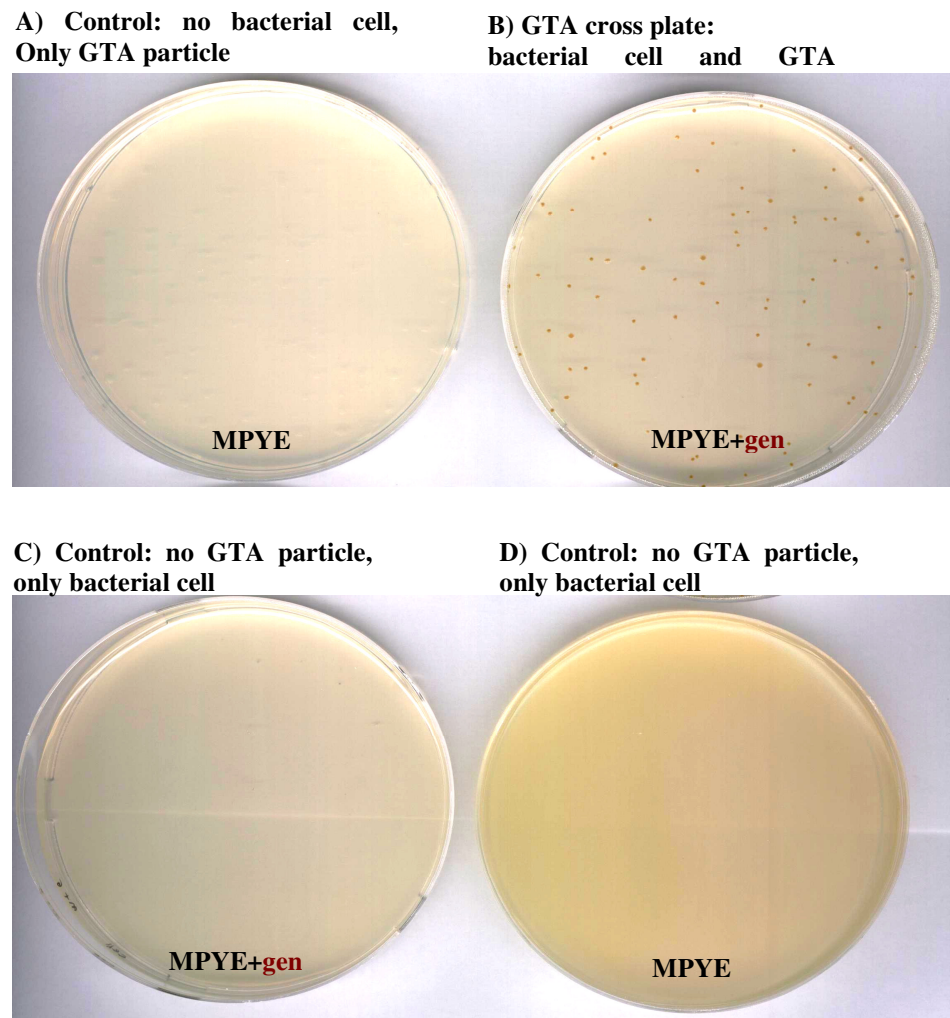


Figure 3.20. The results of GTA cross for YO3 strain. The mutant Hup⁻ colonies became visible on MYPYE+gen plates after 2 days incubation at 34° C (**B**). Control experiments were also performed in the absence of recipient bacterial cell on MYPYE plate (**A**), in the absence of GTA particle on MYPYE+gen plate (**C**) and on MYPYE plate (**D**).

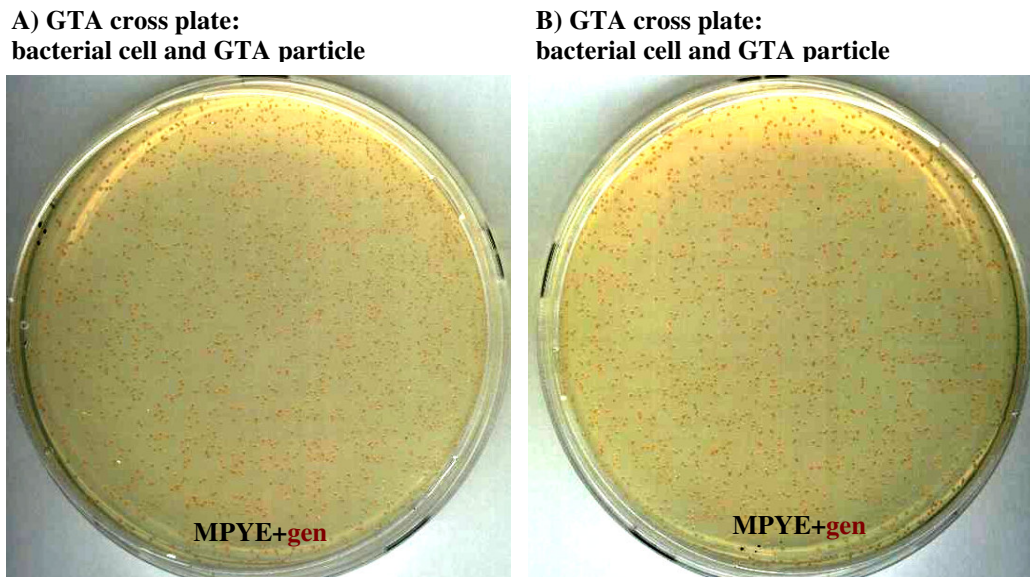


Figure 3.21. The results of GTA cross for YO4 (**A**) and YO4 strains (**B**). The mutant Hup⁻ colonies became visible on MYPYE+gen plates after 2 days incubation at 34° C.

Table 3.3. GTA cross table for Hup⁻ strains.

Donor strain		Recipient strains		Resulted Hup ⁻ strains	
Name	Genotype	Name	Genotype	Name	Genotype
pYO42/Y ₂₆₂	$\Delta hupSL::gen$ in GTA Over-producer strain	MT1131	W. type	YO3	$\Delta(hupSL::gen)$ Hup ⁻
		GK-32	$\Delta(ccoNO::kan)$ cyt cbb_3^-	YO4	$\Delta(ccoNO::kan)$, cyt cbb_3^- $\Delta(hupSL::gen)$, Hup ⁻
		KZ1	$\Delta(cydAB::spe)$ Qox ⁻	YO5	$\Delta(cydAB::spe)$, Qox ⁻ $\Delta(hupSL::gen)$, Hup ⁻

3.13. Confirmation of the chromosomal mutation of uptake hydrogenase

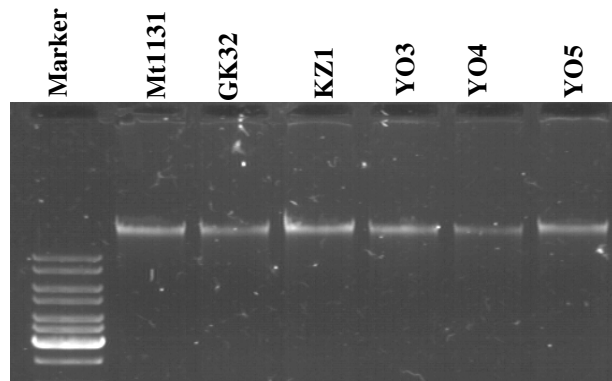
3.13.1. PCR amplification of chromosomal $\Delta hupSL::gen$ insertion-deletion allele.

The PCR amplification of *hupSLC* and $\Delta hupSL::gen$ insertion-deletion allele from chromosomal DNA's of wild type and mutant *R. capsulatus* strains by using the *hupF* and *hupR* primers confirmed that in mutant strains, 4,1 kb *hupSLC* operon was replaced by 3 kb *hupSL::gen* insertion-deletion allele (**Figure 3.22**).

3.13. 2. Hydrogenase activity of Hup⁻ *R. capsulatus* strains.

Hydrogenase activity in whole cells was assayed by following the reduction of methylene blue linked to H₂ oxidation. Activity assay indicated that Hup⁻ strains as in the case of YO3, YO4 and YO5 can not reduce methylene blue by oxidation of H₂ in the absence of uptake hydrogenase so the blue color of the cell suspension did not change over the time (**Figure 3.23**).

A) Chromosomal DNA



B) Control PCR for *hup*⁻ strains

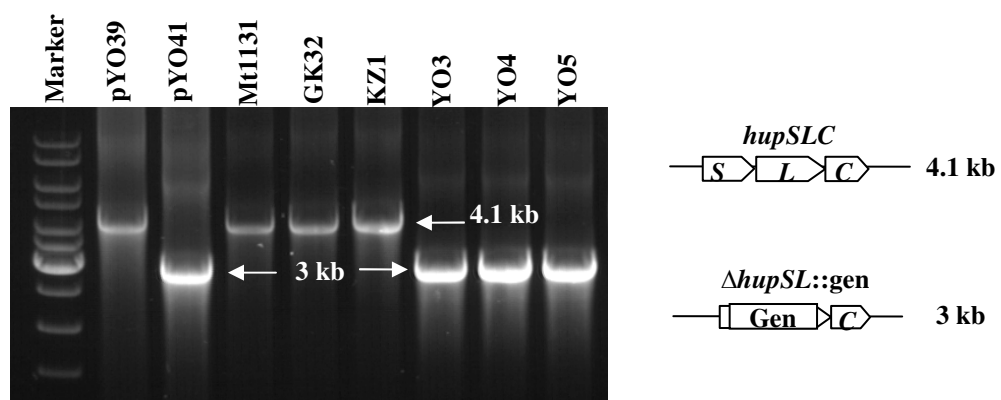


Figure 3.22. Chromosomal DNA's of related strains were isolated and used as a template for PCR amplification of *hupSLC* and $\Delta hupSL::gen$ (**A**). Deletion of *hup* operon was confirmed by PCR amplification of *hupSLC* and $\Delta hupSL::gen$ insertion-deletion allele from chromosomal DNA's of wild type and mutant *R. capsulatus* strains (**B**). pYO39 and pYO41 are the plasmids carrying *hupSLC* and $\Delta hupSL::gen$ in pBSII respectively.

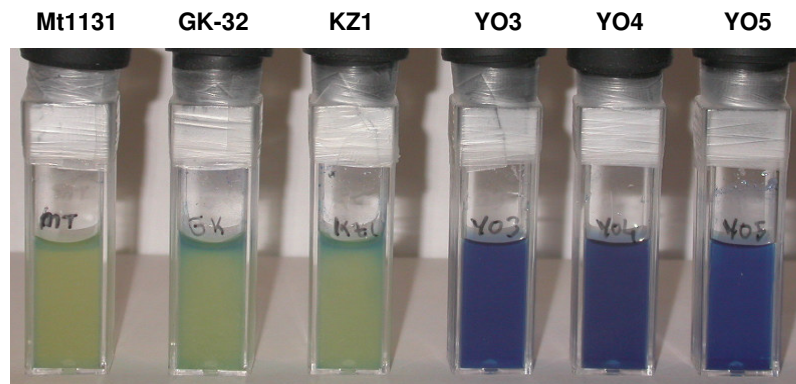


Figure 3.23. Hydrogenase activity of the Hup⁻ strains were assayed by the methylene blue reduction linked to H₂ oxidation.

3.14. Hydrogen production of mutant *R. capsulatus* strains with modified electron carrier cytochromes.

R. capsulatus mutants harboring various modified electron carrier cytochromes were compared with a wild type strain to determine the effect of these mutations on the hydrogen production in malate/glutamate medium. The result of mutant strains containing only the cyt *c*₂ (pHM14/FJ2), only the cyt *c*_y (pFJ631/FJ2) and only the cyt S-*c*_yR35 (pYO135/FJ2) indicated that the total hydrogen production of these mutants decreased by 3 to 5 folds (0.29, 0.33 and 0.17 ml per ml of culture, respectively) compared to that of a wild type strain (0.94 ml per ml of culture) (**Figure 3.24 A, Table 3.4**). Growths of these mutants were slower than that of the wild type (**Figure 1 B**) and their substrate conversion efficiency decreased by about 3 to 5 folds, as listed in **Table 3.4**. The inefficient electron transfer for overall energy production might be at the basis of these observations, as the nitrogenase enzyme needs a lot of ATP molecule to produce hydrogen. In respect to the maximum rate of H₂ production those of pFJ631/FJ2 (cyt *c*_y⁺) and pYO135/FJ2 (cyt S-*c*_yR35⁺) were decreased approximately by 2.5 fold. However the maximum H₂ production rate of pHM14/FJ2 (cyt *c*₂⁺) mutant strain was comparable to that of the wild type although the total amount of hydrogen it produced decreased by 3 fold. The FJ2 strain, which was used as a

control, did not grow by photosynthesis because it has neither cyt c_2 nor cyt c_y for the cyclic electron transfer (**Figure 3.24 B**). Finally, as expected the final pH of all cultures, with the exception of FJ2, increased to around 7.4 -7.5 (**Figure 3.24 C**).

3.15. Hydrogen production of quinol oxidase and cyt cbb_3 oxidase deficient mutants of *R. capsulatus*.

The roles of respiratory enzymes cyt cbb_3 oxidase and alternative Qox on hydrogen production metabolism through the effecting redox signaling pathway was also investigated (**Figure 3.25**). The results demonstrated that although total hydrogen production of GK-32 (cyt cbb_3^-) and KZ1 (Qox $^-$) strains were slightly decreased, the cyt cbb_3^- mutant strain starts earlier to produce hydrogen and hydrogen production rate of this mutant increased approximately 1.8 fold (0.025 ml/ml culture.h) when compared with wild type and Qox $^-$ strains (0.014 and 0.015 ml/ml culture.h respectively) (**Table 3.4**). These observations are in agreement with a regulatory role of the cyt cbb_3 oxidase on the redox balancing systems (Kaplan et al., 2005; Oh et al., 2004). Previously it was shown that under both aerobic and anaerobic growth condition cyt cbb_3 of *R. sphaeroides* has an inhibitory effect on RegB/RegA by enhancing the phosphatase activity of RegB (PrrB) relative to its kinase activity (Kaplan et al., 2005). Moreover, inactivation of the cyt cbb_3 oxidase in *R. sphaeroides* resulted in increased expression of the RegB/RegA (PrrB/PrrA) regulon which includes the regulation of nitrogenase and uptake hydrogenase expression (Oh and Kaplan, 2000). In *R. capsulatus*, the RegB/RegA system indirectly activates the synthesis of nitrogenase by activating expression of the *nifA2* gene and directly represses uptake hydrogenase structural gene expression by binding to the *hupSLC* promoter (Elsen et al., 2000). These observations suggest that inactivation of the cyt cbb_3 oxidase in *R. capsulatus* eliminates its inhibitory effects on the RegB/RegA system, which subsequently activates the expression of the nitrogenase and represses that of the hydrogenase, resulting in earlier and faster induction of hydrogen production.

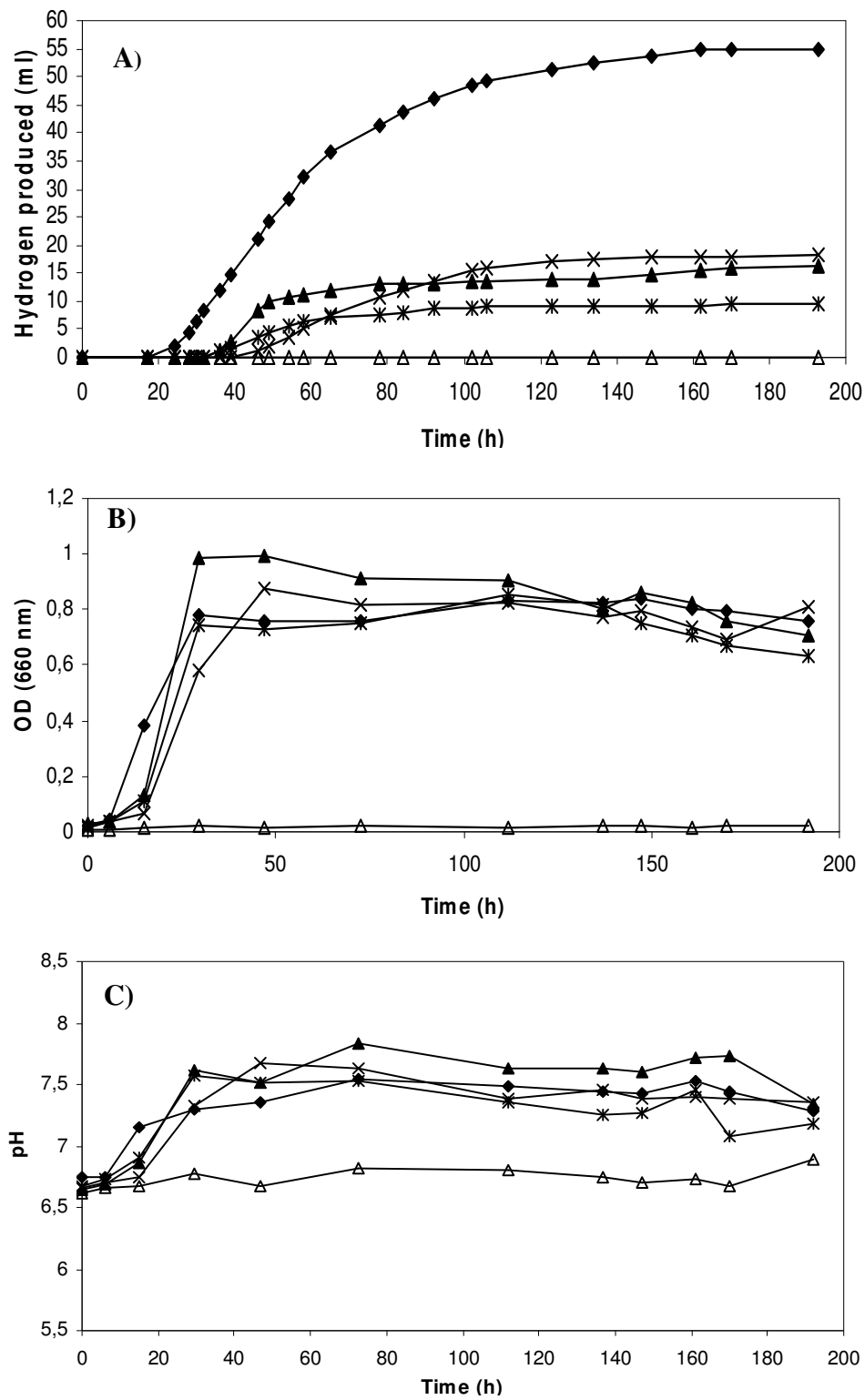


Figure 3.24. Hydrogen production (**A**), phototrophic growth (**B**) and pH of (**C**) mutant *R. capsulatus* strains with different electron carrier cytochromes in malate/glutamate medium (15 mM/ 2mM). ♦: Wild type MT1131; ▲: pHM14/FJ2; x: pFJ631/FJ2; *: pYO134/FJ2-R4; Δ: FJ2.

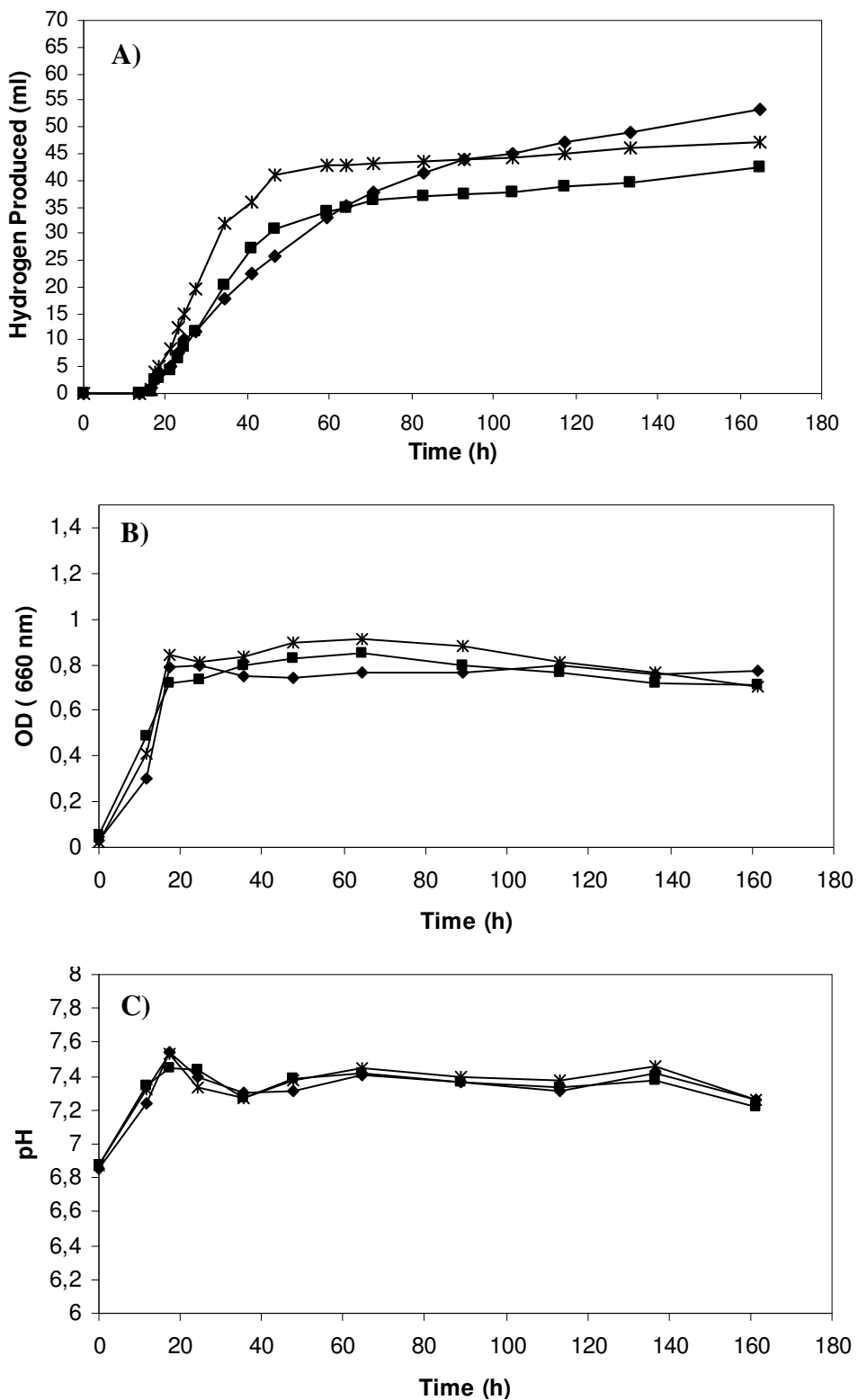


Figure 3.25. Hydrogen production (A), phototrophic growth (B) and pH of (C) Qox⁻ and cyt *cbb*₃⁻ mutants of *R. capsulatus* in malate/ glutamate medium (15 mM/ 2mM). ◆: Wild type MT1131; x: GK-32; ■: KZ1.

3.16. Hydrogen production of uptake hydrogenase deleted derivatives of *R. capsulatus* strains.

In previous studies, inactivation of uptake hydrogenase of *R. capsulatus* resulted in increased total hydrogen production, and efficient substrate conversion by preventing recycling of the nitrogenase produced H₂ (Zorin et al., 1996; Jahn et al., 1994). In addition to electron carrier and terminal oxidase (*cbb₃*⁻ and Qox⁻) mutants, in this study, uptake hydrogenase deleted derivatives of MT1131 (wild type), GK-32 (cyt *cbb₃*⁻) and KZ1 (Qox⁻) strains were obtained (YO3, YO4 and YO5 respectively) and their hydrogen production profiles were investigated (Figure 3.26). The total hydrogen production and substrate conversion efficiency of all Hup⁻ derivatives increased significantly comparing to their wild type parents (Table 3.4). Maximum H₂ production rates of YO3 (Hup⁻) and YO5 (Qox⁻, Hup⁻) (0.019 ml/ml culture.h for both of them) were also increased when compared with their mother strains MT1131 and KZ1 (Qox⁻) (0.014 and 0.015 ml/ml culture.h respectively) (Table 3.4). Like GK-32, the hydrogen production rate of its Hup⁻ derivative YO4 (cyt *cbb₃*⁻, Hup⁻) (0.022 ml/ml culture.h) is higher than that of YO3 and YO5 (Table 3.4).

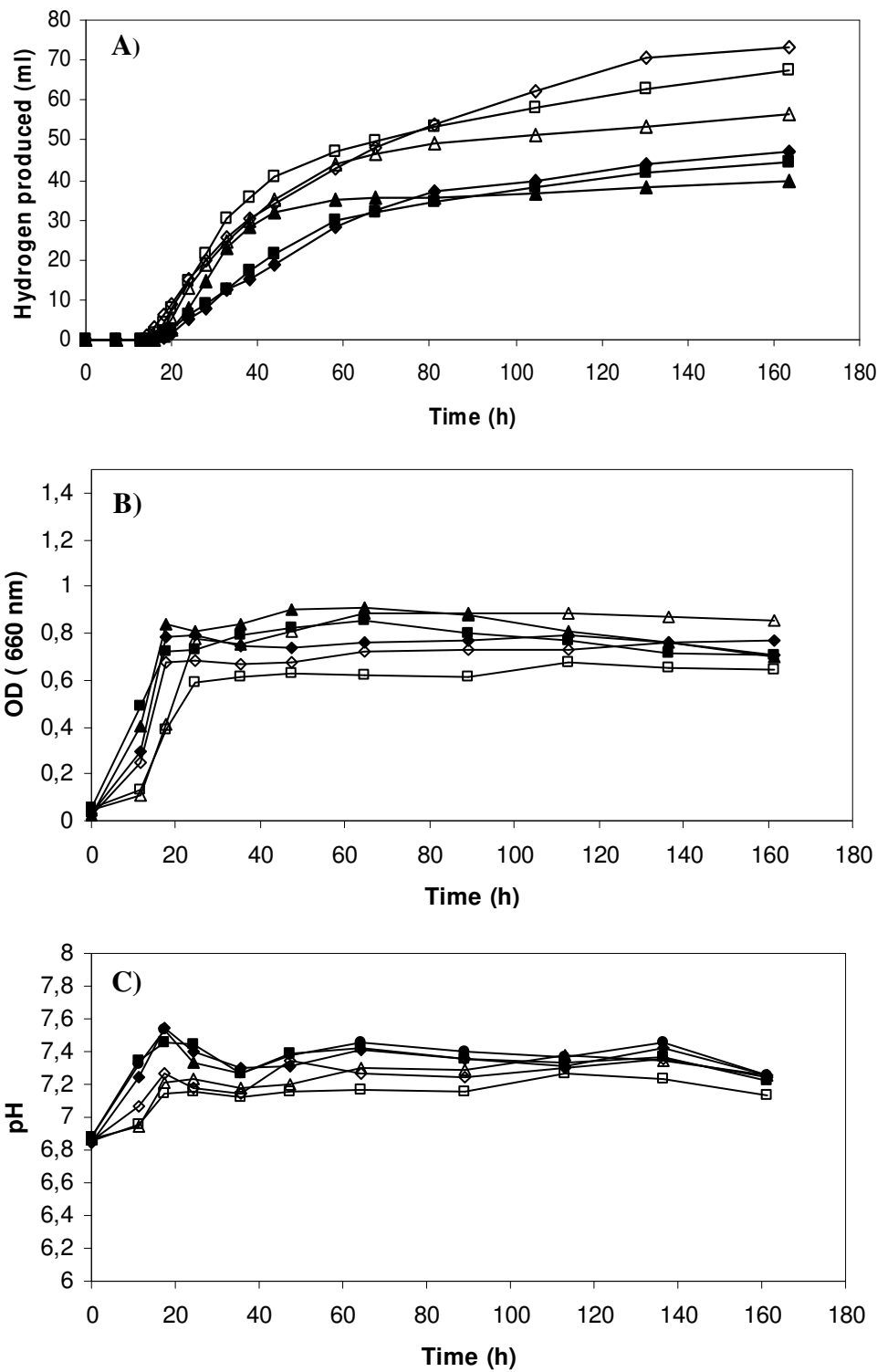


Figure 3.26. Hydrogen production (**A**), phototrophic growth (**B**) and pH of (**C**) Hup⁻ mutants of wild type, Quinol oxidase and cyt *cbb₃* oxidase deleted strains of *R. capsulatus* in malate/ glutamate medium (15 mM/ 2mM). ♦: Wild type MT1131; ▲: GK-32; ■: KZ1; ◇: YO3; Δ: YO4; □: YO5.

Table 3.4. Hydrogen production of wild type and different mutants of *R. capsulatus* in malate/glutamate (15/ 2 mM) growth medium. The data are means of three different experiment determinations.

Strains	Total hydrogen (ml/ml culture)	Max. H ₂ production rate (ml/ml culture.h)	Substrate conversion* efficiency (%)
MT1131 wild type	0.94	0.014	47 %
pHM14/FJ2 (cyt <i>c</i> ₂)	0.29	0.014	15 %
pFJ631/FJ2 (cyt <i>c</i> _y)	0.33	0.0055	16 %
pYO135/FJ2-R4 (cyt S- <i>c</i> _y R35)	0.17	0.0051	9 %
GK-32 (cyt <i>cbb</i> ₃ ⁻)	0.85	0.025	40 %
KZ1 (Qox ⁻)	0.79	0.015	40%
YO3 (Hup ⁻)	1.33	0.019	67 %
YO4 (cyt <i>cbb</i> ₃ ⁻ , Hup ⁻)	1.08	0.022	54. %
YO5 (Qox ⁻ , Hup ⁻)	1.22	0.019	61 %

* Calculations for substrate conversion efficiency was given in Appendix I

3.17. Hydrogen production of the *R. capsulatus* strains in glucose/glutamate medium.

The hydrogen production profiles of wild type and all mutant strains (electron deficient strains, cyt cbb_3^- , Qox $^-$ and Hup $^-$ strains) of *R. capsulatus* were also tested in glucose/ glutamate (10/2 mM) growth medium instead of malate /glutamate medium. In general, the hydrogen production rate and the total hydrogen production of all *R. capsulatus* strains in this medium were slower and less than that of in malate/ glutamate medium (**Table 3.5**). However the difference in hydrogen production properties between the different kinds of mutant strains was also detected in glucose/ glutamate medium. For example as observed in malate medium, the total hydrogen production and substrate conversion efficiency of mutant *R. capsulatus* strains with modified electron carrier cytochromes decreased 2 to 4 folds (**Figure 3.27 and Table 3.5**). In addition, the hydrogen production rate of GK-32 (cyt cbb_3^-) strain was higher than that of wild type and KZ1 (Qox $^-$) strains as shown in malate medium. Moreover, similar to observations in malate medium, the Hup $^-$ strains YO3, YO4 and YO5 produced more hydrogen at higher production rate than that of their Hup $^+$ parent strains MT131, GK-32 and KZ1 respectively in this medium (**Figure 3.28, Table 3.5**). All these results confirmed the hydrogen production profiles of mutant strains that were obtained in malate medium. This experiment also indicated the capacity of *R. capsulatus* to utilize glucose as a carbon source in addition to organic acids. *R. sphaeroides* can not produce any hydrogen at glucose/ glutamate medium.

Table 3.5. Hydrogen production of wild type and different mutants of *R. capsulatus* in glucose/glutamate (10/2 mM) growth medium.

Strains	Total hydrogen (ml/ml culture)	Max. H ₂ production rate (ml/ml culture. h)	Substrate conversion* efficiency (%)
MT1131 wild type	0.64	0.010	24 %
pHM14/FJ2 (cyt <i>c</i> ₂)	0.18	0.002	7 %
pFJ631/FJ2 (cyt <i>c</i> _y)	0.3	0.004	12 %
pYO135/FJ2-R4 (cyt S- <i>c</i> _y R35)	No growth	No growth	No growth
GK-32 (cyt <i>cbb</i> ₃ ⁻)	0.46	0.014	17 %
KZ1 (Qox ⁻)	0.57	0.012	21%
YO3 (Hup ⁻)	0.99	0.019	37 %
YO4 (cyt <i>cbb</i> ₃ ⁻ , Hup ⁻)	0.83	0.019	31 %
YO5 (Qox ⁻ , Hup ⁻)	0.88	0.015	33 %

* Calculations for substrate conversion efficiency was given in Appendix I

The data are means of three different experiment determinations for MT1131, GK-32, KZ1, YO3, YO4 and YO5, two different experiment determinations for pYO135/FJ2-R4 (cyt S-*c*_yR35), pHM14/FJ2 (cyt *c*₂) and pFJ631/FJ2 (cyt *c*_y).

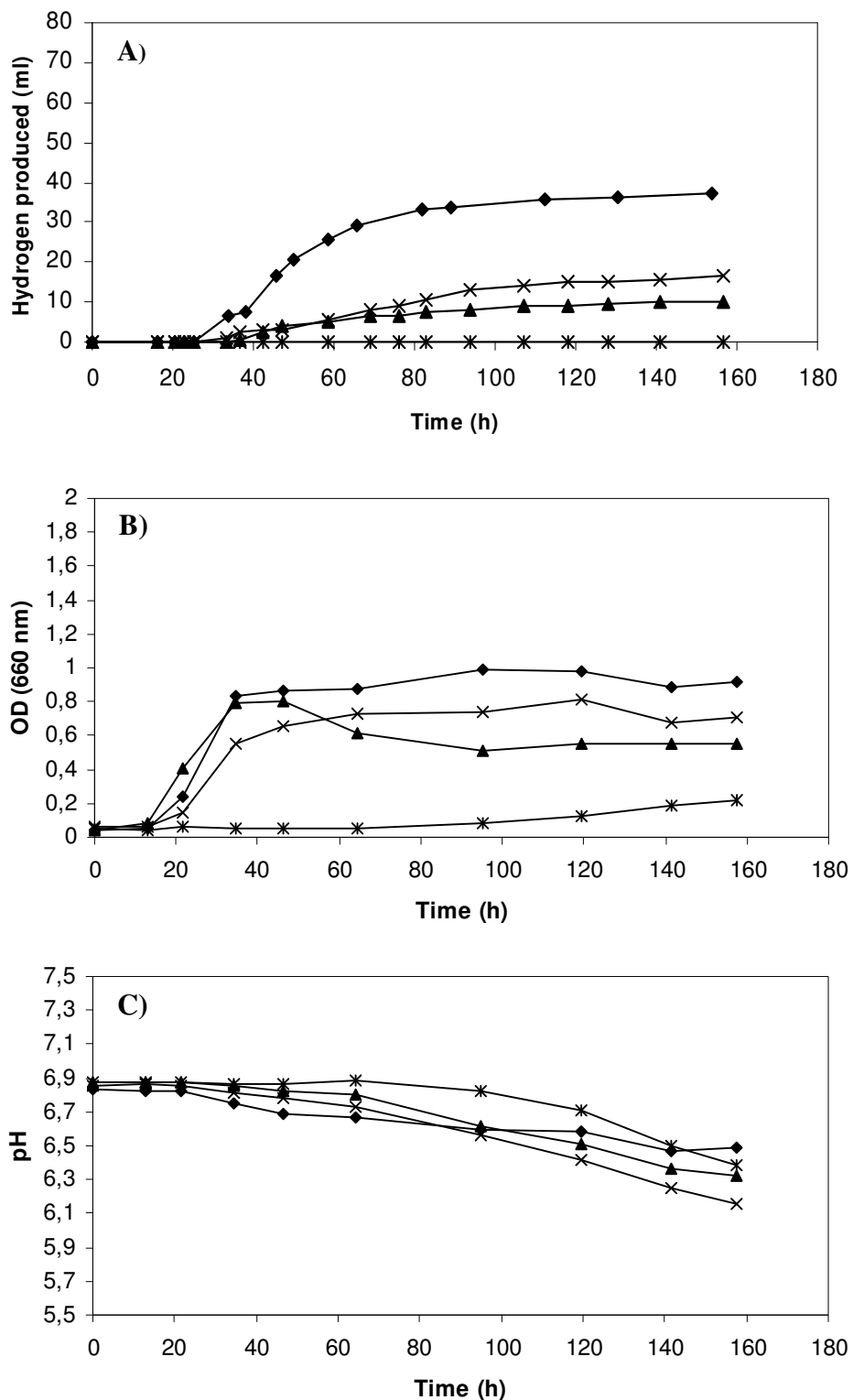


Figure 3.27. Hydrogen production (**A**), phototrophic growth (**B**) and pH of (**C**) mutant *R. capsulatus* strains with different electron carrier cytochromes in glucose/glutamate medium (10 mM/ 2mM). ◆: Wild type MT1131; ▲: pHM14/FJ2; x: pFJ631/FJ2; *: pYO134/FJ2-R4; Δ: FJ2.

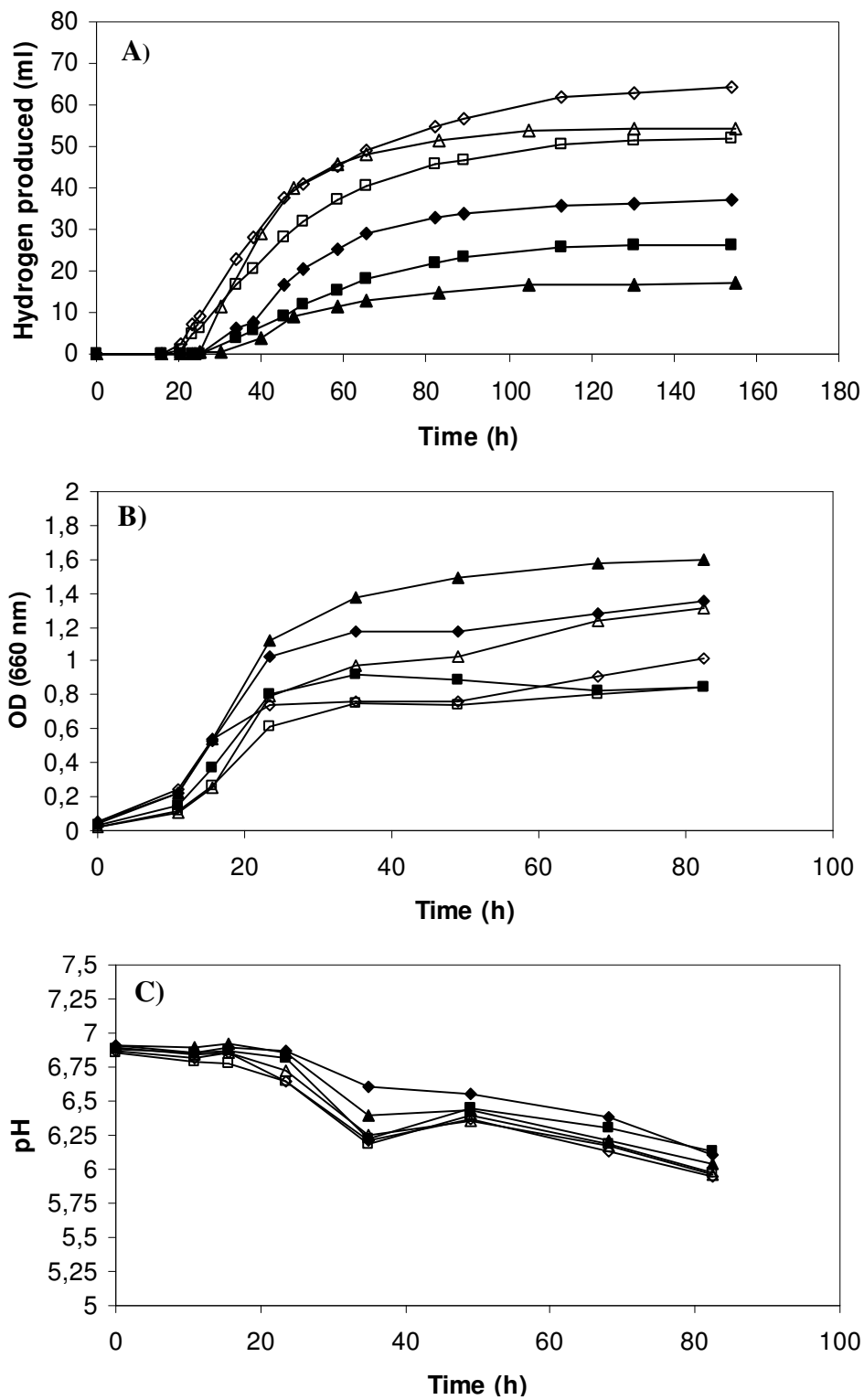


Figure 3.28. Hydrogen production (A), phototrophic growth (B) and pH of (C) Hup⁻ mutants of wild type, Quinol oxidase and cyt *cbb₃* oxidase deleted strains of *R. capsulatus* in glucose/ glutamate medium (10 mM/ 2mM) . ♦: Wild type MT1131; ▲: GK-32; ■: KZ1; ◇: YO3; Δ: YO4; □: YO5.

CHAPTER 4

CONCLUSION

The membrane bound cyt c_y of *R. capsulatus* is attached to membrane by unprocessed long and flexible anchor-linker domain during translocation to periplasm. This linker domain of cyt c_y is long enough to facilitate the movement of its cyt c domain for fast electron transport to photooxidized RC. Because the relative mobility of cyt c_y is limited, compared to cyt c_2 , the cyt c_y pathway is organized in isolated electron-transport chains (close association of the same amounts of RC and cyt c_y per cyt bc_1 complex) allowing rapid re-reduction of P^+ by cyt c_y and rapid re-reduction of cyt c_y by electrons originating from the cyt bc_1 complex. The connection between the cyt bc_1 complex and the RC by cyt c_y is described as tighter than that by cyt c_2 (Jenney et al., 1994; Myllykallio et al., 1998).

To shed further light to the molecular basis of the difference in Ps electron transfer properties of cyt c_y versus cyt c_2 , the soluble versions cyt c_y were sought by eliminating their membrane-anchor and linker domains. It was anticipated that the freely diffusible variant of this electron carrier would not be constrained by their membrane-attachment, and hence reveal electron carrier properties of its cyt c domain. The obtained cyt S- c_y was initially unable to support the Ps growth of a *R. capsulatus* strain lacking both the cyt c_2 and cyt c_y , but they quickly accumulated mutations that increased their steady-state amounts. In the case of cyt S- c_y , its very low amount may reflect its rapid degradation due to its lack of

protective association with its redox partners. It is known that in the absence of the cyt *bc*₁ complex cyt *c*_y is absent when cells were grown in enriched medium (Jenney et al., 1994). The nature of the chromosomal mutation in FJ2-R4 is intriguing, as its effects seem to be restricted to the cyt S-*c*_y and its derivatives, because no increased production of cyt *c*₂ or cyt *c'* is seen in this background. Undoubtedly, determination of the molecular identity of this component, which is out of the scope of this work, is an important future task.

Analyses of the cyt S-*c*_y derivatives with cyt *c* domain substitutions (*e.g.*, K19R or H53Y or K19R+H53Y) indicated that their E_m were very similar to that of the native cyt *c*_y. Neither these mutations nor rendering cyt *c*_y soluble changed drastically their electron carrier properties, while improving their steady-state amounts. The structure of cyt *c*_y is not available but its primary sequence is highly similar (63 % identity and 75 % similarity with 1 % gap over 95 amino acid residues) to that of cyt *c*₅₅₂ of *Paracoccus denitrificans* of known structure (Harrenga et al. 2000; Reincke et al., 2001). A structural model for the cyt *c* domain of cyt *c*_y built by homology modeling using that of cyt *c*₅₅₂ (www.expasy.org/swissmod/SWISS-MODEL.html) indicated that K19 is on the surface of binding interface of the protein near the heme edge and highly solvent exposed (**Figure 4.1 A**). Thus conceivably, the larger side chain of R substituting K at this position may improve binding of cyt *c*_y to the RC via improved electrostatic interactions and limit its degradation. On the other hand, H53Y mutation is located on the surface of opposite site of binding interface and may have possible effect on stability by avoiding protease degradation (**Figure 4.1 B**).

Perhaps one of the most remarkable findings of this work is the mode of ET kinetics exhibited by cyt S-*c*_yR35 derivative cyt S-*c*_y. Light activated RC coupled cyt *c* oxidation kinetics indicated clearly that electron donation by cyt S-*c*_yR35 is much slower than that mediated by either the cyt *c*_y or the cyt *c*₂ (Overfield et al. 1979; Drepper and Mathis, 1997; Axelrod et al., 2002). The rapid kinetics seen with cyt *c*_y has been attributed to its close proximity to the RC and its inability to diffuse freely (Myllykalio et al., 1998; Drepper et al., 1997).

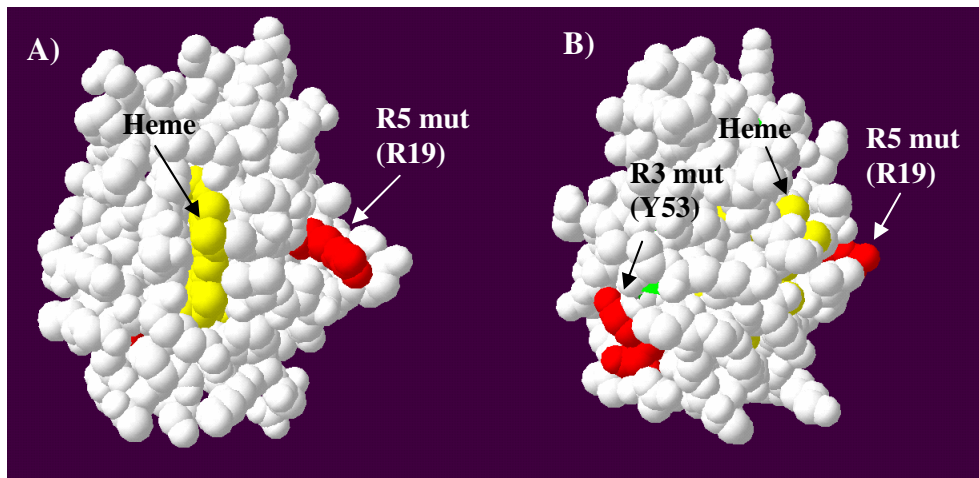


Figure 4.1. Structural model for the cyt *c* domain of cyt *c_y* built by homology modeling using the cyt *c₅₅₂* (www.expasy.org/swissmod/SWISS-MODEL.html). The location of R5 mutation; R19 (A) and R3 mutation; Y53 (B). Heme is indicated by yellow color, mutations are indicated by red colors.

In the case of cyt *c₂*, its kinetics is considered to arise from two distinct populations, with the fast phase reflecting the subpopulation of cyt *c₂* already bound to the RC prior to light activation (Axelrod et al., 2002). The rate of the fast phase is independent from cyt *c₂* concentration, but its amplitude depends on both its concentration and binding affinity to the RC. The rate of the slower phase reflects the fraction of cyt *c₂* that need to diffuse to reach an oxidized RC, and depends on both its concentration and binding affinity to the RC (Drepper et al., 1997; Drepper and Mathis, 1997; Moser and Dutton, 1988, Axelrod et al., 2002). Thus, in the case of cyt S-*c_yR35* kinetics the absence of a fast phase and the prominence of a slower phase indicates that almost no cyt S-*c_yR35* is associated with the RC prior to light activation. Comparing appropriate strains with similar amounts of soluble electron carrier cyts suggests that the binding affinity to the RC of cyt S-*c_yR35* should be lower than cyt *c₂* (Tiede et al., 1993; Overfield et al., 1979; Moser and Dutton, 1988). This deduction is in agreement with the

observation that better Ps^+ growth is correlated with increased steady-state concentrations of cyt S- c_y in various mutants.

It is thought that docking of a freely diffusible electron carrier, like cyt c_2 , to its redox partner such as the RC, is mainly governed by protein-protein interactions mediated by opposite surface charges (Tiede et al., 1993; Long et al., 1989; Caffrey et al., 1992). Therefore, different charge distributions on the docking surfaces of the redox couples affect their mode of interactions. The mutations that change the binding affinity also change the second-order rate constant, k_2 , for electron transfer and are important for docking cyt c_2 onto the RC (Tetreault et al., 2002). Upon docking, additional hydrophobic interactions are required for precise orientation of the redox couples and subsequent optimal ET rates between them, as illustrated by the RC-cyt c_2 (Axelrod et al., 2002), or the cyt bc_1 -cyt c (Hunte et al., 2002) co-crystal structures. The kinetic data available with cyt c_y and cyt S- c_y suggest that such hydrophobic interactions between the cyt c domain of cyt c_y and the RC are efficient enough to mediate fast ET, but the electrostatic interactions are weaker. It is possible that membrane anchoring of such electron carriers would counterbalance their weaker electrostatic interactions in recognizing their redox partners (Baymann et al., 2003). Thus, a lack of tight binding of the cyt c domain of cyt c_y to the RC, which is compensated by its membrane attachment, along with its efficient interaction with the cyt bc_1 complex is consistent not only with the slower oxidation of its soluble version cyt S- c_y , but also with its fast oxidation and re-reduction kinetics of its native form (Jenney et al 1996; Myllykallio et al., 1998). This observation suggests that cyt c_y might be more readily associated in its resting state with cyt c_1 of the cyt bc_1 complex rather than the RC, so that it interacts only transiently with the latter upon light activation in order to accomplish efficient multiple turnovers and Ps growth. Hence, a limited numbers of RC-cyt c_y - cyt bc_1 complex as hardwired photosynthetic units that turn over efficiently can provide vigorous phototrophic growth, as it has been observed upon the discovery of membrane-attached electron carriers (Daldal et al. 1986; Myllykallio et al., 1999).

In summary, this work demonstrated that the cyt *c* domain of the membrane anchored electron carrier cyt *c_y* exhibits slower ET kinetics to the RC upon its production in a freely diffusible form, due to absence of strong protein-protein interactions between these physiological partners. It also raises the intriguing possibility that attaching electron carrier cyts to the membrane allowed them to weaken their interactions with their partners, while restricting their spatial diffusion, so that they accomplish rapid multiple turnovers. Therefore, unlike the freely diffusible electron carriers, which rely on complementary electrostatic interactions and large pools, a small number of membrane-attached electron carrier cyts are sufficient to support growth efficiently.

In the second part of this thesis, the interaction between the electron transfer chain and the hydrogen production metabolism of *R. capsulatus* was investigated to elucidate the control mechanism of electron transfer chain and energy metabolism on hydrogen production. As a bacterium that is able to adapt to different environmental conditions *R. capsulatus* has developed elaborate regulatory mechanisms that control a variety of energy-generating and energy-utilizing biological processes, extending from photosynthesis to respiration to nitrogen fixation and hydrogen oxidation, which are involved in hydrogen metabolism. In this study, the relationship between the electron transfer chain and the hydrogen metabolism was analyzed by using various mutant strains deficient in electron carrier cytochromes, in terminal oxidases, in uptake hydrogenase and in their various combinations. The obtained results showed that the absence of any one of the multiple electron carrier cytochromes decreased the hydrogen production by about 3 to 5 fold (**Table 3.4**) likely due to the inefficiency of the electron transfer reactions required to maintain vigorous energy production. It therefore appears that efficient electron transport during the cyclic photoheterotrophic growth is essential for efficient hydrogen production of *R. capsulatus*.

The terminal oxidase⁻ mutants and their Hup⁻ derivatives were also analyzed for hydrogen production. These results indicated that, interestingly,

although the hydrogen production rate of a Qox^- strain did not change, that of a $\text{cyt } cbb_3^-$ mutant increased by about two fold (**Table 3.4**). This observation might be explained by the activation of nitrogenase gene expression and the repression of hydrogenase gene expression by the RegB/RegA global regulatory system, the activity of which is controlled by the electron flow through the $\text{cyt } cbb_3$ oxidase (**Figure 4.2**).

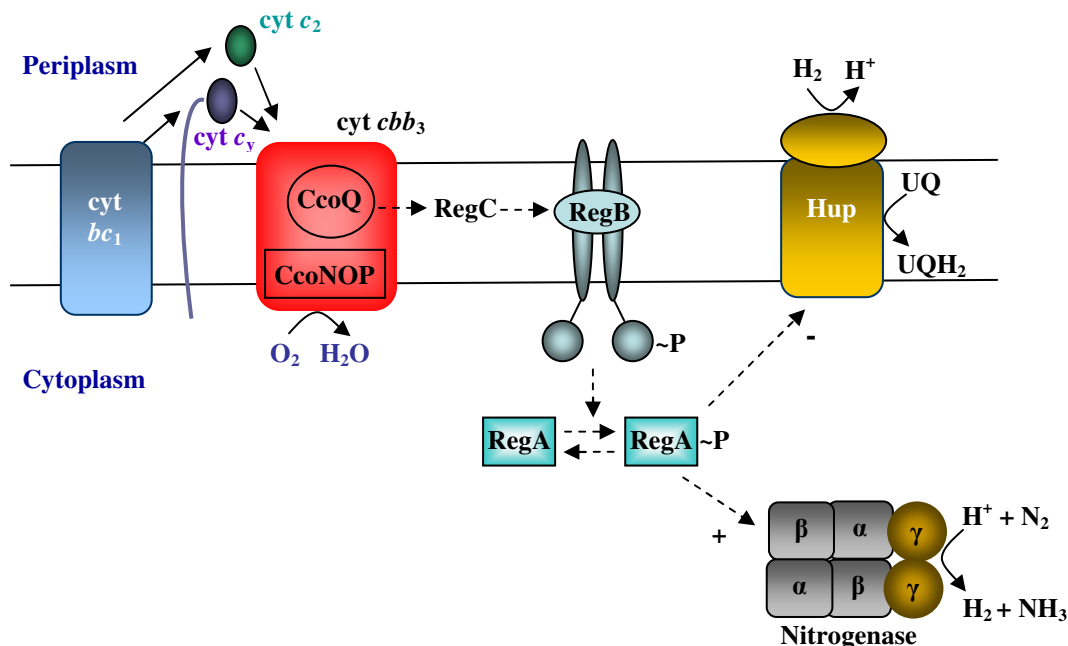


Figure 4.2. Respiratory electron transport pathways and model for redox sensing and signal transduction. The solid and dotted arrows demonstrate the electron and signal flows, respectively. In the absence of the cbb_3 oxidase, electron flow is blocked, which removes the signal, thereby returning RegB in the kinase-dominant mode. This leads to phosphorylation of RegA, resulting in the induction nitrogenase and repression of uptake hydrogenase. Abbreviations: UQH₂-UQ, ubiquinone pool; cyt bc_1 , cytochrome bc_1 complex; cyt c_2 , soluble cytochrome c_2 ; cyt c_y , membrane-bound cytochrome c_y ; cyt cbb_3 , cbb_3 -type cytochrome c oxidase; Hup, uptake hydrogenase

This finding further underlines the importance of the electron transfer chain and its components on redox signaling, and subsequently on hydrogen production metabolism. Moreover, our findings also confirmed that deletion of the uptake hydrogenase from wild type and oxidase⁻ mutants also increased the total hydrogen production and its production rate in agreement with earlier studies (Zorin et al., 1996; Jahn et al., 1994). The overall findings of this work highlights that the hydrogen production profile of the photosynthetic bacterium *R. capsulatus* might be further improved upon genetic modification of its ETC chain, as illustrated here with strains lacking the cyt *cbb₃*⁻ terminal oxidase and the uptake hydrogenase.

REFERENCES

- Albracht, S.P.J., 1994. Nickel hydrogenases: in search of the active site. *Biochim. Biophys. Acta* 1188, 167-204.
- Ambler, R.P., 1991. Sequence variability in bacterial cytochromes *c*. *Biochim. Biophys. Acta* 1058, 42-47.
- Amesz, J., Knaff D. B., 1988. Molecular Mechanisms of Bacterial Photosynthesis. Jhon Wiley & Sons, Chapter 3.
- Axelrod, H. L., Abresch, E. C., Okamura, M. Y., Yeh, A. P., Rees, D. C., and Feher, G., 2002. X-ray structure determination of the cytochrome *c*₂:reaction center electron transfer complex from *Rhodobacter sphaeroides*, *J. Mol. Biol.* 319, 501-515.
- Caffrey M, Davidson E, Cusanovich M, Daldal F., 1992. Cytochrome *c*₂ mutants of *Rhodobacter capsulatus*. *Arch. Biochem. Biophys.* 292 (2): 419-426.
- Cauvin B, Colbeau A, Vignais PM., 1991. The hydrogenase structural operon in *Rhodobacter capsulatus* contains a third gene, *hupM*, necessary for the formation of a physiologically competent hydrogenase. *Mol Microbiol.*; 5 (10): 2519-27.

Baccarini-Melandri, A., Zannoni, D., & Melandri, B. A., 1973. "Energy transduction in photosynthetic bacteria. IV. Respiratory sites and energy conservation in membranes from dark-grown cells of *Rhodopseudomonas capsulata*. Biochim. Biophys. Acta., 314, 298.

Baymann F, Barlow NL, Aubert C, Schoepp-Cothenet B, Leroy G, Armstrong FA., 2003. Voltammetry of a "protein on a rope". FEBS Lett. 539: 91-4.

Benning, M. M., Wesenberg, G., Caffrey, M. S., Bartsch, R. G., Meyer, T. E., Cusanovich, M. A., Rayment, I., Holden, H. M., 1991. Molecular structure of cytochrome c_2 isolated from *Rhodobacter capsulatus* determined at 2.5 Å resolution. *J Mol Biol* 220 pp. 673.

Bockris JO'M., 2002. The origin of ideas on a hydrogen economy and its solution to the decay of the environment. *Int J Hydrogen Energy*;27:731–40.

Camacho, C. J., and Vajda, S., 2001. Protein docking along smooth association pathways, *Proc. Natl. Acad. Sci. U.S.A.* 98, 10636-10641.

Carson, M., 1997. Ribbons. *Methods Enzymol.* 277, 493–505.

Colbeau, A., Richaud, P., Toussaint, B., Caballero, J., Elster, C., Delphin, C., 1993. Organization of the genes necessary for hydrogenase expression in *Rhodobacter capsulatus*. Sequence analysis and identification of two hyporegulatory mutants. *Mol Microbiol* 8: 15–29.

Cramer W.A., Knaff D.B., 1990. Quinone-binding proteins in photosynthetic reaction centers In Energy Transduction in Biological Membranes.

Daldal F., Cheng S., Applebaum J., Davidson E., Prince R., 1986. Cytochrome *c*² is not essential for photosynthetic growth of *Rhodopseudomonas capsulata*. Proc .Natl. Acad. Sci. 83: 2112-2116.

Daldal F., Davidson E., Cheng S., 1987. Isolation of the Structural Genes for the Rieske Fe-S Protein, Cytochrome *b* and cytochrome *c*₁ all components of the Ubiquinol: Cytochrome *c*₂ Oxidoreductase Complex of *Rhodopseudomonas capsulata*. J. Mol. Biol. 194: 1-12.

Daldal F., Gray K., Grooms M., Myllykallio H., Moomaw C., Slaughter C., 1994. *Rhodobacter capsulatus* Contains a Novel *cb*-Type Cytochrome *c* Oxidase without a Cu_A Center. Biochemistry 33:3120-3127.

Daldal F., Mandaci S., Winterstein C., Myllykallio H., Duyck K., and Zannoni D., 2001. Mobile Cytochrome *c*₂ and Membrane-Anchored Cytochrome *c*_y are Both Efficient Electron Donors to the *cbb*₃ and *aa*₃ Type Cytochrome *c* Oxidases during Respiratory Growth of *Rhodobacter sphaeroides*. J. Bacteriology, 183, 2013–2024.

Darrouzet E., M. Valkova-Valchanova, Ohnishi, T and F. Daldal., 1999. Structure and Function of the Bacterial *bc*₁ Complex: Domain movement, Subunit interactions, and Emerging Rationale Engineering Attempts. Journal of Bioenergetics and Biomembranes, vol. 31, No. 3.

Darrouzet E., M. Valkova-Valchanova, C. C. Moser, P. L. Dutton and F. Daldal., 2000. Uncovering the [2Fe2S] domain movement in cytochrome *bc*₁ and implications for energy conversion. Proc. Natl. Acad. Sci. USA 97: 4567-4572.

Das, D., and Veziroğlu, T.N., 2001. Hydrogen Production by Biological Processes: A Survey of Literature. *Int. J. Hydrogen Energy*, 26, pp. 13-28.

Davis G. L., Dibner D.M., Battey F. B., 1986. Basic methods in Molecular Biology, section 8-1, p. 90.

Debus R.J., Feher, G., and Okamura M.Y., 1985. Complex of Reaction Center from *Rhodopseudomonas viridis* R-26: Characterization and Reconstitution with H subunit. *Biochemistr* 24: 2488-2500.

Dischert, W., Vignais P. M., and Colbeau A., 1999. The synthesis of *Rhodobacter capsulatus* *HupSL* hydrogenase is regulated by the two-component HupT/HupR system. *Mol. Microbiol.* 34:995–1006.

Ditta G., Schmidhauser, T., E. Yakobson, P. Lu, X.-W. Liang, D. R. Finlay, D. Guiney, and D. R. Helinski., 1985. Plasmids related to the broad host range vector, pRK290, useful for gene cloning and for monitoring gene expression. *Plasmid* 13:149–153.

Drepper F and Mathis P., 1997. Structure and Function of Cytochrome *c2* in Electron Transfer Complexes with the Photosynthetic Reaction Center of *Rhodobacter sphaeroides*: Optical Linear Dichroism and EPR. *Biochemistry*, 36, 1428-1440.

Drepper F and Mathis P., 1997. Structure and Function of Cytochrome *c2* in Electron Transfer Complexes with the Photosynthetic Reaction Center of *Rhodobacter sphaeroides*: Optical Linear Dichroism and EPR. *Biochemistry*, 36, 1428-1440.

Drepper F, Dorlet P, Mathis P., 1997. Cross-linked electron transfer complex between cytochrome c_2 and the photosynthetic reaction center of *Rhodobacter sphaeroides*. Biochemistry. 36: 1418-27.

Drews D. and Golecki Jochen R., 1995. Molecular Organization, and Biosynthesis of membranes of Purple Bacteria. Kluwer Academic Publishers. Chapter 12.

Dross F, Geisler V, Lenger R, Theis F, Krafft T, Fahrenholz F, Kojro E, Duchene A, Tripier D, Juvenal K and Kröger A., 1992. The quinone-reactive Ni/Fe-hydrogenase of *Wolineilla succinogenes*. Eur J Biochem 206: 93-102.

Eady, R.R., 1996. Structure-function relationships of alternative nitrogenases. Chem. Rev. 96, 3013-3030.

Elsen, S., A. Colbeau, and P. M. Vignais., 1997. Purification and in vitro phosphorylation of HupT, a regulatory protein controlling hydrogenase gene expression in *Rhodobacter capsulatus*. J. Bacteriol. 179:968–971.

Elsen S., Dischert W., Colbeau A., and Bauer C. E., 2000. Expression of Uptake Hydrogenase and Molybdenum Nitrogenase in *Rhodobacter capsulatus* Is Coregulated by the RegB-RegA Two-Component Regulatory System. J. Bacteriol. Vol. 182, No. 10. 2831–2837.

Elsen S, Swem LR, Swem DL, Bauer CE., 2004. RegB/RegA, a highly conserved redox responding global two-component regulatory system. Microbiol Mol Biol Rev. Jun; 68(2):263-79.

Ferguson S.J., Jackson J.B., McEwan A.G., 1987. Anaerobic respiration in the Rhodospirillaceae: characterisation of pathways and evaluation of the roles in the redox balancing during photosynthesis. FEMS Microbiology Reviews 46:117-143.

Gennis, R. B., barquera, B., Hacker, B., Van, D. S. R., Arnaud, S., Crofts, A. R., Davidson, E., Gray, K. A., and Daldal, F., 1993. Journal of Bioenergetics and Biomembranes. 25, 195-209.

Gest, H. and Kamen, MD., 1949. Photoproduction of molecular hydrogen by *Rhodospirillum rubrum*. Science 109, 558-559.

Goltsov V. A., Veziroglu T. N., 2002. A step on the road to Hydrogen Civilization. International Journal of Hydrogen Energy 27 719–723.

Gomelsky, M., and S. Kaplan., 1995. Isolation of regulatory mutants in photosynthesis gene expression in *Rhodobacter sphaeroides* 2.4.1 and partialcomplementation of a PrrB mutant by the HupT histidine-kinase. Microbiology 141:1805–1819.

Gong, X., Paddock, M. L., and Okamura, M., 2003. Interactions between cytochrome c_2 and photosynthetic reaction center from *Rhodobacter sphaeroides*: Changes in binding affinity and electron transfer rate due to mutation of interfacial hydrophobic residues are strongly correlated, *Biochemistry* 42, 14492-14500.

Gray, K.A., Grooms, M., Myllykallio, H., Moomaw, C., Slaughter, C., and Daldal, F., 1994. *Rhodobacter capsulatus* contains a novel cb-type cytochrome c oxidase without a CuA center. *Biochemistry* 33: 3120–3127.

Hall, D.O., Markov, S.A., Watanable, Y and Rao, K.K., 1995. The potential application of cyanobacterial photosynthesis for clean technologies. Photosynthesis Research 46, 159-167.

Hallenbeck P, Benemann JR, 2001. Biological hydrogen production: fundamentals and limiting processes. Int J Hydrogen Energy; 27:1185–94.

Harrenga A, Reincke B, Ruterjans H, Ludwig B, Michel H., 2000. Structure of the soluble domain of cytochrome *c* (552) from *Paracoccus denitrificans* in the oxidized and reduced states. J Mol Biol 21;295(3):667-78.

Hawks, T.R., McLean, P.A. & Smith, B.E., 1984. Nitrogenase from nifV mutants of Klebsiella pneumoniae contains an altered form of the iron-molybdenum cofactor. Biochem. J. 217, 317-321.

Hillmer P, Gest H., 1977. H₂ germetabolism in the photosynthetic bacterium *Rhodopseudomonas capsulate*: H₂ production by growing cultures. J Bacteriol 129:724-731.

Hochkoeppler A., Jenney F., Lang S., Zannoni D., Daldal F., 1995. Membrane Associated Cytochrome *c_y* of *Rhodobacter capsulatus* Is an Electron Carrier from the Cytochrome *bc₁* Complex to the Cytochrome *c* Oxidase during respiration. J. Bacteriol. 177: 608-613.

Hoff AJ., 1988. Nomen estome. The Photosynthetic Bacterial reaction center: Structure nd Dynamics. Pp 98-99. Pleum Press, New York.

Hunte C, Solmaz S, Lange C., 2002. Electron transfer between yeast cytochrome *bc₍₁₎* complex and cytochrome *c*: a structural analysis. Biochim Biophys Acta. 1555: 21-8.

Imhoff F. Johannes., 1995. Taxonomy and Physiology of Phototrophic Purple Bacteria and Green Sulfur Bacteria. Kluwer Academic Publishers. Chapter 1.

Jahn A, Keuntje B, Dorffler M, Klipp W, Oelze J., 1994. Optimizing photoheterotrophic H₂ production by *Rhodobacter capsulatus* upon interposon mutagenesis in the hupL gene, J. Appl Microbiol Biotechnol Jan; 40(5):687-90.

Jee, H.S., Ohashi, T., Nishizawa, Y., and Nagai, S., 1987. Limiting Factor of Nitrogenase System Mediating Hydrogen Production of *Rhodobacter sphaeroides* S, J. Ferment. Technol. 65(2), 153-158.

Jenney Jr., Daldal F., 1993. A novel membrane-associated c-type cytochrome cyt c_y, can mediate the photosynthetic growth of *Rhodobacter capsulatus* and *Rhodobacter sphaeroides*. EMBO J. 12:1283-92.

Jenney Jr. F.E., Prince R.C., Daldal F., 1994. Roles of the soluble cytochrome c₂ and membrane-associated cytochrome c_y. Biochemistry 33:2496-2502.

Jenney Jr. F.E., Prince R.C., Daldal F., 1996. The membrane-bound cytochrome c_y of *Rhodobacter capsulatus* can serve as an electron donor to the photosynthetic reaction center of *Rhodobacter sphaeroides*. Biochimica et Biophysica Acta 1273: 159-164.

Joshi, H. M., and Tabita F. R., 1996. A global two component signal transduction system that integrates the control of photosynthesis, carbon dioxide assimilation, and nitrogen fixation. Proc. Natl. Acad. Sci. USA. 93:14515–14520.

Kaplan S., Donohue T. J., 1992. Genetic techniques in the *Rhodospirillaceae*. Methods in Enzymology 204: 459-485.

Kaplan S, Eraso J, Roh JH., 2005. Interacting regulatory networks in the facultative photosynthetic bacterium, *Rhodobacter sphaeroides* 2.4.1. Biochem Soc Trans. 33(Pt 1):51-5.

Kiel, J.L., 1995. Type-*b* Cytochromes: Sensors and Switches. CRC Press, Boca Raton.

Kiley P. J., and Kaplan S., 1988. Molecular Genetics of Photosynthetic Membrane Biosynthesis in *Rhodobacter sphaeroides*. Microbiological Reviews, p 50-69.

Koch H-G., O. Hwang and Daldal F., 1998. Isolation and characterization of *Rhodobacter capsulatus* mutants affected in cytochrome *cbb*₃ oxidase activity. J. Bacteriol. 180:969-978.

Koku H. Eroğlu İ, Gündüz U, Yücel M, Türker L., 2003. Aspects of the metabolism of hydrogen production by *Rhodobacter sphaeroides*. International Journal of Hydrogen Energy; 27: 1315 – 1329.

Kranz RG and Foster-Hartnett D., 1990. Transcriptional regulatory cascade of nitrogen-fixing genes in anoxygenic photosynthetic bacteria: oxygen- and nitrogen-responsive factors. Mol Microbiol 4: 1793-1800.

Laguri, C., M. K. Phillips-Jones, and Williamson M. P., 2003. Solution structure and DNA binding of the effector domain from the global regulator PrrA (RegA) from *Rhodobacter sphaeroides*: insights into DNA binding specificity. Nucleic Acids Res. 31:6778–6787.

Lehninger L. A., Nelson L. D., Cox M. M., 1993. Principle of Biochemistry.

Long, J., Durham, B., Okamura, M. & Millett, F., 1989. *Biochemistry* 28, 6970–6974.

Lowry, O., Rosebrough, N., Farr, A. & Randall, R., 1951. *J. Biol. Chem.* 193, 265–275.

Ludden, P. W. & Roberts, G. P., 1989. Regulation of nitrogenase activity by reversible ADP ribosylation. *Curr. Top. Cell. Regul.* 30: 23–56.

Madigan, M.T., Martinko, J.M., and Parker, J., 2000. *Brock Biology of Microorganisms*, 9th edition, Prentice Hall Inc.

McEwan, A. G., 1994. Photosynthetic electron transport and anaerobic metabolism in purple non-sulfur bacteria. *Antonie van Leeuwenhoek*: 66, 151–164.

Meyer, T., and Donohue T., 1995. Cytochromes, iron-sulfur and copper proteins mediating electron transfer from the Cyt *bc₁* complex to photosynthetic reaction center complexes, p. 725–745. Kluwer Academic Publishers, chapter 34.

Meyer, J., Kelley, B. and Vignais, P.M., 1978. Nitrogen fixation and hydrogen metabolism in photosynthetic bacteria. *Biochimie* 60, 245-260.

Merrick, M. J., 1992. Regulation of nitrogen fixation genes in free living and symbiotic bacteria. In: *Biological Nitrogen Fixation* (Stacey, G., Burris, R. H. & Evans, H. J., eds.), pp. 835–876, Chapman and Hall, New York, NY.

Merrick M., 1993. Organization and regulation of nitrogen fixation genes. In Palacious R, Mora J and Newton W (eds) *New Horizons in Nitrogen Fixation*, pp 48-54.kluwer Academic press, Boston.

Mitchell, P., 1961. Nature, 191, 144.

Mitchell P., 1966. Chemio Coupling in Oxidative and Photosynthetic Phosphorylation. In H. M. Fox (Ed.), Biological Reviews of the Cambridge Philosophical Society (pp. 445-502).

Miyake, J., Tomizuka, N., and Kamibayashi, A., 1982, "Prolonged Photohydrogen Production by *Rhodospirillum rubrum*", Journal of Fermentation Technology, 60, pp. 199-203.

Moore G.R., Pettigrew G.W., 1990. Cytochromes c: Evolutionary, Structural and Physicochemical Aspects Springer.

Montet, Y., Amara, P., Volbeda, A., Vernede, X., Hatchikian, E.C., Field, M.J., Frey, M. and Fontecilla-Camps, J.C., 1997. Gas access to the active site of Ni-Fe hydrogenases probed by X-ray crystallography and molecular dynamics. Nat. Struct. Biol. 4, 523-526.

Moser, C., and Dutton, P. L., 1988. Cytochrome c and c_2 binding dynamics and electron transfer with photosynthetic reaction center protein and other integral membrane redox proteins, *Biochemistry* 27, 2450-2461.

Mouncey, N. J., and Kaplan, S., 1998. Oxygen regulation of the *ccoN* gene encoding a component of the *cbb3* oxidase in *Rhodobacter sphaeroides* 2.4.1T: involvement of the *FnrL* protein. *J. Bacteriol.* 180, 2228-2231.

Myllykallio H., Jenney Jr., F. Moomaw C., Slaughter C., Daldal F., 1997. Cytochrome c_y of *Rhodobacter capsulatus* Is Attached to the Cytoplasmic Membrane by an Uncleaved Signal Sequence-Like Anchor. J. Bacteriol. 179: 2623-2631.

Myllykallio H, Drepper F, Mathis P and Daldal F., 1998. Membraneanchored cytochrome c_y mediated microsecond time electron transfer from the cytochrome bc_1 complex to the reaction center in *Rhodobacter capsulatus*. Biochemistry 37: 5501–5510.

Myllykallio, H., Drepper, F., Mathis, P. & Daldal, F., 1998. Membrane-Associated Cytochrome c_y of *Rhodobacter capsulatus* Is an Electron Carrier from the Cytochrome bc_1 Complex to the Cytochrome c Oxidase during Respiration. Biochemistry 37, 5501–5510.

Myllykallio, H., D. Zannoni and F. Daldal., 1999. Rhodobacter sphaeroides cyt c_y is a membrane-attached electron carrier that is deficient in photosynthesis but proficient in respiration. Proc. Natl. Acad. Sci. USA 96:4348-4353.

Nomenclature Committee of the International Union of Biochemistry (NC-IUB)., 1989. Nomenclature of electron-transfer proteins. Eur. J. Biochem. 200, 599-611.

Oh, J.I. and Kaplan, S., 1999. The cbb_3 terminal oxidase of *Rhodobacter sphaeroides* 2.4.1: structural and functional implications for the regulation of spectral complex formation. *Biochemistry*, 38, 2688–2696.

Oh, J. I., and Kaplan, S., 2000. Redox signaling: globalization of gene expression, EMBO J. 19, 4237-4247.

Oh J. I, Ko IJ, Kaplan S., 2004. Reconstitution of the *Rhodobacter sphaeroides* *cbb₃*-PrrBA signal transduction pathway in vitro. Biochemistry 22; 43 (24):7915-23.

Ooshima H., Takakuwa S., Katsuda T., Okuda M., Shirasawa T., Azuma M.and Kato J., 1998. Production of Hydrogen by a Hydrogenase-Deficient Mutant of *Rhodobacter capsulatus*. Journal of Fermentation and Bioengineering Vol. 85, No. 5, 470-475.

Overfield, R. E., Wraight, C. A., and Devault, D. C., 1979. Microsecond photooxidation kinetics of cytochrome *c₂* from *Rhodopseudomonas sphaeroides*: In vivo and solution studies, *FEBS Lett.* 105, 137-142.

Öztürk Y., 2001. Construction and Analysis of a Soluble Version of The Membrane-Attached Cytochrome *c_y* in *Rhodobacter capsulatus*. Master thesis.

Pettigrew, G.W. and Moore, G.R., 1987. Cytochromes *c*. Biological Aspects. Springer-Verlag, Berlin - Heidelberg - New York.

Prince, R. C., E. Davidson, C. Haith, and F. Daldal., 1986. Photosynthetic electron transfer in the absence of cyt *c₂* in *Rhodopseudomonas capsulata*: cyt *c₂* is not essential for electron flow from the *bc₁* complex to the photochemical reaction center. Biochemistry 25: 5208–5212.

Prince R. C., 1990. Bacterial photosynthesis: From Photons to Δp The Bacteria, Vol.XII. Chapter 5.

Prince, R. C., Cogdell, R. J., and Crofts, A. R., 1974. The photo-oxidation of horse heart cytochrome *c* and native cytochrome *c₂* by reaction centers from *Rhodopseudomonas sphaeroides* R-26, *Biochim. Biophys. Acta* 347, 1-13.

Reincke B, Perez C, Pristovsek P, Lucke C, Ludwig C, Lohr F, Rogov VV, Ludwig B, Ruterjans H., 2001. Solution structure and dynamics of the functional domain of *Paracoccus denitrificans* cytochrome c(552) in both redox states. *Biochemistry*. 40 :12312-20.

Reith J.H., Wijffels, R.H. and Barten H., 2003. Status and perspectives of biological methane and hydrogen production. *Dutch Biological Hydrogen Foundation*. ISBN: 90-9017165-7.

Richaud, P., Colbeau, A., Toussaint, B., and Vignais, P.M., 1991. Identification and sequence analysis of the hupR gene which encodes a response regulator of the NtrC family required for hydrogenase expression in *Rhodobacter capsulatus*. *J. Bacterio*. 1173: 5298–5392.

Roh JH, Smith WE, Kaplan S., 2004. Effects of oxygen and light intensity on transcriptome expression in *Rhodobacter sphaeroides* 2.4.1. Redox active gene expression profile. *J Biol Chem*. 5;279(10):9146-55.

Sambrook, J., E. F. Fritsch, and T. Maniatis., 1989. Molecular cloning: a laboratory manual. Cold Spring Harbor Laboratory Press, Cold Spring Harbor, N.Y.

Sargent, F., Bogsch, E.G., Stanley, N.R., Wexler, M., Robinson, C., Berks, B.C. and Palmer, T., 1998. Overlapping functions of components of a bacterial Sec-independent protein export pathways. *EMBO J*. 17, 3640-3650.

Saribas A. S., Mandaci S., and Daldal F., 1999. An Engineered Cytochrome *b₆ c₁* Complex with a Split Cytochrome *b* Is Able to Support Photosynthetic Growth of *Rhodobacter capsulatus*. *Journal of Bacteriology*, p. 5365–5372 Vol. 181, No. 17.

Sauder, J.M., MacKenzie, N.E., and Roder, H., 1996. Kinetic mechanism of Folding and Unfolding of *Rhodobacter capsulatus* Cytochrome *c*₂. *Biochemistry*. 35 16852-16862.

Schägger, H., and Von Jagow, G., 1987. Tricine-sodium dodecyl sulfate-polyacrylamide gel electrophoresis for the separation of proteins in the range form 1–100 kDa. *Anal Biochem* 166: 368–379.

Scolnik, P., M. Walker, and B. Marrs., 1980. Biosynthesis of carotenoids derived from neuosporene in *Rhodopseudomonas capsulata*. *J. Biol. Chem.* 255:2427–2432.

Smith, B.E., 1999. Structure, function, and biosynthesis of the metallo sulfur clusters in nitrogenases. *Adv. Inorg. Chem.* 47, 159-218.

Sistom, W.A., 1960. requirement for sodium in the Growth of *Rhodopseudomonas sphaeroides*. *J. Gen. Microbiol.* 22: 778.

Stackebrandt, E., Murry, R.G.E., and Trüper, H.G., 1988. *Proteobacteria* classis nov., a name for the phylogenetic taxon that includes the “Purple bacteria and their relatives.” *Int. J. Syst. Bacteriol.*

Stam, H., Stouthamer, A.H., and Van Verseveld, H.W., 1987, FEMS Microbiol. Rev., 46, pp. 73-92, cited in Sasikala *et al.*, 1993.

Tetreault, M., Cusanovich, M., Meyer, T., Axelrod, H. & Okamura M., 2002. *Biochemistry* 41, 5807–5815.

Tetreault M., Rongey S., Feher G., and Okamura, M., 2001. Interaction between cytochrome *c*2 and the photosynthetic reaction center from *Rhodobacter sphaeroides*: Effects of charge-modifying mutations on binding and electron transfer, *Biochemistry* 40, 8452-8462.

Thomas, P.E., Ryan, D., and Levin, W., 1976. An improved staining procedure for the detection of the peroxidase activity of cyt *P450* on sodium dodecyl sulfate polyacrylamide gels. *Anal Biochem* 75: 168–176.

Tichi MA, Meijer WG, Tabita FR., 2001. Complex I and its involvement in redox homeostasis and carbon and nitrogen metabolism in *Rhodobacter capsulatus*. *J Bacteriol.* 183(24):7285-94.

Tiede D. M., Dutton P. L., 1993. Electron Transfer between Bacterial Reaction Centers and Mobile *c*-Type Cytochromes. In The Photosynthetic Reaction Center.

Tindall,B.J., and Grant, W:D., 1986. The anoxygenic Phototrophic bacteria. *Soc.Appl.Bacteriol. Symp. Ser.* 13, 115-155.

Toussaint, B., de Sury d'Aspremont, R., Delic-Attree, I., Berchet, V., Elsen, S., Colbeau, A., 1997. The *Rhodobacter capsulatus hupSLC* promoter: identification of cis-regulatory elements and of trans-activating factors involved in H₂ activation of *hupSLC* transcription. *Mol Microbiol* 26: 927–937.

Trumppower B.L., Gennis R B., 1994. Energy Transduction by Cytochrome Complexes in Mitochondria and In Bacterial Respiration. *Annu. Rev. Biochem* 63:675-716.

Vignais P. M., Colbeau, A., Willison J. C., and Jouanneau Y., 1985. Hydrogenase, Nitrogenase and Hydrogen Metabolism in Photosynthetic Bacteria. *Adv. Microbial Phys.* 26, 154-234.

Vignais P. M., B. Dimon, N. A. Zorin, A. Colbeau, and S. Elsen., 1997. HupUV proteins of *Rhodobacter capsulatus* can bind H₂: evidence from the H-D exchange reaction. *J. Bacteriol.* 179:290–292.

Vignais PM., Billoud B., Meyer J., 2001. Classification and phylogeny of hydrogenases. *FEMS Microbiology Reviews* 25 455-501.

Volbeda A., Charon, M.H., Piras, C., Hatchikian, E.C., Frey, M. and Fontecilla-Camps, J.C., 1995. Crystal structure of the nickel-iron hydrogenase from *Desulfovibrio gigas*. *Nature* 373, 580-587.

Yen, H.C., Hu, N.T., and Marrs, B.L. (1979) Characterization of the gene transfer agent made by an overproducer mutant of *Rhodopseudomonas capsulata*. *J Mol Biol* 131:157–168.

Youvan Dougles C. and Bylina Edward J., 1989. Photosynthesis in *Rhodospirillace*. Chapter 5.

Zajic J.E., Kosaric, N. and Brosseau, J.D., 1978. Microbial production of hydrogen. *Advances in Biochemiacal Engineering* 9, 57-109.

Zannoni, D., Melandr, B. A., and Baccarini-Melandri, A. (1976) Composition and function of the branched oxidase system in wild-type and respiratory mutants of *Rhodopseudomonas capsulata*. *Biochim. Biophys. Acta*, 423: 413-430.

Zannoni D., Daldal F., 1993. The role of *c*-type cytochromes in catalyzing oxidative and photosynthetic electron transport in the dual functional plasma membrane of facultative phototrophs. Arch. Microbiol. 160:413-423.

Zannoni D., 1995. In R.E. Blankenship, M.T. Madigan and C.E. Bauer (eds), Anoxygenic Photosynthetic Bacteria (pp 949-71) Kluwer Academic Publishers.

Zeilstra-Ryalls, J. H., and S. Kaplan., 1995. Aerobic and anaerobic regulation in *Rhodobacter sphaeroides* 2.4.1: the role of the *fnrL* gene. J. Bacteriol. 177:6422–6431.

Zeilstra-Ryalls, J. H., and Kaplan, S., 1996. Control of *hemA* expression in *Rhodobacter sphaeroides* 2.4.1: regulation through alterations in the cellular redox state, J. Bacteriol. 178, 985-993.

Zorin N. A., Lissola T., Colbeau A and Vignasis P.M., 1996. Increased hydrogen photoproduction by *Rhodobacter capsulatus* strains deficient in uptake hydrogenase. J Mar Biotechnol 4:28-33.

Zufferey, R., Preisig, O., Hennecke, H., and Tho'ny-Meyer, L. (1996) J. Biol. Chem. 271, 9114-9119.

APPENDIX A

BACTERIAL GROWTH MEDIUMS

Sistrom's Minimal Medium (Med A) liquid

	<u>For 1L</u>
(NH ₄) ₂ SO ₄ [10%]	5 ml
Sodium (or Potassium) Succinate [10%]	20 ml
NaCl [10%]	5 ml
L-Glutamic acid [5%, pH:7]	2 ml
L-Aspartic acid [2%, pH:7]	2 ml
Macroelement solution	20 ml
Potassium phosphate [1M, pH:6.8]	20 ml

are completed up to 1 L and autoclaved. When the temperature is 50-55°C, sterile 10 ml 100X Vitamin is added and mixed.

Med A-Plate

	<u>For 1L</u>
(NH ₄) ₂ SO ₄ [10%]	5 ml
Sodium (or Potassium) Succinate [10%]	20 ml
NaCl [10%]	5 ml
L-Glutamic acid [5%, pH:7]	2 ml
L-Aspartic acid [2%, pH pH:7]	2 ml

are completed with dH₂O to 920 ml. 15 g agar [1.5%] is added, and autoclaved. Sterile 20 ml macroelement solution, 20 ml potassium phosphate [1M, pH:6.8], and

10 ml 100X vitamin are added and mixed when the temperature of the medium is 50-55°C.

Stock Solutions of Med A

A) Microelements Solution

<u>For 1 L</u>	
ZnSO ₄ .7H ₂ O	10 g
EDTA	2.5 g
FeSO ₄ .7H ₂ O	5 g
H ₃ BO ₃	1.14 g
MnSO ₄ .H ₂ O	1.54 g
CuSO ₄ .5H ₂ O	3.92 g
Co(NO ₃) ₂ .6H ₂ O	2.5 g

are dissolved in 1 L dH₂O, autoclaved and stored.

B) Macroelements Solution

<u>For 1 L</u>	
Nitrilotriacetic acid	10 g
MgSO ₄ .7H ₂ O	29.5 g
CaCl ₂ .2H ₂ O	3.3 g
FeSO ₄ .7H ₂ O	9.9 g
Microelements Solution	50 ml

are dissolved in 800 ml dH₂O, pH is adjusted with KOH to 6.8-7. The volume is completed to 1 L with dH₂O and autoclaved.

C) Vitamins (100X)

<u>For 1 L</u>	
Nicotinic acid	100 mg
Thiamin HCl	25 mg
Biotin (40 µg/ml stock)	12.5 ml

are dissolved in 1 L dH₂O, sterilized with 0.22 µm filter, and stored at +4°C.

Liquid MPYE-Medium (enriched Medium)

<u>For 1 L</u>	
Bacto pepton (0.3%)	3 g
Yeast extract (0.3%)	3 g
MgCl ₂ (1,6 mM)	1.6 ml
CaCl ₂ (1 mM)	1 ml

are dissolved in dH₂O. pH is adjusted with NaOH to 7 and autoclaved.

MPYE-Plate

For 1 L liquid MPYE medium, 15 g agar (1.5%) (Difco-Bacto agar) is added and autoclaved.

Liquid LB Medium (Luria Broth)

<u>For 1 L</u>	
Bacto tryptone	10 g
Yeast extract	5 g
NaCl	10 g

are dissolved in 800 dH₂O, pH is adjusted with NaOH to 7.5. The volume is completed to 1 L with dH₂O and autoclaved.

LB-Plate

For 1 L liquid LB medium, 15 g agar (1.5%) (Difco-Bacto agar) is added and autoclaved.

Minimal medium of Biebl and Pfennig (BP)

<u>For 1 L</u>	
KH ₂ PO ₄	0.5 g
MgSO ₄ · 7H ₂ O	0.2 g
NaCl	0.4 g
Na-glutamate (2 mM)	0.36 g
CaCl ₂ · 2H ₂ O	0.05 g
DL-Malic Acid (15 mM)	2.0 g
Vitamin Solution	1 ml
Trace Element Solution SL7	1 ml
Fe-citrate Solution	1 ml

Stock Solutions of BP medium

A) Trace Element Solution

<u>For 1 L</u>	
HCl (25% v/v)	1 ml
ZnCl ₂	70 mg
MnCl ₂ · 4H ₂ O	100 mg
H ₃ BO ₃	60 mg
CoCl ₂ · 6H ₂ O	200 mg
CuCl ₂ · 2H ₂ O	20 mg
NiCl ₂ · 6H ₂ O	20 mg
NaMoO ₄ · 2H ₂ O	40 mg

B) Fe-citrate Solution

0.5 g Fe-citrate is dissolved in 100 ml distilled water and sterilized by autoclaving.

C) Vitamin Solution

For 1 L

Thiamine	500 mg
Niacin (Nicotinate)	500 mg
Biotin	15 mg

* Growth mediums, solutions and buffers are sterilized by autoclaving at 121°C for 30 min.

APPENDIX B

ANTIBIOTICS AND SOLUTIONS

Tetracycline

For 100 ml 1.25 mg/ml stock solution;

125 mg tetracycline is dissolved in 100 ml 50% (v/v) Ethanol / water, and sterilized with 0.22 µm filter, and stored in dark at -20°C.

Kanamycin

For 100 ml 5 mg/ml stock solution;

500 mg kanamycin is dissolved in 100 ml dH₂O, filter sterilized, and stored at -20°C.

Ampicillin

For 100 ml 10 mg/ml stock solution;

1 gr ampicillin is dissolved in 100 ml dH₂O, filter sterilized, and stored at -20°C.

Spectinomycin

For 100 ml 5 mg/ml stock solution;

500 mg spectinomycin is dissolved in 100 ml dH₂O, filter sterilized, and stored at -20°C.

Gentamicin

For 100 ml 5 mg/ml stock solution;

500 mg gentamicin is dissolved in 100 ml dH₂O, filter sterilized, and stored at 4°C.

EDTA (Ethylene-tetraacetic acid) (0.5 M)

For 250 ml EDTA solution, 46.5 g EDTA is dissolved in 150 ml dH₂O, and pH is adjusted with NaOH to 8. The volume is completed to 250 L with dH₂O and autoclaved.

SDS Solution (10%)

0.1 g Sodium Dodecyl Sulphate (SDS) was dissolved in 1ml of ddH₂O

Acrylamide Solution (49.5 %)

For 100 ml solution, 48 gr Acrylamide, and 1.5 gr bisacrylamide are dissolved in 60 ml dH₂O. 5 gr of BIO-RAD AG501x8D bed resin is added and stirred for 1 hr. The volume is completed to 100 ml and filtered through Whatman filter paper. The stock solution is kept in dark at 4°C.

Ammonium persulfate (APS) (10%)

0.1 gr of APS is dissolve in 1 ml of dH₂O. It should be made fresh daily.

TMBZ (3,3',5,5'-Tetramethylbenzidin) staining solution

For 100 ml solution, 45 mg TMBZ is dissolved in 30 mL Methanol (peroxides free) and mixed with a stir bar to dissolve TMBZ completely. The beaker is sealed with parafilm and cover completely with aluminum foil to block out all light. 70 mL 0.25 M Na-Acetate (pH 5.0) is added to complete 100 ml.

Sodium Acetate solution (0.25 M, pH 5.0)

For 500 ml solution, 17.01 gr Na-Acetate is dissolve in 400 mL of dd H₂O and pH is adjusted to 5.0 with glacial acetic acid. The volume is completed to 500 ml.

RNase Solution

	<u>For 1 ml</u>
RNase	10 mg
Tris/HCl (1M, pH: 7.5)	10 µl (final 0.01 M)
NaCl (5M)	3 µl (final 0.015 M)

The volume is completed to 1 ml and boiled at 110°C for 40 min. The solution is filter sterilized and stored at -20°C.

Solutions Used for Lowry Method to Determine Amount of the Protein

Solution A: 2 g Na₂CO₃ is dissolved in 0.1 N NaOH than volume completed to 100 ml with ddH₂O.

Solution B: 1 g CuSO₄. H₂O is dissolved in 1000 ml ddH₂O.

Solution C: 2 g Sodium Potassium tartarate are dissolved in ddH₂O

Solution D: Solution B and C are mixed (1/1 ratio) (It is daily prepared).

Solution E: 1 ml solution D was added in 50 ml solution A (It is prepared just before used).

APPENDIX C

BUFFERS

TBE Buffer (20X)

For 1 L

Tris Base (1 M)	121 g.
Boric Acid (1M)	61.7 g.
EDTA .2H ₂ O (20 mM)	7.44 g.

are dissolved in 1 L dH₂O, and sterilized by autoclaving.

TAE Buffer (50X)

For 1 L

Tris Base	242 g
Asetic acid Glacial	57.1 ml
EDTA. 2H ₂ O (0,5 M, pH:8)	100 ml

The volume is completed to 1 ml with dH₂O, and sterilized by autoclaving.

TE buffer

For 100 ml

Tris Base (1 M, pH:7.5)	1 ml
EDTA.2H ₂ O (0.5 M, pH:8)	200 µl

The volume is completed to 100 ml with dH₂O, and sterilized by autoclaving.

Stock buffers for the Schagger Gel:

a) Gel Buffer (3M Tris, 0.3% SDS, pH 8.45) (3X)

36.33 gr Tris and 0.3 gr SDS is dissolved in about 40 ml water. pH is adjusted to 8.45 with HCl and the volume is completed up to 100 ml.

b) Anode Buffer (2M Tris, pH 8.9) (10X)

For 100 ml solution, 24.22 gr Tris is dissolved in 80 ml water. pH is adjusted to 8.9 with HCl and the volume is completed up to 100 ml.

c) Cathode Buffer (1M Tris, 1M Tricine, 1 % SDS, pH 8.25) (10X)

For 200 ml solution, 24.2 gr Tris 35.84 gr Tricine and 0.6 g SDS were dissolved in 200 ml water. pH is not adjusted (it should be around 8.25)

MOPS/KCl buffer (50 mM/1 mM, pH:7)

For 500 ml

MOPS	5.78 gr
KCl	0.37 gr

are dissolved in 400 ml dH₂O, and pH is adjusted with HCl to 7. The volume is completed to 500 ml with dH₂O, and sterilized by autoclaving (store at -4°C).

MOPS/KCl buffer (50 mM/100 mM, pH:7)

For 500 ml

MOPS	5.78 gr
KCl	3.7 gr

are dissolved in 400 ml dH₂O, and pH is adjusted with HCl to 7. The volume is completed to 500 ml with dH₂O, and sterilized by autoclaving (store at -4°C).

DNA Loading Dye:

	<u>For 10 ml</u>
Bromophenol blue	0.025g
Glycerol (100%)	5 ml
EDTA.2H ₂ O (0,5 M, pH:8)	200 µl
TBE (10X)	5 ml

Protein loading dye

	<u>For 1 ml</u>
10% SDS	400 µl (final con; 4%)
100 % Glycerol	120 µl (final con; 12%)
1 M Tris (pH:7)	50 µl (final con; 50 mM)
0.5 % Bromophenol blue	40 µl (final con; 0.01%)

The volume completed to 1 ml by adding 390 µl d H₂O.

GTA Buffer:

	<u>For 100 ml</u>
1 M Tris-HCl pH=7.8	1ml (final con:10 mM)
1 M MgCl ₂	100 µl (final con:1 mM)
1 M CaCl ₂	100 µl (final con:1 mM)
5 M NaCl	20µl (final con:1 mM)
BSA-fraction V (Sigma)	0.05 gr (final con:500 µg/ml)

The volume is completed to 100 ml with dH₂O. The buffer is sterilized by filtered aseptically through a 0.2 µ disposable filters and stored at -20°C.

APPENDIX D

CHEMICALS

Acetic acid (Merck, 100056)
Acrylamide (J.T.Baker 79-06-1)
Agar (Difco, 0140-01)
Agarose (Research organics 1170A) cat. number 9012-36-6
Ammonium persulfate [APS] (Sigma, A-9164)
Ampcillin (Sigma, A-0166)
L-Aspartic acid (Sigma, A-9256)
Bacto Peptone (Difco, 0118-17-0)
Bacto Tryptone (Difco, 0123-17-3)
Biotin (SIGMA)
BSA [Bovine Serum Albumin] (Sigma, A-9647)
N, N'-Methylene- bis-Acrylamide (Sigma, M-7256)
CaCl₂.2H₂O (MERCK)
Chloroform (Carlo Erba reagent, 334353)
CoCl₂.6H₂O (MERCK)
CuCl₂.2H₂O (MERCK)
DNase [DeoxyribonucleaseI, from bovine pancreas] (Sigma, DN-25)
dNTP set (MBI): cat. # R0181
EtBr [Ethidium Bromide] (Sigma, E-8751)
Glycerol, cell culture tested (Sigma, G-2025)
Glycerol, Electrophoresis grade (Sigma G-8773)
HCl (MERCK)
H₃BO₃ (MERCK)

Hydrogen peroxide [(H₂O₂), 30%] (Aldrich, Chemical Co., 21, 676.3)
L-Glutamic acid (Sigma, G-1251)
Fe-citrate (MERCK)
Kanamycin (Sigma, K-4378)
Lysozyme (Sigma, L-7651)
Malic Acid (MERCK)
MgSO₄.7H₂O (MERCK)
2-Mercaptoethanol (Electrophoresis Regent, Sigma, M-7154)
Methanol (Carlo Erba reagent, 309203)
MOPS [3- (N-Morpholino) propanesulfonic acid] (Sigma, M-9381)
Niacin (SIGMA)
NiCl₂.6H₂O (MERCK)
Phenol (Sigma, P-4557)
KH₂PO₄ (MERCK)
Proponal (Merck, 100995)
RNase A (from bovine pancreas) (Bioehringer mannheim, 83686728)
SDS (Lauryl sulfate) (Sigma, L-5750)
Sigmacote® (Sigma, SL-2)
Sodium acetate (Merck, 6268.1000)
NaCl (MERCK)
NaOH (MERCK)
Sodium Glutamate (MERCK)
NaMoO₄.2H₂O (MERCK)
Succinic Acid [Disodium Salt Hexahydrate] (Sigma, S-9637)
Temed (Sigma, T-7024)
Tetracycline Hydrochloride, Crystalline (Sigma, T-3383)
Thiamine (SIGMA)
Tris Base (Trizma base, J.T. Baker 77-86-1)
Tricine (Electrophoresis Grade) Sigma T-7911
TMBZ (Aldrich Chemical Co., 86, 033-6)
Yeast Extract (Difco, 0127-17-9)
ZnCl₂, MnCl₂.4H₂O (MERCK)

APPENDIX E

RESTRICTION ENDONUCLEASES AND DNA MODIFYING ENZYMES

RESTRICTION ENDONUCLEASES

*Bal*I (MBI): cat.# 1211

*Bam*HI (MBI): cat.# ER0051

*Bgl*III (MBI): cat.# ER0081

*Dpn*I (MBI): cat. # ER1701

*Eco*RI (MBI): cat.# ER0271

*Hind*III (MBI): cat.# ER0501

*Kpn*I (MBI): cat.# ER0021

*Pst*I (MBI): cat.# ER0611

*Xba*I (MBI): cat # 0681

POLYMERASES

Pfu DNA polymerase (MBI): cat. # EP0501

LIGASES

T4 DNA Ligase (MBI): cat. # EL0331

PHOSPHATASES

Calf Intestine Alkaline Phosphatase (CIAP) (MBI): cat. # ER EF0341

APPENDIX F

hupSLC OPERON AND PLASMID MAPS

Sequence of *hupSLC* operon with upstream and downstream sequences:

GAAGCCGGACAGGCCGAGGCCGTGGCGTGACGGGCGGCTTTTCAAATTCCAGACTTGCAACCAGACCGCAGAAATTCCCTTGCCGATCAAGGCATTCTGACGCAGGGCGCTCCGCCAACAGATGGGGCCTGGCTGGGTCAAGGCCCTGTCGCGGCCGAAAATTGGAAAGCAACTGACCGAAGTGGAAATGGAATCGGTAAAATACTTCGGTTTTTACGTGACAAATCACACACCA TTGAAAAACAAGGAAAATTTCCT

CGCACAATTGCCGTTCTCATGGCGAAACCGCCAACCATGAGAATTCCACTTACCCATGGCGCCGAGGAGGTCA CGCGCGCTACAAGGCAAGGGAGGGACAATTGTCGGACATCGAAACATTCTATGACGTGATGCCGCTCAGGGGATCACCCGG CGCAGCTTCACTGAAGTTCTGCTCACCGCAGCAGTTGGGCTTGGGCCCTTCGTGCCGAAAATGCCGAAGCCATGG AAACGAAGCCGCACCCGGTCGCTGGGTGATGGCTGAATGCACCTGCTGTTGGAAAGCTTCGCTCATCCGCTCGGCCAT CGCTGCCAAGGATGTCGCTCTGATGATCTCGCTGATTACGACGACACCTGATGCCGCCCGGTACGCCCGGA AGGCCCTTCGAGGAAACCATGCCAAATAACAGGCAACTACATCTGCCGAGGGCAACCCGCCGCTCAAGGAAGACG GGATGTCGCTCATGCCGGCAAGCCCCTTGCGAGAAGCTGCCGACGCCGGCAAGGGCAGATCATCAGTGG GGGGCTGTGCGTCTATGGCTGCGTGAGCCGGCGCCGACCCAGGGACGCCGGTGACAAGGTGATCACCGA CAAGCCGATCATCAAGGTCGGGCTGCCCGATGCCGAGGTGATGACCGCGTCATCACCTACATGTCGACCTCGACC GGATGCCGGAACTGGACCGTCAGGGCCCGCGATGTTACAGCCAGCGCATCCACGACAAATGCTACGCCGCCGAT TTCGACGCCGGCAATTGCGAACACTGGGACGACGAAAACGCCGCAAGGGTATTGCCCTCTACAAGATGGGCTGCAAGGG CCCGACCCATACAACCGCTGTTGACCGCTGCGCTGAAACGCCGGCTCAGCTCCGATCCAGTCCGTCACGGCTGATCG GCTGTTCCGAGGACGGGCTCTGGGATCACGGGAGCTCTATGACCCGGTCAAGGACATCAAGGAAATTGGCATCGAGGACG GCCGACCCAGATGCCGTCAGGGCCACCCGGCTTGCGGCCCTGCCGCCCCATGCCGGGCTCCGGTCAAAACGCCG GCAGAAAAGAACGAGGGCGTAAGCCATGACGACCAAACGCCGAAACGGCTCACCTCGACAACGCCGCAAGCGATCG TCGTGGATCCGTCAACCGGATCGAAGGCCACATGCCGCTGCGAAGTGAACGTCAGGACATCACCAACGCCGTC TCGACGGGACGATGTCGCGCCCTGAAAGTGAACGTCAGGACATGCCGCGACGCCCTGGGCTTACCGAACGGAT CTGCGGTGTCGACCGGACCCATGCCGTCACCTCGGTCCGCCGGTCAAAGCGCTGGGATCACCATCCCCGACAAT CGAACATCGATCCGCAACATGATGCAACGTCAGGACATGCCGACCCATATCGCATTCTACACACTGCATGCCGTGGAT TGGGTGAACCCGGTCAATGCCGCTGCCGCGATCCGAAAGGCCGACCTCGGAACCTCGCAGCAGATGGTTGCCAGCCATCGC GTCTGGCTTCCCGCTATTCGCGACGTCGAGAAGGGCTGAAAGAAATTCCGCTGAAATCCGGCAGCTGGGCTGTTCAAGAACG GCTACTGGGACAATCCGGCTACAAGCTGCCCGAAGGCCGATCTGATGGCGACGACGCAATTCTGGAAGCGCTGGATCTG CAAAAGGAAGTGGTCAAGGCCACAGATCTGCCGCAAGAACCGCATCCGACTGGCTGTGGGATCACCATCCCCGACAATG GATCAACGTCGATGGCGTGGCGCGGTGCGATCAACATGGAGCGGCTGAACCTCGTCTCTCGATCATCGACCGCTGCA CCGAATTACCCGCAACGTCATCTGCCGACCTCAAGCCATGCCGCTTCTACAAGGAATGGCTATGGCGGGCTG TCAGGGCAATCGGTCTCTATGCCGACATCCGAAACCCGAATGATTCTAGCGCCGGTCAGCTGCACTGCCGCCGG GGCATCATCACCGCAACCTGAACCGAGGTGATGACGTCGACAGCAGGCCGACAGCGTGGCAGGAATCTGTCGACCAATT CCTGGTATGATTACGGGAGCCGGCATGGGCTGCACTCCCTGGGACGGCCGGACGGCGAAATTGAGCTGGGCGGAAAC CTGAAAGGCACCCGCAACCATCGAGAACATCGACGAGGCCGAAATATTCTGGATCAAGGCGCCGCTGGCGCGAA TGCGATGGAGGTGGGCGCTGGCCGCTACGCGCAAGGGCCACGGAGACATCAAGAACCGAGTCGAGGGCC TGCTGCCGACATGAACCTGCCGTTTCCGGCTGTTCTCGACGCTGGGCCGACTGCCGCGGGCTCTGGAGGCGGAATAC TGCTGCCGCTGCAAAGCACTTCTCGACAAGCTGGTACCAACATCAAGAACGGGACAGCTGCGACCGCGAATGTCGAGAA ATGGGATCCCTGACCTGCCGAGGAGGCAAGGGCTGGCATGACCGAGGCCGCGCGCTGGCCATTGGTCA AGATCAAGGACGCCGATCGAGAACACTATCAATGCGTGTGCGACGACCTGGAACGGCTGCCGCCGACAGCAAGGAATAT CGCGCCCTTCGAGGCCCTGCTGTAACACGAGAAGATGCCGAAAGAGCCGGTCGAGATCTGCCGACGCTCACAGCT TCGATCGTGGCTGCCGCTGGACGATGTCGCGCAAGGCCGCCCCCTGACCAACCGCTCAAGGTCCGGTAGGGGATGCCATGCCG GCCATGAAGGGAGTTCCGACGAAAGGATCAATGCCCGTCCGGCCGGATGAAATCTCGAGGCTCGCACTGCCGACTACCGG CGACGCCACCCCGGAGGACCTAGAAAGCATCCGGCGCGTACCTCCGCTATGCTACGAGGGCGGGTCCGGGCTGGCACT GGGTCAACGCCGCTGGCGATCACCATCTGGTGGTCACCGGCTATTCTCATGCCCTGCCGCTGCCCTGATGCCAGATGCCGAG GCCACCGGACAGTCGATGGGCTACATCGCTGCCGCACTGCCGCCGGGGTGTGATGCGTGGGTTTTGCCG CATCTACTGGCCTCTGGACGCCAACCGCCACGCCCTGGCAGATGTTCTACATCCGATCTTACAACGCCGACTGGGAAGGAAT TCGCTTCTCGAGCTGCCGCTGGTATTCTCTTGAAGAAGAGGCCGAGAAATACATGCCACACCCGCTGCCGATGCCG ATGTTCACCTCATCACCTGGGATCACCTCATGATGATCACCGGCTGGGCTTATGCCGAGGCCGGGGCAGGGGG CGTGACCGACGCCGCTGGTGGGCTATGCAAAACAGCCAGGGCTGCACAGTGCACCATCTGGGATGT

GGCGATCGT GATCTTCGGCATCCATATCTACGCCGCGTGC CGAAGACGTGATGAGCCGCCAGTCGATGGTCTCGACG
ATGATCTCGGGCACCGAACCTCAAGGACGACCGGATCGAGTGACTGGAAAGAAGCTTG

AACCGGGCGCAGAGT GATCTGTGCTCGGTTATTGTGGAATATACTTCAAACCTTATAAGTGGTAACAAGGTT TCC
AGAATTGGCGATTCCGACTCTTGC GGTTTCCGGGCGACGGGGTCGATCATGGGCATCGCAACGTGCTTGGGCCACGA
CGGTCTAGGGAGGGACCCATGCCAGCAACCTGAACGGGTTCTGTTCTGGGCATCGCAACGTGCTTGGGCCACGA
GGCTTGGCGTGCCTGTGTC

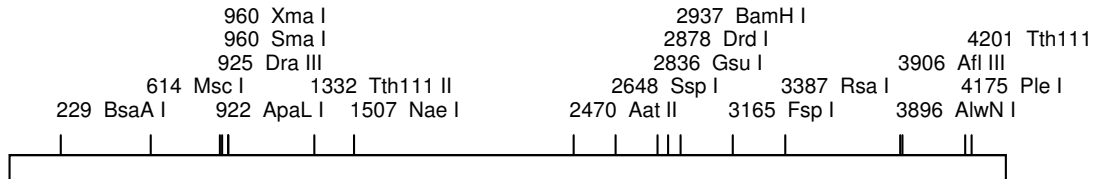


Figure F1. Restriction Map of *hupSLC* operon.

Absent site

Afl II c/ttaag
EcoR V gat/atc
Pml I cac/gtg
Ase I at/taat
Esp I gc/tnagc
Sac I gagct/c
Asp718 g/gtacc
Hpa I gtt/aac
Sca I agt/act
Avr II c/ctagg
Kpn I ggtac/c
Sfi I ggccnnnn/nggcc
Bgl II a/gatct
Mlu I a/cgcgt
BspM II t/ccgga
Mse I t/taa
Spe I a/ctagt
BstB I tt/cgaa
Nde I ca/tatg
Spl I c/gtacg
Bsu36 I cc/tnagg
Nhe I g/ctagc
Xba I t/ctaga
Cla I at/cgat
Not I gc/gccccgc
Xca I gta/tac
Dde I c/tnag
Nsi I atgca/t
Xho I c/tcgag
Dra I ttt/aaa

Enzyme Site unique

BsaA I yac/gtr
Msc I tgg/cca
ApaL I g/tgcac
Dra III cacnnn/gtg
Sma I ccc/ggg
Xma I c/ccggg
Tth111 II caarca
Nae I gcc/ggc
Aat II gacgt/c
Ssp I aat/att
Gsu I ctggag
Drd I gacnnnn/nngtc
BamH I g/gatcc
Fsp I tgc/gca
Rsa I gt/ac
AlwN I cagnnn/ctg
Afl III a/crygt
Ple I gagtc
Tth111 I gacn/nngtc

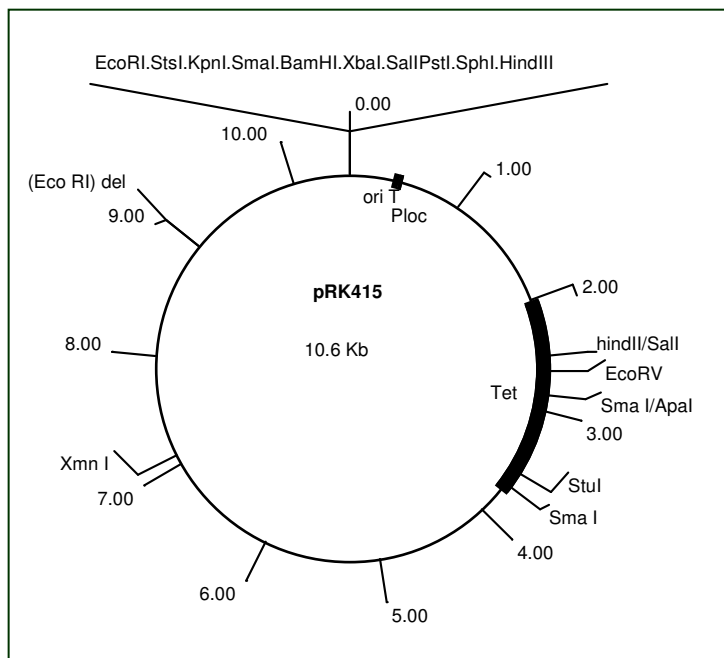
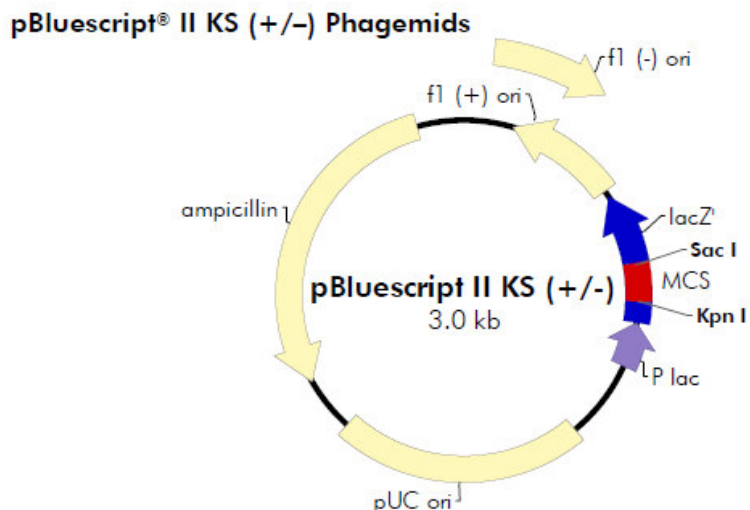
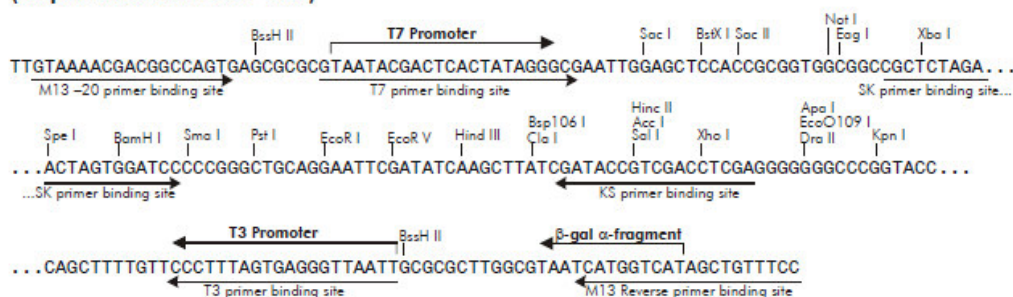


Figure F2. Map of the pRK415 Plasmid vector.



pBluescript II KS (+/-) Multiple Cloning Site Region (sequence shown 598–826)



Feature	Nucleotide Position
f1 (+) origin of ss-DNA replication [pBluescript KS (+) only]	135–441
f1 (-) origin of ss-DNA replication [pBluescript KS (-) only]	21–327
β -galactosidase α -fragment coding sequence (<i>lacZ'</i>)	460–816
multiple cloning site	653–760
T7 promoter transcription initiation site	643
T3 promoter transcription initiation site	774
<i>lac</i> promoter	817–938
pUC origin of replication	1158–1825
ampicillin resistance (<i>bla</i>) ORF	1976–2833

Figure F3. Map of the pBluescript Plasmid vector (Stratagene).

APPENDIX G

OPTICAL DENSITY-DRY WEIGHT CALIBRATION CURVES

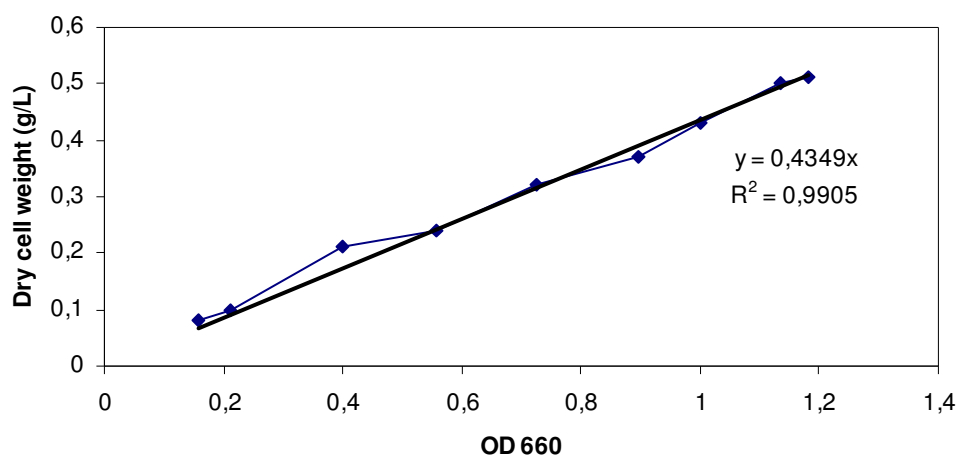


Figure G1. Calibration curve and the regression trend line for dry cell weight versus OD₆₆₀ of MT1131.

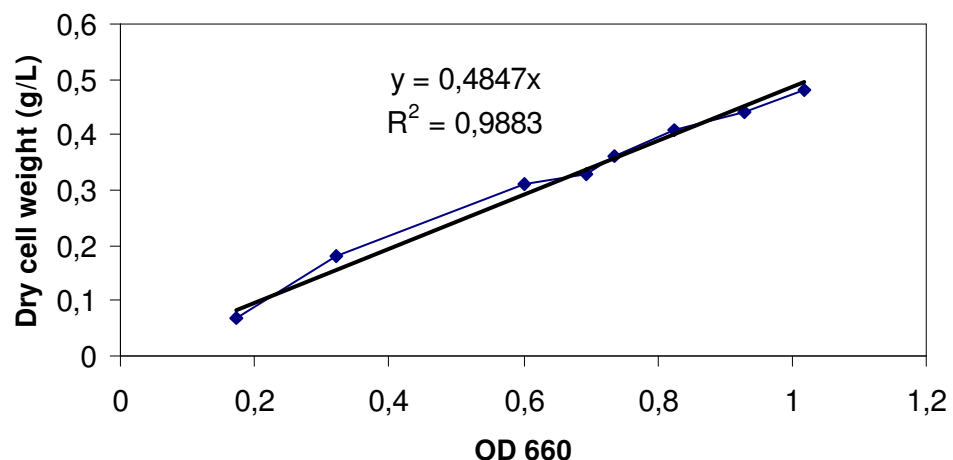


Figure G2. Calibration curve and the regression trend line for dry cell weight versus OD₆₆₀ of GK-32.

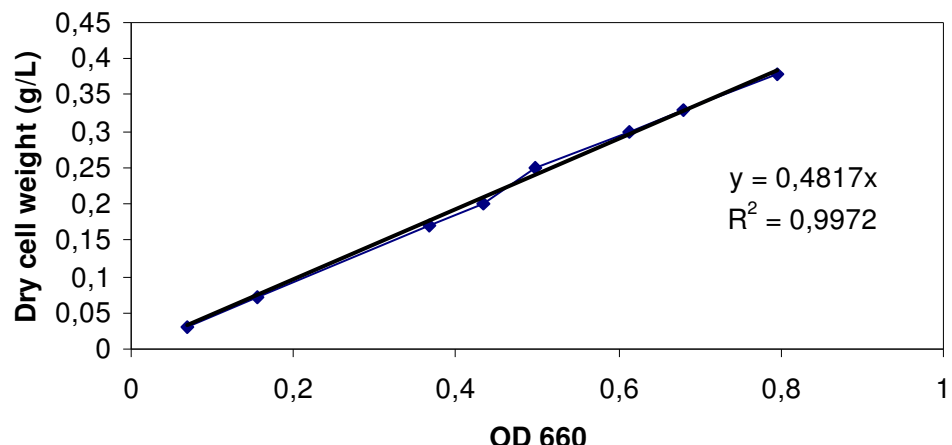


Figure G3. Calibration curve and the regression trend line for dry cell weight versus OD₆₆₀ of KZ1.

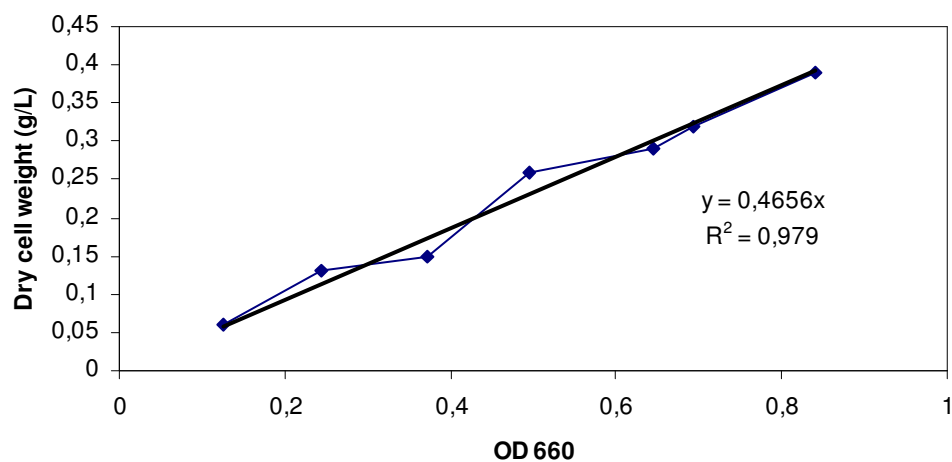


Figure G4. Calibration curve and the regression trend line for dry cell weight versus OD₆₆₀ of YO3.

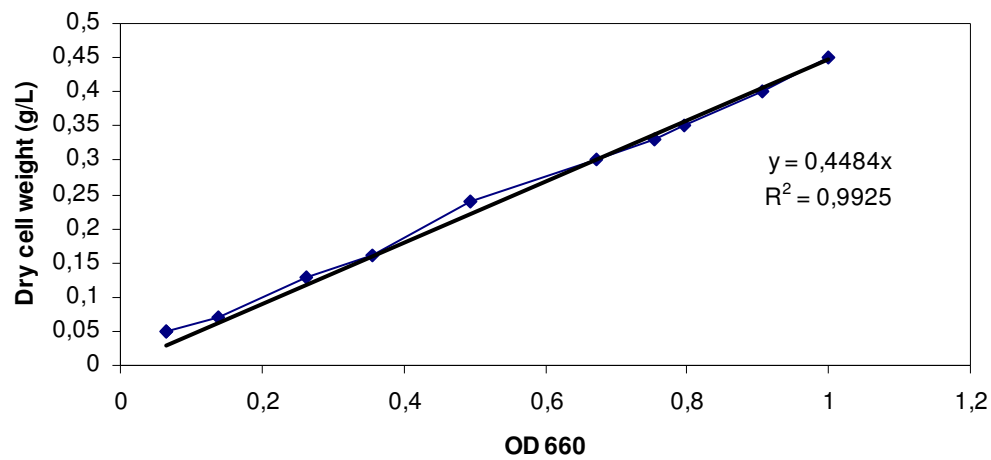


Figure G5. Calibration curve and the regression trend line for dry cell weight versus OD₆₆₀ of YO4.

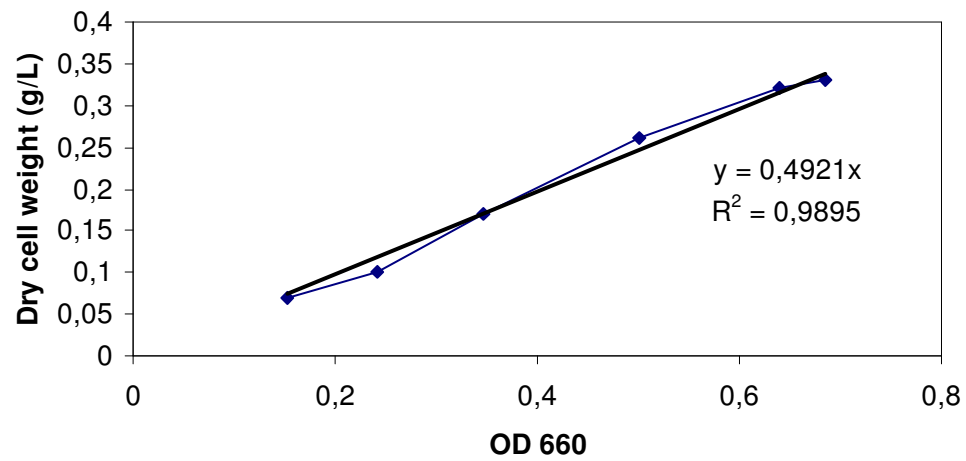


Figure G6. Calibration curve and the regression trend line for dry cell weight versus OD₆₆₀ of YO5.

APPENDIX H

EQUIPMENTS USED IN THIS STUDY

PCR, Eppendorf, Mastercycler gradient

34 °C and 37 °C Etuve (Nuve EN 500)

34 °C and 37 °C shaker-incubator (Nuve SL 350)

4 °C- 99 °C Incubator, Memmert

Anaerobic jar (Oxoid)

Gas Generating Kit (BR038B)

Anaerobic catalyst (BR55)

Electrophoresis Systems

Miniprotein II Biorad

Sigma-Aldrich Techware Protein Electrophoresis System

DNA Electrophoresis System

Power supplies

Biorad Model 200/2.0 Power supply

Biolab, PS 9009 TX, Apelex, Power supply

Heat Blocks

Dry Bloc (Techne DB 2A, Dry-Block)

Shaker-heater (IKA RCT basic)

Autoclave (V/O Medoxport rk-100-2)

pH meter (Metrohm 744)

Micropipettes, Pipetman®, Gilson

0-20, 0-200 and 100-1000 µl pipettes

Centrifuges

Desktop centrifuges (Biofuge fresco Heraeus instruments)

Micro 20 centrifuge, Hettich

Megafuge 2.0R Heraeus seatech)

Sorval RC5C-Santrifuge

Sorval RC 28S

Sorvall Ultracentrifuges OTD75B

Coolers

+4 °C Refrigerators

+4 °C Room

-20 °C deepfreeze, Bosh

-85 °C deepfreeze, Nuaire -85 ultraslow freezer

French® Pressure Cell Press, SIM-AMINCO

Spectrophotometer (Biorad, SmartSpect™ 3000)

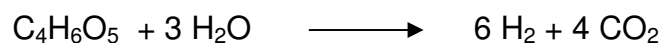
Scales

UV Transalluminator

Vortex (IKA MSI Minishaker)

APPENDIX I

CALCULATIONS FOR SUBSTRATE CONVERSION EFFICIENCY



- 6 moles H_2 are produced from 1 mole malate
- 4950×10^{-6} moles are produced from 825×10^{-6} mole malate (55 ml of 15 mM malate was used in experiments, Mwt of malate;134.09)
- 4950×10^{-6} moles $\times 22.4 \text{ L/moles} = 110880 \times 10^{-6} \text{ L (110, 88 ml) H}_2 \text{ gas}$

Substrate conversion efficiency (%):
$$\frac{\text{Total H}_2 \text{ produced} \times 100}{110.88}$$

VITA

PERSONAL INFORMATION

Surname, Name: Öztürk, Yavuz

Nationality: Turkish (TC)

Date and Place of Birth: 28 October 1974, Kağızman/Kars

Marital Status: Single

Phone: +90 262 641 23 00 extension: 4021 or 4022

Fax: +90 262 646 39 29

Email: yavuz.ozturk@gmbae.tubitak.gov.tr

EDUCATION

Degree	Institution	Year of Graduation
PhD	METU Biotechnology department	December 2005
MS	METU Biotechnology department	May 2001
BS	METU Biology department	June 1998

WORK EXPERIENCE

Year	Place	Enrollment
1999- Present	TÜBİTAK-Gen Mühendisliği Biyoteknoloji Araştırma Enstitüsü	Research Scientist
2001 (7 mount) 2003 (6 mount)	Biology department, UPENN USA	Visiting scholar

FOREIGN LANGUAGES

Advanced English,

PUBLICATIONS

1. Öztürk Y and et al. Soluble Variants of Membrane-anchored cytochrome c_y of *Rhodobacter capsulatus* and *Rhodobacter sphaeroides* as Photosynthetic and Respiratory Electron carriers (in preparation).
2. Öztürk Y, Yücel M, Daldal F, Mandacı S, Gündüz U, Türker L, Eroğlu İ. Hydrogen Production by Using *Rhodobacter capsulatus* mutants with Genetically Modified Electron Transfer Chains. International Journal Hydrogen Energy, special issue (Accepted).
3. Öztürk Y. ve Mandacı, S. "Energy Transduction and electron carrier Protein in *Rhodobacter capsulatus*" Turkish Bulgarian Workshop on Plant Biotechnology May 27-30, 2001 TÜBITAK, MRC, RIGEB-NCAS, AgroBioinstitute.J. Biotechnol.& Biotechnol. Eq.15/2001/2, Supplement.1.

ATTENDED SYMPOSIUM AND MEETINGS

1. Öztürk Y, Yücel M, Mandacı S, Gündüz U, Türker L, Eroğlu İ. Hydrogen Production by Using *Rhodobacter capsulatus* Harboring Genetically Modified Electron Carrier Cytochromes. Proceedings International Hydrogen Energy Congress and Exhibition IHEC 2005 Istanbul, Turkey, 13-15 July 2005
2. Öztürk Y, Yücel M, Mandacı S, Gündüz U, Türker L, Eroğlu İ. Effect of Genetically Modified Electron Carrier Cytochromes on Hydrogen Production in *Rhodobacter capsulatus*. Cost meeting 2004.
3. Öztürk, Y. Mandacı, S. and Daldal, F. Novel Soluble Derivatives of *Rhodobacter capsulatus* cytochrome c_y . 11th International Symposium on Phototrophic Prokaryotes-ISPP2003, Tokyo, Japan (24-29 August, 2003)

4. Öztürk, Y, Mandacı, S., Osyczka,A. Prince,R.C., and Daldal, F. A soluble form of cytochrome c_y as an electron carrier in *Rhodobacter capsulatus*. Gordon conrerence, Roger Williams University, Bristol, RI, USA (June 22-27, 2003)
5. Öztürk Y, Mandacı, S. Daldal, F. A Soluble Form of Cytochrome c_y as An Electron Carrier in *Rhodobacter capsulatus*. Twentieth Eastern Regional Photosynthesis Conrrence, Woods Hole, Massachusetts, USA (Aprilll-13, 2003)
6. Öztürk, Y. Mandacı, S. and Daldal, F. Novel Electron carriers of *Rhodobacter capsulatus*. 28th FEBS meeting; Istanbul-Turkey (October 20-25, 2002)
7. Öztürk, Y., Mandacı, S.(May 14-18, 2000) 'Genetic Engineering of a Novel Electron Carrier Cytochrome, Cyt s- c_y , in *Rhodobacter capsulatus*', 2nd Balkan Botanical Congress, Istanbul-Turkey
8. Öztürk, Y., Mandacı, S, F. Severcan "Sitokrom cyt c_y varyantlarının mutasyon analizleri ve sitokrom cyt c_y proteininin çözümün formunun yapılması", 13. Ulusal Biyofizik Kongres, 4-7 Eylül 2001

PARTICIPATION IN COURSES

1. Powerful technique for functional and structural analysis of protein: Site-directed mutagenesis., 1999, Daldal, F., Mandacı, S., Aygün, S., Öztürk, Y., Tubitak-MAM, Gebze, Kocaeli
2. Molecular Biology/Mutagenesis/Genom-Proteom., 2000, Daldal, F., Mandacı, S., Aygün, S., Öztürk, Y., Tubitak-MAM, Gebze, Kocaeli.
3. Moleküler Biyoloji/Mutagenez/Genom-Proteom: Lisansüstü teorik ve uygulamalı eğitim kurs kitabı, (S Mandacı, S. Aygün, & Y. Öztürk Eds.) TÜBİTAK-MAM. Gebze/Kocaeli, 2001.

4. Moleküller Biyoloji Yöntemleri. Lisansüstü uygulamalı eğitim kurs kitabı.
TÜBİTAK-GMBAE, Gebze/Kocaeli, 2002.
5. Bitki Biyogüvenlik Araştırmaları Uygulamalı Eğitim Programı ISBN-975-403-259-9. TÜBİTAK-GMBAE. Gebze/Kocaeli, 2002.
6. Moleküller Biyoloji-Yönlendirilmiş mutagenez Temel bilgiler ve Denysel uygulamar, TÜBİTAK-GMBAE, Gebze/Kocaeli, 2004.

HOBBIES

Traveling, swimming, nature, reading historical novels, computer technologies, movies, motor sports